CORA Cork Open Research Archive
Cartlann Taighde Oscailte Chorcaí

Title	A novel macroinvertebrate biomonitor for metals in the freshwater environment
Authors	O'Callaghan, Irene
Publication date	2022-08-24
Original Citation	O'Callaghan, I. 2022. A novel macroinvertebrate biomonitor for metals in the freshwater environment. PhD Thesis, University College Cork.
Type of publication	Doctoral thesis
Rights	© 2022, Irene O'Callaghan. - https://creativecommons.org/licenses/by-nc-sa/4.0/
Download date	2026-10-31 09:48:28
Item downloaded from	https://hdl.handle.net/10468/13574

UCC
University College Cork, Ireland
Coláiste na hOllscoile Corcaigh

Ollscoil na hÉireann, Corcaigh

National University of Ireland, Cork



A novel macroinvertebrate biomonitor for metals in the freshwater environment

Thesis presented by

Irene O'Callaghan, B.Sc. (Hons.) M.Sc.

ORCiD: 0000-0002-9030-2824

for the degree of

Doctor of Philosophy

University College Cork

School of Biological, Earth & Environmental Sciences

Head of School/Department: Prof Astrid Wingler

Supervisors: Dr Timothy Sullivan, Dr Dara Fitzpatrick

2022

Declaration

This is to certify that the work I am submitting is my own and has not been submitted for another degree, either at University College Cork or elsewhere. All external references and sources are clearly acknowledged and identified within the contents.

I have read and understood the regulations of University College Cork concerning plagiarism and intellectual property.



Irene O'Callaghan

For Mom.

To live is to fly.

Someday when we meet up yonder,
We'll stroll hand in hand again;
In a land that knows no partin',
Blue eyes cryin' in the rain.

"Courage is being scared to death, but saddling up anyway."

~ John Wayne

Table of Contents

Declaration ii

Acknowledgements xi

List of Publications xiii

Journal Publications xiii

Conference Presentations xiv

Ancillary Works xvi

Nomenclature xvii

Abstract xxi

* * *

Chapter I: Exordium 1

Chapter II: Background 4

Transport and Fate of Pollutants 5

Emerging Contaminants 9

Engineered Nanomaterials 9

Toxicity of Nanomaterials 11

Uptake and Bioavailability in Benthic Fauna 22

Biomonitoring 26

Approaches to Environmental Analysis 29

Direct Measurement 29

Determination of Bioavailable Fraction 31

Traditional Biomonitoring *33*

Passive Sampling *35*

Bioaccumulative Amplification *35*

Chapter III: *Asellus aquaticus* as a Biomonitor 39

The Isopod, *Asellus aquaticus* 43

Potential Mechanisms 46

Freshwater as a Loose Term *47*

Isolated Pollutant Uptake, Sequestration & Excretion *48*

Synergistic & Antagonistic Effects *54*

Other Stressors in the Environment *57*

Use of *Asellus aquaticus* as a Biomonitor 62

Suitability in Principle *62*

Application in Lab and Field *64*

Some Observations *69*

Chapter IV: On Thiophilicity 72

Metallothionein 73

MT in Macroinvertebrates 74

The Thiophilic Scale 75

Materials and Methods 78

Environmental Sampling *78*

Chemical Analysis *81*

Determination of Bioaccumulation Factor (BAF) *81*

Determination of Thiophilicity *82*

Statistical Analysis *83*

Comparative Analysis *84*

Results and Discussion 86

Correlation Between Thiophilicity and BAFs *86*

Comparison of Previously-Published Works *91*

Further Discussion *94*

The Special Case of Pb *96*

Thiophilicity Determines Bioaccumulation 98

Chapter V: Bioaccumulative Amplification in Practice 100

Methodology 100

Field Sampling *100*

Chemical Analysis *102*

Data Analysis *103*

Results 103

Discussion 106

Chapter VI: Laboratory Evaluation of Method 112

Methodology 114

Experimental Set-up *114*

Physical Characterisation of Analytes *115*

Chemical Analysis *116*

Data Analysis *116*

Results 117

Analyte characterisation *117*

Toxicity tests *120*

Bioaccumulation assays *120*

Discussion 123

Preferential Uptake of Nanomaterials over Bulk Analogues *123*

Heterogenous Accumulation of Polymetallic Ions *126*

Elevated Bioaccumulation of Tungsten *127*

Final Thoughts *128*

Chapter VII: Modelling the Impact of Moulting 129

Conceptualizing the Impact of Moulting 131

Existing Models *131*

Choice of Approach *133*

Assumptions *135*

The Conceptual Model *137*

Impact of Moulting *141*

Derivation of Key Equations 143

Differential Rate Equations *143*

Growth Factor *143*

Closed-Form Expressions *144*

Steady-State Equations *144*

Simulation 145

Objectives *145*

Simulation Parameters *146*

Simulation Results *146*

Discussion 149

Contribution of Moulting *149*

Validity of Simulated Example *152*

Reducing Variability due to Moulting *155*

Chapter VIII: In Conclusion 162

* * *

References 166

Table of Figures 219

Table of Tables 224

Appendix A: Thiophilicity Study: Field Data 225

Appendix B: Thiophilicity Study: Meta-Analysis 228

Appendix C: Field Data 253

C1. Measured water concentrations 253

C2. Measured sediment concentrations 254

C3. Measured macroinvertebrate concentrations 255

Appendix D: Lab Data 256

D1. TiO2 exposure assays 256

D2. BaTiO3 exposure assays 256

D3. WC exposure assays 257

Appendix E: Moulting Model: Data 258

E1. V Concentration Factors, from (Miramand et al., 1981) 258

E2. Ni Concentrations, from Figure 4 of (Hall, 1982) 259

E3. Ni Concentrations, from Figure 2(a) of (Hall, 1982) 259

E4. Extracted Data, from (Bergey and Weis, 2007) 260
E5. Extracted Data, from (Hennig, 1984) 260
E6. Extracted Data, from (Keteles and Fleeger, 2001) 260
E7. Extracted Data, from (Reinecke *et al.,* 2003) 261

Appendix F: Moulting Model: Details 262
F1. Accumulation Data from (Miramand *et al.,* 1981) 262
F2. Simulated Exoskeleton Pollutant Concentration 263
F3. Error when Modelling Moulting as a Continuous Process 263
F4. Expanding the Model Derivation 263
F5. Derivation of Parameters from (Miramand *et al.*, 1981) 266
F6. Derivation of Parameters from (Hall, 1982) 268
F7. Continuous Approximation 270
F8. Sample Implementation 271

Acknowledgements

There are several people without whom this thesis might never have been written, and to whom I am greatly indebted, and others still that, were it not for their input and support, this work would not have the spirit that it has.

This research would not have been possible had it not been for the financial support of the Irish Research Council and the Environmental Protection Agency (Ireland). I was honoured to have been awarded a Government of Ireland Postgraduate Scholarship (GOIPG/2018/3351), and I wish to acknowledge that their funding has not only made this work achievable, but has provided me with the independence and creative space that I so greatly enjoyed over these past few years.

Many thanks to the staff in the School of BEES, for their kind support during the course of my studies, and to many of my fellow students for their continuous encouragement and hours of chat. I must also extend my gratitude to those at the ERI and the School of Chemistry, namely my co-supervisor, Dara Fitzpatrick, for his advice, assistance, and time.

My deepest gratitude is due to my primary supervisor, Tim Sullivan, for his guidance, patience, and moral support. This work would, undoubtedly, have been difficult without his academic input, but perhaps of even greater

contribution to its completion were the many cups of coffee, laughs, and his unwavering belief in my abilities.

In the end, my most heartfelt appreciation is reserved for my beloved family. Were it not for them, I would never have begun on this journey, let alone have seen it through to completion. To my father, Liam, my brothers, Billy and Martin, and Martin's dear family, I owe so much more than I can express. Endless support and encouragement seem to come so easily from them, no doubt a reflection of the goodness in their hearts.

I am forever grateful to my grandparents, Gloria and Robert, of the Navajo Nation, for the prayers and genuine kindness. Their letters are a source of joy, and my life is so much the richer for their part in it.

My dearest canine companion, Jazz, has kept me company in the darkest of nights, and placed her head on my knee when my hurt has been in need of her healing, and for that I owe her a lot of donuts. And to my dear Yann, words cannot express the volume of love and encouragement you have given me, but I am eternally thankful.

Finally, this work is dedicated to my desperately missed mother, Gina, who's recent passing has torn my life apart. She has been my most devoted friend and my greatest ally for the entirety of my life, and there is no doubt in my mind that, had it not been for her unending love and kindness, I would not be who I am.

List of Publications

Journal Publications

O'Callaghan, I., Harrison, S. S. C., Fitzpatrick, D., and T. Sullivan. "The freshwater isopod Asellus aquaticus as a model biomonitor of environmental pollution: A review." *Chemosphere* 235 (2019): 498-509.

O'Callaghan, I., and T. Sullivan. "Shedding the load: moulting as a cause of variability in whole-body metal concentrations." *Journal of Crustacean Biology* 40 (2020): 725-733.

O'Callaghan, I., Fitzpatrick, D., and T. Sullivan. "Thiophilicity is a determinant of bioaccumulation in benthic fauna." *Environmental Pollution* 294 (2022): 118641.

O'Callaghan, I., Fitzpatrick, D., and T. Sullivan. "The bioaccumulative biomonitor: a novel approach to measuring metallic pollution in the benthic environment." *Manuscript in preparation.*

O'Callaghan, I., Fitzpatrick, D., and T. Sullivan. "Factors influencing the bioaccumulation of metallic pollutants in a benthic macroinvertebrate." *Manuscript in preparation.*

Conference Presentations

O'Callaghan, I., and T. Sullivan. "*Asellus aquaticus* as a potential biomonitor of trace metal pollution in freshwaters." Environ: 29th Irish Environmental Researchers' Colloquium, Carlow (2019).

O'Callaghan, I., Harrison, S. S. C., Fitzpatrick, D., and T. Sullivan. "The benthic isopod *Asellus aquaticus* as a model biomonitor for metallic nanoparticle pollution in freshwater systems." SETAC Europe 29th Annual Meeting, Helsinki (2019).

O'Callaghan, I., and T. Sullivan. "The effects of surfactants on the microbial biofilm associated with the benthic isopod *Asellus aquaticus*." 17th International Conference on Chemistry and the Environment, Thessaloniki (2019).

O'Callaghan, I., and T. Sullivan. "On the micro-structural features of a pollution-tolerant freshwater isopod, *Asellus aquaticus*." ESA Annual Meeting, Louisville, KY (2019).

O'Callaghan, I., and T. Sullivan. "Trace metal bioaccumulation in freshwater macroinvertebrates: a comparative approach of lab and field studies." SETAC Europe 30th Annual Meeting, Online (2020).

O'Callaghan, I., and T. Sullivan. "Modelling the effect of moulting on metallic pollutant accumulation in freshwater macroinvertebrates." Environ: 30th Irish Environmental Researchers' Colloquium, Online (2020).

O'Callaghan, I., and T. Sullivan. "Destroyed, not defeated: Ireland's legacy of aquatic pollution." IFSA Annual Scientific Meeting, Online (2021).

O'Callaghan, I., and T. Sullivan. "Uncharted waters: UV filters in the freshwater environment." Environ: 31st Irish Environmental Researchers' Colloquium, Online (2021).

O'Callaghan, I., Fitzpatrick, D., and T. Sullivan. "A metric for the relative accumulation of metals in benthic fauna." IFSA Annual Scientific Meeting, Dublin (2022).

O'Callaghan, I., Fitzpatrick, D., and T. Sullivan. "Intrinsic properties of metallic contaminants govern bioaccumulation behaviour: An *ex-situ* comparison of bulk metallic, nanomonometallic and nanopolymetallic bioaccumulation in benthic isopods." SETAC Europe 32nd Annual Meeting, Copenhagen (2022).

O'Callaghan, I., Fitzpatrick, D., and T. Sullivan. "Improving freshwater contaminant quantification by drawing upon intrinsic bioaccumulative properties." Environ: 32nd Irish Environmental Researchers' Colloquium, Belfast (2022).

Ancillary Works

Sullivan, T., and I. O'Callaghan. "Recent advances in biomimetic antifouling materials: a review." Biomimetics 5.4 (2020): 58.

O'Callaghan, I., and T. Sullivan. "Legacy Sediment Contamination." Policy Report, *compiled for* An Fóram Uisce (2021).

Sullivan, T., and I. O'Callaghan. "Understanding the Source, Behaviour and Fate of Nanoplastics in Aquatic Environments." in *Influence of Microplastics on Environmental and Human Health: Key Considerations and Future Perspectives* (Ed. Y. Lang), CRC Press: Boca Raton, FL (2022).

Nomenclature

A	Absorbance
$[a]$	Concentration adsorbed to macroinvertebrate surface
ACF	Accumulation factor
Ag-NP	Silver nanoparticle
β_k	Regression coefficient
B	Body compartment
BAF	Bioaccumulation factor
BAF_S	Sediment-associated bioaccumulation factor
BAF_W	Water-associated bioaccumulation factor
BCF	Bioconcentration factor
BLM	Biotic ligand model
BPA	Bisphenol A
c	Concentration of attenuating species
CN	Coordination number
CNS	Central nervous system
CuO-NP	Copper oxide nanoparticle
$D_0(R)$	Bond dissociation enthalpy of RO
$D_S(R)$	Bond dissociation enthalpy of RS
DLVO	Derjaguin, Landau, Verwey, Overbeek theory
DNA	Deoxyribonucleic acid
DO	Dissolved oxygen

DTPA	Diethylenetriamene pentaacetate
E	Exoskeleton compartment
ε	Molar absorptivity or extinction coefficient
ε	Residual
EDTA	Ethylenediaminetetraacetic acid
ENM	Engineered nanomaterial
FA	Fluctuating asymmetry
FIAM	Free Ion Activity Model
G:A	*Gammarus* : *Asellus* ratio
GC-MS	Gas chromatography – mass spectrometry
GF-AAS	Graphite furnace – atomic absorption spectroscopy
GUTS	General unified threshold model of survival
$[i]$	Concentration ingested by macroinvertebrate
ICP-MS	Inductively-coupled plasma – mass spectrometry
K_{OW}	Octanol-water partition coefficient
k_a	Rate of uptake *via* surface adsorption
k_i	Rate of uptake *via* ingestion
k_r	Rate of uptake *via* respiration
k_t	Rate of translocation from body to exoskeleton
l	Path length of beam within absorbing medium
LC-MS	Liquid chromatography – mass spectrometry
LOD	Limit of detection
M	A metal species

MNP	Metallic nanoparticle
MO	Metal-oxygen complex
MP	Microplastic
MS	Metal-sulfur complex
MT	Metallothionein
MWCNT	Multi-walled carbon nanotube
NOM	Natural organic matter
$O2^{\cdot -}$	Super oxide radical
$OH^{\cdot}$	Hydroxyl radical
ϕ_i	Incidental light flux
ϕ_t	Transmitted light flux
PAH	Polycyclic aromatic hydrocarbon
PBPK	Physiologically-based pharmacokinetic model
PGE	Platinum group element
PHF	Polyhydroxy fullerene
PS-NP	Polystyrene nanoplastic
QD	Quantum dot
$[r]$	Concentration respirated by macroinvertebrate
ROS	Reactive oxygen species
S	Thiophilicity
T	Transmittance
T_M	Moult period
t	time

TBARS	Thiobarbituric acid reactive substance
TiO_2-NP	Titanium dioxide nanoparticle
TKTD	Toxicokinetic toxicodynamic
TS	Thiophilic scale
UV	Ultraviolet
ZP	Zeta potential

Abstract

Clean water is vital to human and ecological health. Freshwaters are relied upon for drinking water abstraction and sanitation, and they are the foundation of many ecosystems. Nonetheless, freshwaters are threatened across the globe by increasing quantities and varieties of emerging contaminants. Our ability to identify and respond to freshwater contamination is limited by our comprehension of fundamental aquatic mechanisms, and the cost and sensitivity of quantitative analytical techniques. This thesis aims to address these issues, through the investigation of bioaccumulative amplification of environmental metal concentrations using benthic macroinvertebrates.

Bioaccumulative amplification is an approach employing the natural bioaccumulation of environmental contaminants by benthic macroinvertebrates as an *in-situ* preparation step in the analytical process, thus relaxing the effective limits of detection. Field evaluation of the technique shows substantial improvement in method sensitivity over the direct quantification of contaminants in the water phase. Lab-based evaluation demonstrates the applicability of this technique to both bulk and nano-scale contaminants, and in both *ex-situ* and *in-situ* environments.

A fundamental relationship between elemental thiophilicity and bioaccumulative potential is described herein, and is evaluated in both field

investigation and meta-analysis of existing datasets. This relationship holds across varying taxa and environmental conditions, and in both marine and freshwater systems. The finding supports the hypothesis that metallothionein is responsible for the biological homeostasis of physiological metals and aids in the protection against metal toxicity. The thiophilic scale is thus presented as a tool for predicting the bioaccumulative potential and ecological risk of a given contaminant.

To date, the process of bioaccumulation has been modelled as an input-only process. Ecdysis, or moulting, is presented as a process that leads to periodic removal of accumulated contaminants. This process is shown to have a significant impact on measured bioaccumulated concentrations. A resulting error is introduced into bioaccumulation studies that overlook this process; steps to minimise this error are also discussed.

Chapter I

Exordium

The widespread monitoring of freshwater metal contaminants is impaired by the difficulty and cost associated with accurate analysis, and the inaccuracy of cheaper alternatives. This thesis aims to address the resulting need for more precise and affordable techniques.

This work will proceed as follows. Chapter II, *Background*, offers an introduction to both well-understood and emerging freshwater contaminants, their impacts on the benthic environment, and the suitability of benthic fauna as biomonitors for these classes of contaminant. It also surveys common approaches to environmental quantification of contaminants, and discusses the advantages of the bioaccumulative amplification approach. Chapter III, *Asellus aquaticus as a Biomonitor*, further explores the suitability of benthic macroinvertebrate biomonitors through the example of a candidate species, the freshwater isopod *Asellus aquaticus*.

The subsequent chapters provide insight into and validation of the bioaccumulative amplification approach. Chapter IV, *On Thiophilicity*, presents new insights into the process of bioaccumulation of metal contaminants. Most importantly, it delivers a novel framework for the relative bioavailability of elemental contaminants according to their position on the thiophilic scale, and offers experimental justification for this statement. It is this finding that would appear to be of greatest impact outside the field of environmental science.

Chapter V, *Bioaccumulative Amplification in Practice*, presents experimental field data that validate the implementation of the bioaccumulative amplification approach in place of direct measurement of the overlying water phase. These results are followed by complementary lab-based experiments described in Chapter VI, *Laboratory Evaluation of Method*, that investigate the influence of thiophilicity on the uptake and accumulation of bulk metallic, nanomonometallic and nanopolymetallic compounds. Taken together, these chapters offer an appraisal of the bioaccumulative amplification approach in practice.

Chapter VII*, Modelling the Impact of Moulting*, investigates practical issues associated with the process of ecdysis that occurs in many benthic macroinvertebrates. It demonstrates why this periodic biological mechanism can alter the interpretation of bioaccumulative processes, and provides instruction on how this phenomenon can be compensated for.

A final summary and parting comments are offered in Chapter VIII, *In Conclusion*.

Ultimately, this body of research aims to present a novel technique capable of overcoming many of the setbacks associated with existing methods.

Chapter II

Background

Portions of this chapter have been published in:

O'Callaghan, I., Harrison, S. S. C., Fitzpatrick, D., and T. Sullivan
"The freshwater isopod Asellus aquaticus as a model biomonitor of environmental pollution: A review."
Chemosphere 235 (2019): 498-509

O'Callaghan, I., and T. Sullivan
"Shedding the load: moulting as a cause of variability in whole-body metal concentrations."
Journal of Crustacean Biology 40 (2020): 725-733

O'Callaghan, I., and T. Sullivan
"Legacy Sediment Contamination."
Policy Report, compiled for An Fóram Uisce (2021)

Portions of this chapter have been disseminated at:

Environ: 29th Irish Environmental Researchers' Colloquium, Carlow (2019)
SETAC Europe 29th Annual Meeting, Helsinki (2019)
IFSA Annual Scientific Meeting, Online (2021)
Environ: 31st Irish Environmental Researchers' Colloquium, Online (2021)

Tó'éí'iiná. Water is life. Perhaps more vital than any other heteronuclear molecule, water is essential to the health of ecosystems and human communities across the globe. People rely on surface waters for drinking water, sanitation, and food supplies. Clean water is an important precondition to strong and successful biotic communities (Hallouin et al., 2018; Keeler et al., 2012).

Unfortunately, freshwater system contamination is seen worldwide. A variety of contaminants are responsible for this deterioration of ambient water quality. These contaminants may enter the hydrosphere *via* a number of (primarily anthropogenic) pathways (Javed, 2005; Klavinš et al., 2000; Salt et al., 1995; Stead-Dexter & Ward, 2004).

Our ability to respond to this threat to freshwater health depends upon the breadth of our understanding of contamination processes, and our ability to detect and quantify existing contamination.

Transport and Fate of Pollutants

Pollutants enter the freshwater environment in many ways, including, but not limited to, domestic and industrial outflow, road run-off, agricultural run-off and natural leaching from mineral-rich soil (Buzier et al., 2011; Maceda-Veiga et al., 2012; Moldovan et al., 2001). The mobility, transport and fractionation of a metal species are defined by the chemistry of the molecule, as well as the physicochemical and biological characteristics of the river system (Sakan et al., 2009). The nature of the pollutants entering the environment is not known *a priori*, but it must be assumed that the elements could be found in any state.

The metallic pollution of freshwater systems has been of significant concern for many decades (Förstner & Prosi, 1979; Nriagu, 1990; Sahu & Basti,

2021). Concentrations of metals in waterways that are in excess of natural background levels are often attributed to anthropogenic pressures (Saleem et al., 2015; Thevenon et al., 2011). Metal pollutants in freshwater systems may undergo precipitation or adsorption to suspended particles, which are then deposited as sediments (Atkinson et al., 2007). The metals can be present in very small concentrations, which makes quantification, or, in many cases, even detection, very difficult. The effects are no less detrimental to the ecosystem, however, due to the potential for bioaccumulation, the gradual build-up of a chemical substance within an organism, and biomagnification, an increase in the concentration of a chemical as it transfers from lower to higher trophic levels (Suedel et al., 1994).

Other factors may also influence the speciation of metals, including weather, or even the presence of benthic dwellers. A significant relationship between metal speciation and heavy rainfall events has been observed, as the increased flow rate and load causes metal-containing sediments to become re-suspended (Meylan et al., 2003).

Similarly, the disturbance of sediment by organisms is responsible, although at a small scale, for the resuspension of metals (Atkinson et al., 2007). Sediment, the layers of sand particles, silt, clay, eroded rock and degraded organic matter that comprises the floor of lakes and rivers, is a vital component of the overall waterbody. This sediment operates as a sink for

many contaminants - absorbing them from the water, retaining them for sometimes decades or longer, and eventually releasing them back into the overlying waters (O'Callaghan & Sullivan, 2021). Changes in sediment load and composition, and increased suspended sediment can impact upon the density and structure of benthic communities (Koiter et al., 2013; Palmer et al., 2000; Ryan, 1991), and the concentration and transfer of dissolved oxygen within the sediment is vital to the survival of benthic biota (K. Wang et al., 2021). The solid, stationary sediment phase is antipodal to the dynamic nature of the water phase. Pollution input to waterways is washed downstream, and while the impacts of this pollution may linger long after the source has been removed, the residence time of the pollutant within the water column is relatively short (Brodie et al., 2012; U.S. Environmental Protection Agency, 2005). The freshwater sediment, however, is a much more stable environment. The porous nature of sediments, as well as the accumulation of decomposing organic matter, promotes the entrapment of pollutants, allowing them to reside for a much longer time. These pollutants can then be released, either gradually (due to the sediment-water interactions) or suddenly (due to storm events or anthropogenic disturbances) (O'Callaghan & Sullivan, 2021). The sediment could be compared to a battery, storing contaminants for a long period of time, and discharging them at a later date.

Speciation distinguishes between free metal ions in solution, complexed metals in solution (which may be organic or inorganic in nature), adsorbed particles and colloidal particles. Furthermore, size fractionation differentiates between particles of various sizes. Particles are measured on a micrometre (μm) scale, and larger sized particles may be removed from solute by way of filtration. However, particles smaller than the pores of the filter (typically 0.45 μm) are referred to as dissolved fractions (Tuccillo, 2006). While it is not feasible to remove these particles on a large scale by simple filtration, a number of methods have been proposed for their removal, including sorption of the particles within a biofilm (Späth et al., 1998; Veglio & Beolchini, 1997). The size of a particle could be of great significance in the context of freshwater biota.

Free metal ions are thought to be more reactive than complexed metals in freshwater, which implies greater toxicity, and, thus, a more urgent need for understanding (Allen et al., 1980). The free ion activity model (FIAM) has been put forward as a tool for assessing potential metal-organism interactions, and for determining the uptake and toxicity of all cationic metals. However, the FIAM makes the assumption that the activity of the free ion is directly related to the reactivity of the chemical species (P. L. Brown & Markich, 2000). The need for further expansion of our understanding and modelling of these processes based on field data has been identified, as the FIAM, while useful in a laboratory setting, is theoretical,

and its applicability to real-world scenarios must be validated (Meylan et al., 2004). Despite efforts to examine the relationship between metal speciation and humic substances (Mantoura et al., 1978), there also remains a need for practical studies to fully understand these interactions (Tipping et al., 2002).

Emerging Contaminants

Contaminants of emerging concern are those that are unregulated at this time, but widely employed in commonly used products, and may cause harm and may potentially persist in the environment. Due to a lack of long-term data, the ecological risk of such compounds is difficult to ascertain (Noguera-Oviedo & Aga, 2016; Taheran et al., 2018).

These emerging contaminants can take many forms, and be found in a range of sizes and shapes, and with varying composition or surface chemistry. For this reason, determining the eventual fate of these materials has proven difficult, and numerous studies have highlighted potential pathways into the aquatic environment (Batley et al., 2012; Ding et al., 2022; Lv et al., 2014; Malakar et al., 2021).

Engineered Nanomaterials

A nanomaterial is, in most cases, described as any material that has one or more dimensions in the nanometre scale or lower (Jeevanandam et al., 2018), however, they have also been defined as sub-100 nm scale (Piccinno et al.,

2012). While naturally-occurring nanomaterials are a known phenomenon, increasing quantities of nanomaterials are man-made, and are commonly termed Engineered Nanomaterials (ENMs) (Jeevanandam et al., 2018; Piccinno et al., 2012). This term typically refers to metallic nanoparticles (MNPs), Quantum Dots (QDs) and nanoplastics, taken to be defined as a plastic particle with at least one dimension less than 1 μm (Pinto da Costa, 2016; ter Halle & Ghiglione, 2021), but more exotic nanomaterial categories exist, such as cellulose-based and ceramic nanoparticles (Bifari et al., 2016; Gangadoo et al., 2020; I. Khan et al., 2019; Wu et al., 2020).

The potential impact of nanomaterials on the freshwater environment is of growing concern (Revel et al., 2017). However, while recent studies have examined the potential mechanisms that nanomaterials may undergo in controlled scenarios, much remains unknown about the mechanistic fate of these materials in the natural environment (Hayes & Sahu, 2020; Shen et al., 2019). The hydrosphere is a likely sink for these materials, due to their proximity to sources of anthropogenic discharge, as well as their role as an endpoint for most wastewater treatment plants (Karbalaei et al., 2018).

Direct measurement of nanomaterial concentrations in the environment is extremely difficult, and attempts to determine their prevalence have been largely restricted to theoretical fate modelling (Gottschalk et al., 2013). Most existing studies considering the environmental impact of nanomaterials have focused on the ecotoxicological potential of these materials. Little attention

has been paid to the mechanisms these materials undergo in the environment, whether chemical and physical processes underlying their environmental transformations and ecotoxicity, or the biological process of trophic transfer. Our resulting understanding of the mechanistic fate of these materials in the environment is limited. This has resulted in a void in our understanding of the risk associated with ENM use and release, beyond the awareness that they are toxic to a selection of aquatic organisms (Lehutso et al., 2020).

Toxicity of Nanomaterials

The majority of studies pertaining to the mechanistic effects of nanomaterials in the freshwater environment have focused on experimentally quantifying the toxicity of the nanomaterial of interest on a particular test organism or group of organisms, and have mainly considered the possibility of toxicity from reactive oxygen species (ROS) production and/or direct physical contact leading to cell membrane damage. This discussion will address several common themes in the literature, while also identifying under-represented, but potentially fertile paths of inquiry.

Nanospecific Mechanisms

Most studies have considered the toxic effects of ROS as a potential primary mechanism of toxicity, with some studies exclusively focusing on this mechanism. There are many mechanisms (both endogenous and exogenous)

which can result in production of ROS, just as there are many examples of ROS; but their common feature is their ease of production in water (in the case of exogenous production) and their potential toxicity arising from their highly reactive nature, which induces oxidative stress in the organism. ROS production can be increased by UV exposure or elevated temperatures, which makes ROS toxicity potentially dependent on experimental conditions. Because ROS are generally reactive with many chemical compounds, they can induce a wide variety of negative effects in the organism, including cell membrane and DNA damage.

Many studies have proposed toxicity through the generation of ROS by nanomaterials. A strong example in favour of the ROS mechanism is the observation of cultured algal density increasing in the presence of polyhydroxy fullerenes (PHF) (Gao et al., 2011). Nanoscale fullerenes are widely touted as antioxidants, with strong radical scavenging properties, so it could be surmised that PHF scavenging ROS, and thus lessening oxidative stress, reduces algal stressors. Similarly, (Feng et al., 2019) saw increased growth inhibition of an algae from polystyrene nanoparticles (PS-NPs) after inhibition of an intrinsic antioxidant response, while (Taylor et al., 2016) found that the ion-specific toxicity of silver compared to Ag-NPs to a cyanobacteria correlates with the ROS-producing ability of ionic silver.

ROS production is especially likely in the context of a known photocatalyst, TiO_2-NPs. TiO_2-NPs are often termed "UV filters" due to

their ability to absorb and reflect UV light, but are also known to act as a catalyst under heightened UV irradiation. In the freshwater environment, a likely mechanism is the production of the hydroxyl radical, the mechanism for which is described graphically in Figure 1: Illustration of the photocatalytic mechanisms TiO2-NP may undergo when subjected to UV irradiation, where the radiation energy (hv) is greater than the band gap energy. Reactive Oxygen Species (ROS) produced include the hydroxyl radical (OH ·), superoxide radical ($O2^{\cdot -}$) and the non-radical reactive hydrogen peroxide (H2O2) molecule. .

Some studies support this, showing both increased toxicity of, and increased ROS production by TiO_2-NPs under UV irradiation (Dalai et al., 2014; Fu et al., 2015; Li et al., 2017; Sendra et al., 2017).

Conversely, it should be pointed out that many studies may have overestimated the ubiquity of ROS as a mechanism of toxicity, and, in doing so, overlooking other potential mechanisms. For example, (Wormington et al., 2017) suggests observed mitigation of toxic effects of TiO_2-NPs after the addition of Natural Organic Matter (NOM) is solely due to less abundant ROS, based on a fluorescence assay-based determination of ROS concentrations, but while the influence of UV attenuation was experimentally discounted, the mechanism of damage as a result of direct contact was not considered. Some studies have found compelling evidence

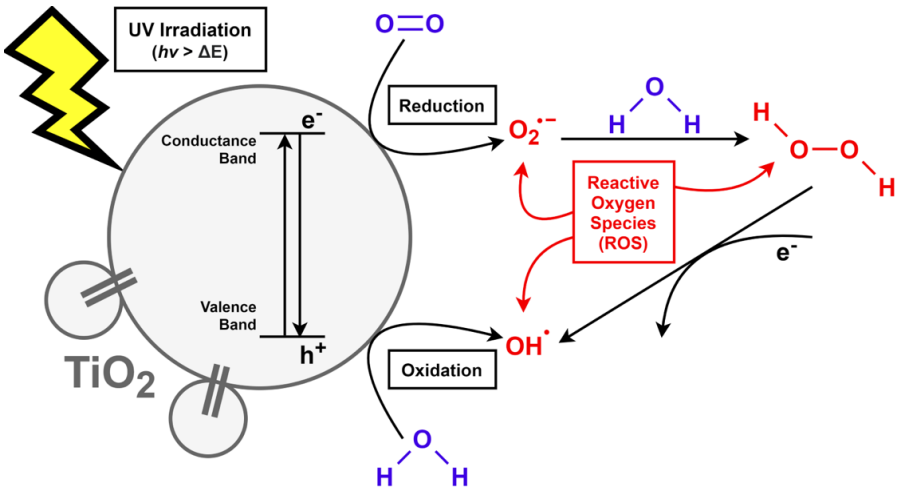


Figure 1: Illustration of the photocatalytic mechanisms TiO_2-NP may undergo when subjected to UV irradiation, where the radiation energy (hv) is greater than the band gap energy. Reactive Oxygen Species (ROS) produced include the hydroxyl radical (OH ·), superoxide radical ($O_2 \cdot^-$) and the non-radical reactive hydrogen peroxide (H_2O_2) molecule.

for the combined effects of ROS-induced toxicity and damage resulting from direct contact between the nanomaterial and the cell (L. Q. Chen et al., 2013; Dalai et al., 2014; Feng et al., 2019; Sendra et al., 2017; J. Zhao et al., 2017).

Other chemical mechanisms beyond the production of ROS have been suggested to explain the toxicity of nanomaterials. One question that perennially arises within the literature is that of the nanospecific toxicity hypothesis. This hypothesis supposes that unusual properties of nanoscale materials are responsible for nanospecific mechanisms of toxicity. An equally popular hypothesis is that the toxicity of nanomaterials arises from leaching of the ionic core metal(Donaldson & Poland, 2013; Fard et al., 2015).

Ion Leachate

A compelling argument in favour of the latter is the higher toxicity of many ionic species compared to their analogous nanoparticular phases, with a number of studies presenting evidence of increased toxicity of the ionic forms (Garner et al., 2018; Intrchom et al., 2018; Lin et al., 2019; Pham, 2019; Qian et al., 2016). A strong argument in favour of toxicity *via* leaching of ions is the finding that varying the coating of Ag-NP results in different toxic behaviour, but the toxicity of leachate from the nanoparticulate form is unaffected by coating type, and further, similar to the toxicity of

$AgNO_3$ salts (C. M. Zhao & Wang, 2012). A similar correlation of toxicity with Ag-NP dissolution was seen in (Sendra et al., 2017). This result would be explained by the theory that different coatings would alter the rate of leaching, thus altering the concentration of leached ions. An interesting group of studies present the example of biotransformation of Au & Ag to the less toxic nanoparticulate form as a detoxification mechanism (Feurtet-Mazel et al., 2016; Kadukova, 2016; Sedlakova-Kadukova & Pristas, 2019).

Despite such convincing arguments to the affirmative, evidence in support of the contrary hypothesis abounds. Studies of mesosilver, CdTe quantum dots and CuO-NPs show differences in toxic effects compared to ionic forms which strongly suggest the existence of nanospecific toxic effects (Ambrosone et al., 2012; Falfushynska et al., 2015; Kleiven et al., 2019; Ma et al., 2017; Poynton et al., 2012; Taylor et al., 2016). The use of glutathione to immobilise the Ag^+ leachate from Ag-NP demonstrated toxicity to algae which cannot be attributed to the leachate, so is likely nanospecific in nature (Miao et al., 2010). It is almost certain that any nanospecific mechanisms that exist typically operate in conjunction with ionic toxicity; and, furthermore, that their relative importance depends on conditions and exposure species (Z. Chen et al., 2018; Taylor et al., 2016).

Genotoxicity

An interesting, but less explored, effect of nanomaterials is disruption of the genetic material, or genotoxicity. Often considered to be caused by oxidative stress, genotoxicity has been observed after exposure to a wide range of nanomaterials (Ali et al., 2012; Bobori et al., 2020; Fahmy & Sayed, 2017; Koehle-Divo et al., 2018; Vicari et al., 2018). Some studies have found genotoxicity to be more prevalent in the presence of nanoparticles when compared to related bulk materials (Bhuvaneshwari et al., 2016). Most curiously, significant genotoxicity has been observed at relatively low analyte concentrations (Ambrosone et al., 2012; Sumi & Chitra, 2019). However, this possible line of inquiry is largely under-explored.

Secondary Mechanisms

While most studies can attribute the observed toxic effects of nanomaterials to one of the primary mechanisms outlined above, there are undoubtedly a plethora of processes associated with the release of nanomaterials into the freshwater environment. Some of these secondary effects have been observed in the literature. A number of carbon-based nanomaterials have been observed to deplete the nutrient content of a solution, with a detrimental effect to resident algal cultures (J. Zhao et al., 2017). A more unusual example is the intensive heteroaggregation of multi-walled carbon nanotubes (MWCNT) to microalgae, resulting in the algae being

encapsulated in a nanomaterial shell that inhibits access to environmental nutrients (Munk et al., 2017). Fullerenes ingested by the zebrafish *Danio rerio* have been shown to reduce the food conversion ratio, seemingly through the inhibition of digestive enzymes (Tao et al., 2016). TiO_2-NPs have been shown to inhibit the nitrogen-fixing process of cyanobacteria *via* a mechanism that appears to be different from that responsible for growth inhibition; additionally, there appears to be a dose-dependent generation of cyanophysin granule polypeptides (CGP) (Cherchi & Gu, 2010), a storage polymer synthesised as a means of storing nitrogen reserves (Obst et al., 2002).

Meanwhile, polyhydroxy fullerenes (PHF) can improve algal growth through scavenging of ROS compounds, but are equally easily biodegraded by photolysis into a nutritional form (Gao et al., 2011). Similar growth-enhancing effects have been observed in studies of low-concentration TiO_2-NPs and algae (Cardinale et al., 2012; Kulacki & Cardinale, 2012). It has been hypothesised that this could result from an increase in photosynthetic efficiency due to electrochemical changes at the NP-cell interface (Cardinale et al., 2012).

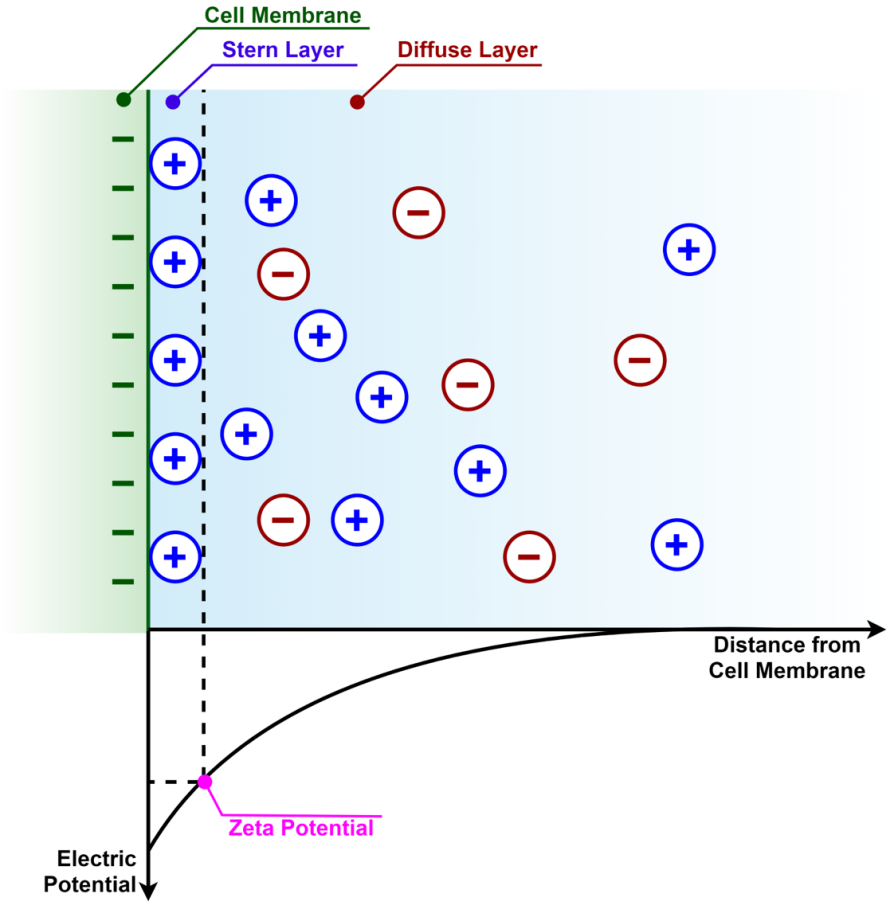


Figure 2: Illustration of electrochemical mechanisms near the charged surface of a cell membrane. The Zeta Potential is defined as the Electric Potential at the interface between the Stern Layer, containing charges strongly bound to the surface, and the Diffuse Layer, containing charges loosely attracted to the surface.

Electrostatic Interactions

The influence of electrostatic interactions on NP-cell heteroaggregation is an important consideration that warrants further study. Surface charge, usually quantified *via* zeta potential (ZP), is likely a vital parameter governing the aggregation of microorganisms, in particular, with nanoparticles, and, thus, the subsequent NP toxicity. The relationship between the ZP and the distribution of charges around a cell surface is illustrated in Figure 2. Opposite nanoparticle and cell membrane surface charges can attract the particle to the cell, promoting aggregation.

Conversely, charges of similar polarity will repel the particle away from the cell. This effect has been observed in the supposed non-toxicity of negatively-charged nanoparticles to negatively-charged bacteria. In this scenario a change in functional group is sufficient for the toxic effect to reappear if the new compound is positively charged (Deryabin et al., 2015; Feng et al., 2019; Y. Liu et al., 2019; J. Zhao et al., 2018). Additionally, ZP is often taken to be a good predictor for the stability of a colloidal solution. ZP magnitudes in excess of ± ~30 mV are taken to be stable (Munk et al., 2017), and, hence, located in homoaggregates with reduced bioavailability. DLVO (Derjaguin, Landau, Verwey, Overbeek) theory would describe the adhesion of the particle to the cell membrane in terms of competing van der Waals and electrostatic double layer forces; however, in the presence of significant

homoaggregation, the competing processes of homo- and heteroaggregation must also be considered.

Alongside the plurality of NP-cell and NP-NP interactions that could occur, the natural freshwater environment is a complex soup of compounds which are equally likely to interact with the nanomaterial. The potential influence of naturally occurring organic compounds on nanomaterial toxicity equally constitutes an important process and a potentially intractable problem. In many studies, the presence of organic matter has been shown to reduce nanomaterial toxicity, although the mechanisms proposed are various and often uncertain. Observed processes include changes to ZP, and, thus, aggregation dynamics (Angel et al., 2015; J. Zhao et al., 2018); scavenging of free radicals, leading to ROS quenching (Liang et al., 2020; Wormington et al., 2017); and heteroaggregation with nanomaterials, rendering a less bioavailable form by altering the surface chemistry of the nanomaterial, or through increased steric hindrance (Bone et al., 2012; R. Khan et al., 2019; J. Zhao et al., 2018). However, these effects were not universal, and found to be both dose-dependent (Y. Liu et al., 2019) and dependent on the nature of the organic matter (Liang et al., 2020), and sometimes reacted differently in the presence of other inorganic compounds (X. Liu et al., 2014), raising the question of potential synergistic and antagonistic behaviours. Furthermore, organic matter was sometimes found to promote bioaccumulation and increase cell damage due to polystyrene NPs (PS-NPs) (Liang et al., 2020).

Scientific interest in elucidating the mechanistic fate of nanomaterials in the freshwater environment is welcome, as our understanding of the impacts of nanomaterials partially depends on our ability to elucidate the mechanisms that these contaminants undergo in the aquatic environment.

Uptake and Bioavailability in Benthic Fauna

The long-term toxicity of many contaminants to aquatic life, even in small concentrations below lethal doses, is partly due to the tendency of fauna to bioaccumulate these trace amounts (Palma et al., 2015). Benthic macroinvertebrates are particularly at risk of freshwater pollution, as they are in near-constant contact with both the sediment and water.

The physical uptake of contaminants by benthic macroinvertebrates from the surrounding environment may occur through several possible mechanisms: ingestion, respiration and/or surface adsorption. These pathways (illustrated in Figure 3) result in the movement of contaminants from the sediment and overlying water column into the organism. Some amount of contaminants may subsequently be removed from the organism through excretion or desorption of surface adsorbed contaminants. Contaminants remaining within the organism may be bioaccumulated by transportation of metabolically-available contaminants from the alimentary tract, gills or through permeable surface pores, into the cells of the organism by way of complexation to receptor proteins (Rainbow, 2006).

Figure 3: Illustration of common uptake (ingestion and adsorption), depuration (excretion) and bioaccumulation pathways of metal contaminants in the freshwater isopod, Asellus aquaticus. Uptake and depuration pathways occur at the organism-environment interface, while bioaccumulation occurs within the cell through the binding of contaminants with receptor molecules. Additional pathways of uptake and depuration include respiratory intake of suspended contaminants from the water phase and desorption of surface-bound contaminants, respectively.

In order to quantify the pollutants that are bioavailable to benthic fauna, it is necessary to consider both the types of pollutants initially introduced to the environment, as well as the numerous processes which may transform the nature of the pollutants present in the environment.

However, environmental concentrations are not necessarily equivalent to concentrations bioaccumulated in the organism. Various processes can occur which may modify the state of pollutants once they have entered the environment. These mechanisms may have an effect on the bioavailability of a metal species in the freshwater environment.

Metal speciation depends on a number of physicochemical factors such as pH, temperature, dissolved oxygen content (DO) and the availability of nitrogen- and sulphur-containing ligands with which the metals may form biologically compatible complexes. All of these factors, and more, determine the ultimate fate of the metal species in the aquatic environment, as they influence the bioavailability and toxicity of the metal (Kuppusamy & Giridhar, 2006; Pagnanelli et al., 2003).

There is also an indication that pH plays an important role in the uptake of metal species. pH dictates the cation and anion partitioning between the solid and liquid phases, and has an effect on the behaviour of the metal, meaning it may alter relevant properties (Warren & Haack, 2001). While the common assumption is that a decrease in pH correlates to an increase in

metal uptake, there have been a number of studies that contradict this, having seen an increased uptake under neutral conditions, compared to a lower pH (Gerhardt, 1993). The authors identify several possible explanations:

a) At low pH, H^+ and the metal ion may compete for binding sites and/or the sensitivity of the carrier molecules for some metals may be lowered.

b) At higher pH, metals may be adsorbed or co-precipitated and therefore less bioavailable.

c) Surface adsorption onto the organism may account for increased metal levels at neutral pH.

d) The organisms used for the experiment may have been from a site with pH neutral water, with the lowering pH resulting in stress and less ingestion by the organisms.

A number of other studies have given consideration to the correlation between pH and metal uptake (Campbel & Stokes, 1985; Courtney & Clements, 2000; Kar et al., 2008; Sako et al., 2009), but there remains much demand for further investigation.

Biomonitoring

Biomonitoring is defined as the use of an organism, whether whole, in part, or communal, to determine the quality of the environment, and it is commonly used as a method of detecting and quantifying contaminants present in the environment (Markert, 2007). Biomonitoring is generally employed for the quantification of environmental pollutants, wherein a measurable parameter may be the abundance of an identified biomonitor species in a geographical area, or under a defined set of conditions (Bonada et al., 2006; Ketelaars & Frantzen, 1995).

Differing species show varying degrees of sensitivity and tolerance to various types of pollutants, with measurable responses ranging from growth inhibition to population die-off. It is by this end that a number of biotic indices have emerged, whereby the relative abundance of a species with a known tolerance to a pollutant can be used to extrapolate the severity of the pollution event (MacNeil et al., 2002).

A primary application of an aquatic biomonitor is the measurement of presence and bioavailability of contaminants in the environment, and hence an indication of environmental concentrations (Flessas et al., 2000; Johnson et al., 1993). Consequently, an unusually restrictive, but, in the context of this thesis, perhaps more interesting definition of the term "biomonitor" is stated, in a 1995 study by Rainbow, as "a species which accumulates heavy

metals in its tissues, and may therefore be analysed as a measure of the bioavailability of the metals in the ambient habitat" (Rainbow, 1995).

Metals may enter the aquatic environment by means of natural processes, such as metals leaching into rivers following a forest fire in an adjacent location, or through anthropogenic disturbance (Richardson et al., 2001). Anthropogenic activities contribute a significant fraction of metals entering the hydrosphere (Callender, 2003). The monitoring of metal concentrations in waterways traditionally requires offline chemical analysis methods which may be costly, time-consuming and may not fully reflect the time-averaged conditions of the water system (Markert et al., 1999). This has led to a search for alternative methods of monitoring. The implementation of a biomonitor is a reasonable solution.

A distinction must be made between total and bioavailable pollutant concentrations in order to appreciate the advantage of biomonitoring over direct measurement of the pollutants. Various physicochemical processes can render a pollutant biologically inert. These can be divided into environmental processes, that influence the "environmental availability," and internal biological processes within an organism, that influence the "toxicological bioavailability" of the pollutant (Peijnenburg et al., 1997). While total pollutant concentrations can be determined directly through chemical analysis, accounting for the concept of bioavailability requires either the application of measured environmental parameters to a model of

the environmental processes (the *a priori* approach, often the application of partition coefficients to measured total pollutant concentrations), or direct measurement of accumulated concentrations within the organism of interest (the *a posteriori* approach). The classification of pollutants according to their bioavailability and toxicity, such as the Priority Substances List of the Water Framework Directive and subsequent amendments (European Commission, 2000, 2008), is a similar approach to the former. Biomonitors exemplify the latter, as the measured biological concentrations are the result of both the environmental availability and toxicological bioavailability processes, and, therefore, offer an insight into the results of these processes without requiring knowledge of the processes themselves. This approach avoids the need to fully understand or characterise such processes, so long as the biomonitor is chosen such that the toxicological bioavailability encountered is representative for the ecosystem under study.

Benthic dwellers have been suggested as an ideal biomonitor of river and lake pollution, as they are generally present in large numbers, and have been found to strongly accumulate metals (El Gawad, 2009). As they do not typically displace themselves over large distances, they are considered to be a fair representation of conditions in the area in which they are found (Adriaenssens et al., 2006). Benthic species are often predated upon, potentially filling the role of a keystone species, and contamination of these species may have far reaching consequences for ecosystem health (Fleeger

et al., 2003; Swartwout et al., 2016; Thorp & Bergey, 1981). As illustration of this statement, the following chapter will examine the suitability of a candidate biomonitor species, the benthic isopod *Asellus aquaticus*.

Approaches to Environmental Analysis

Environmental monitoring is typically carried out at scale and across long timeframes, and benefits from granularity of accuracy and cost. In this section, we examine some of the most common approaches to the analysis and quantification of contaminants in the freshwater environment. A graphical summary of these is presented in Figure 4.

Direct Measurement

Direct measurement consists of sample acquisition, most often of the overlying water, followed by on-line or off-line analysis. While advanced analytical techniques can be employed in the direct measurement of contaminants in a freshwater system, these methods are cost-prohibitive, particularly for small-scale projects, and often require specialist technical knowledge, limiting the performance of analysis to trained persons. This results in a limitation to the number of samples that can be taken, or the number of sites that can be monitored. While there exist less costly and simpler methods of analysis, these methods are less accurate, less precise and offer analysis of decidedly fewer analytes.

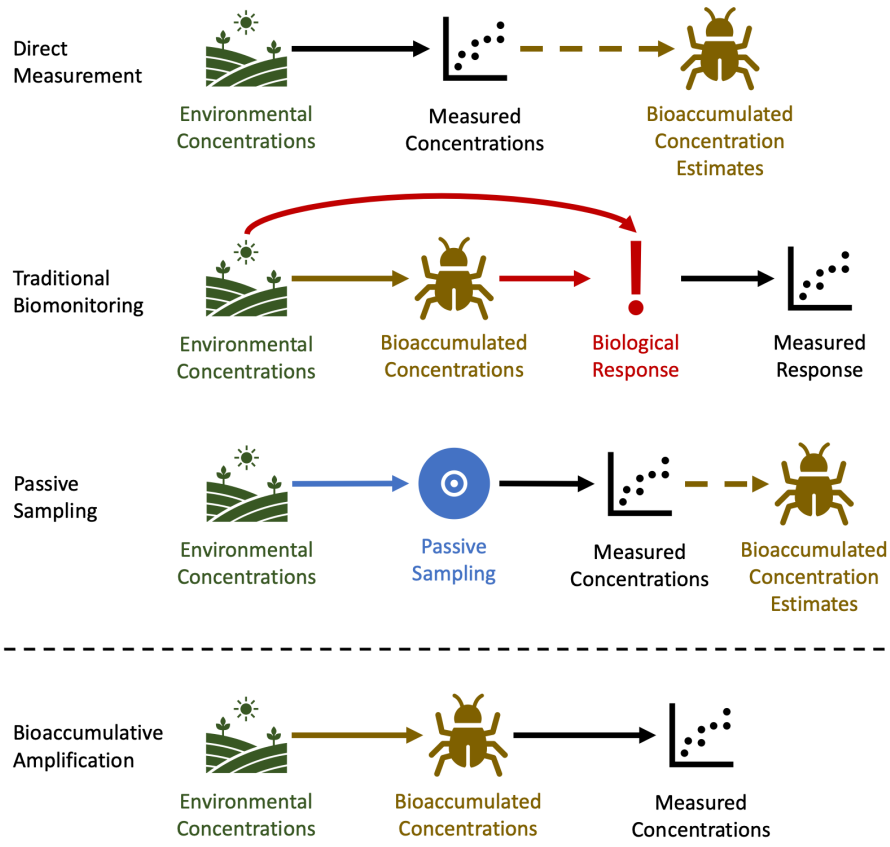


Figure 4: Comparison of existing techniques for the quantification of environmental contaminants. Direct measurement can be costly for some analysis types, and relies on post-hoc estimation of ecological impact from environmental concentrations. Traditional biomonitoring assumes that a biological response acts as an effective proxy for environmental presence and/or impact of a contaminant. Passive sampling improves upon direct measurement by selectively amplifying target analytes, but suffers from the additional drawbacks of fouling and selectivity. This thesis proposes that bioaccumulative amplification offers many advantages over these established methods.

Furthermore, one could imagine that direct sampling of a freshwater system is analogous to taking a photograph. The analysis performed offers a result that is correct only at the moment of sampling, and unless sampling and analysis is carried out repeatedly, and, better still, in real-time, it gives little in the way of a long-term overview of contaminant load in the system.

The riverbed acts as a sink for many freshwater contaminants (U.S. EPA, 2005). In this way, sampling of the sediment phase, rather than the water phase, could make some headway in overcoming the aforementioned issue of temporal resolution, but requires an additional step of digestion, and this may prove difficult in the case of a gravelly substrate. Complex methods of digestion require the use of *Aqua regia*, or similar, and many commercial labs contracted to perform analysis will refrain from carrying out such efforts.

Determination of Bioavailable Fraction

Direct measurement of environmental concentrations does not answer the question of the ecological risk to freshwater biota, as the bioavailability of contaminants can be influenced by factors including speciation, complexation and environmental conditions. Of more interest to the environmental scientist and ecologist is the bioavailable fraction of contaminants.

This bioavailable fraction of contaminants within the benthic environment is difficult to determine, and highly variable depending on contaminant,

complexation and environmental conditions. By way of illustration, a recent study (Jaiswal & Pandey, 2020) has ascertained a link between the oxygen content of the environment and the associated bioavailability of a series of metal contaminants. The authors found that decreasing DO correlated with increasing concentrations of bioavailable metals at the sediment-water interface. However, the study employed the EDTA single-step extraction method (Ure, 1996), wherein EDTA is employed as a chelating agent to capture metal ions and render them available for analysis. This method equates any extractable metals with environmental bioavailability, and assumes that anything that is not captured by the chelating agent is biologically unavailable. This theory holds only if one applies the simplifying definition of the bioavailable fraction as the pool of contaminants that can potentially be uptaken due to their free state in the environment, rather than the contaminants that are uptaken and accumulated due to their biological compatability.

Efforts have been made to develop a procedure that could allow for estimation of the bioavailable fraction, with several methods most commonly employed including not only the aforementioned EDTA separation, but variations on this method that make use of alternative chelating agents, such as CH_3COOH (B. Liu et al., 2017) or DTPA (J.-X. Wang et al., 2021). It has been suggested that a sequential multi-step extraction method, such as BCR-701 (Pueyo et al., 2001) or that proposed

by Tessier (Tessier et al., 1979), is more accurate and reproducible than a simpler single-step extraction. Recent scholarship has suggested the use of the protease K digestive enzyme as a bioinspired means of determining the bioavailable fraction, with relative success when compared to traditional extraction methods (Rosado et al., 2016).

Despite these, and many more, efforts, there remains a significant gap in the knowledge and a requirement for a simple, accurate means of determining the reality of the ecological risk that freshwater contaminants pose. These extraction methods, while straightforward and low-cost, rely on the assumption that unbound metals in the environment are analogous to bioavailable metals. Similarly, the use of enzyme-based methods holds only for metals that are accumulated directly *via* the ingestion pathway, and allows no consideration of alternative pathways such as respiration or surface adsorption. Both approaches only tell part of the story, and neither accounts for a possible analyte-selective bioaccumulation process, as will be described in the subsequent chapter.

Traditional Biomonitoring

The straightforward approach of traditional biomonitoring, whether by use of an individual indicator species, or by employing an index-based population assessment, has its advantages; this method is low-cost, requiring little in the way of specialist equipment, it is relatively universal, accounting

for geographical and condition-specific variations in community assemblages, and it requires very little technical knowledge or expertise beyond the ability to carry out a basic sampling procedure and identify key species of interest. Given these advantages, it is often the preferred method for community engagement and citizen science programmes, and can prove useful in the initial assessment of a site.

This approach does, however, suffer from a series of drawbacks. As the species employed in these surveys, or at least those that indicate good water quality, are typically considered "sensitive", seasonal or site variations, however minor, can result in an unexpected alteration of assemblages present at a sampling site. Aspects such as weather or interference with riparian vegetation can introduce uncontrolled bias into the results of a survey. Additionally, while little expert knowledge is required, it should not be taken for granted that species are easy to distinguish from one another, as some species can look very similar to the untrained eye.

The greatest disadvantage associated with the traditional biomonitoring approach is its lack of selectivity. A measure of impact, in this case, is simply an indication of *an* impact; it indicates that something in the system is amiss, but it gives no clue as to what that is. Should a survey result in a positive indication of something wrong within the system, further analysis will be required to determine what it is, and while biomonitoring may be valuable

as an early-warning system, the subsequent actions required to elucidate useful information about the system may take too long.

Passive Sampling

The passive sampling method is a preparation step that assists with direct sampling. A stationary sampler is placed within the environment and allowed to collect contaminants for a set period of time. The sampler is then retrieved and analysed for medium-term average contaminant concentrations. This passive sampling approach offers better temporal scale than instantaneous direct measurement, and better selectivity than traditional biomonitoring, but suffers from two major drawbacks: analyte specificity and fouling.

Passive samplers are developed for specific target analytes, so a monitoring effort is constrained by the range of target analytes catered for. Multiple samplers may be required if there are multiple analytes of interest. Fouling, which is the undesired adherence of micro- and macro-organisms to a surface, occurs when any engineered structure is placed within the aquatic environment for any length of time. Passive samplers are at risk of fouling that may impede their effectiveness, ultimately rendering them useless in the latter stages of long deployments.

Bioaccumulative Amplification

An alternative approach to those described above has been investigated as part of the research described in this thesis. Natural bioaccumulative

processes within organisms offer an opportunity to selectively amplify chemical concentrations before the use of direct analytical quantification. In particular, benthic macroinvertebrates provide an ideal medium for taking advantage of bioaccumulative amplification, as they have been shown to bioaccumulate a wide range of contaminants and are widespread and abundant throughout freshwater systems worldwide.

Bioaccumulation is typically considered the enemy of the ecologist, as it can concentrate environmental contaminants to levels that exceed ecotoxicological limits. This process, however, can greatly assist in the measurement of these contaminants. Bioaccumulation of contaminants by benthic macroinvertebrates has often been reported to result in higher tissue concentrations than in the surrounding sediment (Bryan & Darracott, 1979). It is almost certain to result in higher tissue concentrations than in the surrounding water phase, as sediment concentrations far exceed water concentrations. It follows that analysis of the post-bioaccumulation concentrations found in aquatic fauna can, through amplification of environmental concentrations, relax effective limits of detection (LODs), allowing for the quantification of contaminants that might otherwise fail to be detected in the water (Phillips, 1977).

This approach has similarities to the passive sampling approach, as it consists of an *in-situ* preparation stage that increases the measured analyte concentration and increases the temporal window of analysis.

Bioaccumulation over the lifetime of the organism effectively smooths out any short-term fluctuations or environmental noise, and benthic macroinvertebrates are readily digested by microwave-assisted digestion with the addition of a dilute HNO_3 solution, eliminating the need for complicated digestion procedures.

Both approaches differ in that passive sampling is specific to arbitrary analytes, depending on the construction of the sampler, while bioaccumulative amplification is specific only to those analytes that are more bioavailable. For this reason, there is no loss of yield due to the choice of sampler, and the measured concentrations are accurate depictions of the ecologically-relevant fraction of freshwater contaminants, leading to valuable insights regarding the risks to freshwater biota.

Unlike techniques that aim to isolate the bioavailable fraction from environmental samples, however, the samples produced by bioaccumulative amplification are obtained post-bioaccumulation. Hence, we quantify the actual bioavailable fraction, rather than the result of a simulated bioaccumulation process.

The bioaccumulation process is not hindered by environmental fouling, as benthic biota remove most surface fouling through ecdysis (O'Callaghan & Sullivan, 2020), and does not require the interpretation of biological responses that underpin traditional biomonitoring. Traditional

biomonitoring relies on the qualitative measurement of a biological response that may be triggered by other unknown parameters than the presence of contamination; conversely, concentrations post-bioaccumulative amplification are real-world representations and their analysis produces an accurate, quantitative measurement of ecologically-relevant environmental pollution.

The use of benthic macroinvertebrates as a medium for bioaccumulative amplification offers the distinct advantage of increased contaminant contact over passive samplers, as these samplers are placed in the water phase, while benthic fauna live at the interface of both the overlying water and the more contaminant-rich sediment phase.

Chapter III

Asellus aquaticus as a Biomonitor

Portions of this chapter have been published in:

O'Callaghan, I., Harrison, S. S. C., Fitzpatrick, D., and T. Sullivan
"The freshwater isopod Asellus aquaticus as a model biomonitor of environmental pollution: A review."
Chemosphere 235 (2019): 498-509

Portions of this chapter have been disseminated at:

Environ: 29th Irish Environmental Researchers' Colloquium, Carlow (2019)
SETAC Europe 29th Annual Meeting, Helsinki (2019)
ESA Annual Meeting, Louisville, KY (2019)

The sensitivity and tolerance of a particular species must be considered, as different species have been found to react differently to the presence of pollutants (De Jonge et al., 2008; MacNeil et al., 2002). In particular, the isopod species, *Asellus aquaticus*, has been identified as a potential biomonitor, due to its greater tolerance for metal pollution (Whitehurst, 1991) and its wide range, which has not been greatly affected by human impact (Verovnik et al., 2005).

A. aquaticus (as shown in Figure 5) has been widely studied, and the life history and population distribution of the species is well-documented



Figure 5: The freshwater isopod, Asellus aquaticus, has been proposed as a suitable candidate species for use in biomonitoring programmes due to its abundance, range, position at the base of the aquatic food web and tolerance to various contaminants.

Image source: "Asellus aquaticus" by Stephen J. McWilliam, iNaturalist (CC0 1.0 Universal).

(Adcock, 1979; Sket, 1994; Steel, 1961; Williams, 1962). The species is increasingly employed as a biomonitor of environmental contamination and has been used for more novel, and recently identified, environmental pollutants, ranging from polycyclic aromatic hydrocarbons (PAHs) and endocrine-disrupting compounds, to radionuclide contaminants and tungsten carbide (WC) nanoparticles (De Lange et al., 2006; Ekvall et al., 2018; Fuller et al., 2018; Weltje, 2006).

The majority of studies on *A. aquaticus* to date have focused on metal contamination in freshwaters, the bioaccumulative capabilities of *A. aquaticus* and its effectiveness as a biomonitor. Most studies have focused on a subset of metals, including Cd, Cu, Zn and As, but platinum-group elements (PGEs), such as Pt, Pd and Rh have also been examined due to their prevalence in road runoff, and there has also been some work performed on studying the accumulation of Fe, Hg, Pb and Al in *A. aquaticus* (outlined in Table 1).

A previous review by (Goodyear & McNeill, 1999) summarised reports of the bioaccumulation of Zn, Cu, Pb and Cd in a number of aquatic macroinvertebrates, while a more recent review by (Ruchter et al., 2015) gave an overview of the effects of PGEs and their fate in the environment. This chapter examines the current body of knowledge pertaining to the benthic isopod, *A. aquaticus*, with particular attention to the species' bioaccumulation of metals and possible explanations

Table 1: A selection of studies investigating the interaction between various metal species and Asellus aquaticus.

Reference	Analyte(s) of Interest
Ekvall et al., 2018	W
Van Ginneken et al., 2018	Cu, Cd, Pb
Joachim et al., 2017	Cu
Van Ginneken et al., 2017	Cu, Cd, Pb
Palma et al., 2015	Cr, Cu, Zn, As, Cd, Pb
Van Ginneken et al., 2015	Cu, Cd, Pb
Kaya et al., 2014	Fe, Cu, Zn, Cd, Pb
Hunting et al., 2013	Cu
Haus et al., 2007	Cr, Cu, Zn, Cd, Sb, Pt, Pb
Bouskill et al., 2006	Cu, As
Tulonen et al., 2006	Cr, Cd, Hg, Pb
Akyüz et al., 2001	K, Ca, Mn, Fe, Ni, Cu, Zn, Br, Rb, Sr, Y, Zr, Cd, Cs, Ba, Hg, Pb
Canivet et al., 2001	Cr, As
Moldovan et al., 2001	Rh, Pd, Pt
Elangovan et al., 1999	Al
Rauch and Morrison, 1999	Pt
Van Hattum et al., 1996	Cu, Zn, Cd
Ham et al., 1995	Cd
Sures and Taraschewski, 1995	Cd, Pb
Migliore and de Nicola Giudici, 1990	Cr, Fe, Ni, Cu, Zn, Cd, Hg, Pb
de Nicola Giudici et al., 1988	Cu, Cd
de Nicola Giudici et al., 1987	Cu
Green et al., 1986	Cd
Fraser, 1980	Pb
Fraser et al., 1978	Pb

for its resistance to pollutants, as well as providing evidence for its suitability as a biomonitor of environmental pollution.

The Isopod, *Asellus aquaticus*

Asellus aquaticus is a freshwater isopod. Widely distributed throughout much of Europe, and commonly associated with a temperate climate, it has been recorded as far south as the Mediterranean, and as far north as Scandinavia (Maltby, 1991). The species is primarily associated with the b-mesosaprobic waters of the palearctic, which is an area defined by high concentrations of dissolved oxygen, low oxygen consumption and significant mineralisation of organic materials with end-products such as nitrates (Nicola Giudici et al., 1988). It has been suggested that *A. aquaticus* feeds primarily on decaying vegetation, microscopic algae and small invertebrates, and is known to scrape at the surface of leaves in order to selectively ingest microbial and fungal growth (Graça et al., 1993; Moore, 1975; Rossi & Fano, 1979). Several subspecies have been discovered, including *Asellus aquaticus infernus*, found in Romania, *A. a. cavernicolus*, *A. a. aquaticus* and *A. a. carniolicus*, all found in Slovenia (Sket, 1994; Sworobowicz et al., 2015; Turk S, 1996; Turk-Prevorcnik & Blejec, 1998).

A. aquaticus is abundant across much of its range, and this distribution has rarely been influenced by anthropogenic impacts (Verovnik et al., 2005). It is tolerant to poor water quality and organic pollution (Maltby, 1995). It is,

however, sensitive to sustained high temperatures, which has a negative effect on rates of growth, survival and reproduction (Di Lascio et al., 2011).

There has been some debate about the life cycle of the species, with a number of different breeding periods recorded, namely, winter breeding, summer breeding and year-long breeding. It is suggested that *A. aquaticus* may completely replace two generations in one year, with the first overwintering generation breeding and dying in spring or early summer. The second generation grows, breeds and dies during the summer and is followed by the third generation, which survives the next winter, to again breed in the spring (Chambers, 1977). This would explain why both summer breeding and winter breeding have been observed. It has been suggested that the autumnal reproductive stasis may be explained by the lesser number of daylight hours during that period, and this leads to avoidance of breeding during less favourable, lower temperatures (Økland, 1978). One study noted that the overwintering spring individuals had a faster relative growth rate than the smaller individuals of the second generation (Adcock, 1979).

The size of an adult individual varies greatly over the species' range. Males of the species are generally found to be larger than females (Adams et al., 1985). There has been some suggestion that the size of *A. aquaticus* is related to the environment in which it lives, as individuals from clean water sites tend to be larger than those from polluted sites (Maltby, 1991; Tolba & Holdich, 1981), and, similarly, smaller individuals may be present in locations

with higher temperature readings (Aston & Milner, 1980). A link may be drawn between tolerance of pollutants and the size of the individual (Kiffney & Clements, 1996). It is, therefore, important to take specimen size into account when gathering samples.

Biomonitoring studies including *A. aquaticus* as part of a wider cohort of biomonitor species have been carried out over a wide geographical and temporal range (Bascombe et al., 1988; Cao et al., 1996; Ketelaars & Frantzen, 1995). One such example is the *Gammarus* : *Asellus* (G:A) ratio. The G:A ratio is based on the observation that *Gammarus pulex* and *Asellus aquaticus* frequently appear at the same location, but *G. pulex* is significantly less tolerant to organic pollution than *A. aquaticus*. If *A. aquaticus* is abundant at a site, but *G. pulex* not, the water at that site is thought to be polluted beyond the tolerance limit of *G. pulex* (Whitehurst, 1991). This index offers a simple, quick method of determining the severity of organic pollution in a freshwater system; however, the success of this method is very much dependent on the presence of both species in a river system (MacNeil et al., 2002). It should be noted that the difference in abundance between *G. pulex* and *A. aquaticus* may, alternatively, be due to competition between the two species, and that it may be as a result of this that they generally occur at different zones in a river system (Graça et al., 1994).

Similarly, *A. aquaticus* has been found to be more tolerant than other macroinvertebrate species to various types of pollutants. It was determined

that the species is more tolerant than the amphipod, *Crangonyx pseudogracilis*, to inorganic pollution in all but the case of Al^{3+} and Mn^{2+} (Martin & Holdich, 1986). Another study compared *A. aquaticus* to *Ephoron virgo* and *Chironomus riparius*, and notes that of these three species, only *A. aquaticus* is limited to feeding from the sediment, while *E. virgo* and *C. riparius* can alter between sediment and water feeding (De Lange et al. 2005). This could greatly influence the types of pollutants *A. aquaticus* is exposed to.

Potential Mechanisms

While many studies have investigated the effects of freshwater pollution on *A. aquaticus*, there remains a lack of firm understanding of the theoretical basis behind these results. Here, an overview is provided of the various proposed environmental and biological pathways of metal pollutants. To begin with, the different forms in which pollutants can be present in the vicinity of the isopod are examined, and the manner in which processes in the freshwater environment produce each of these forms. Consideration is given to the proposed mechanisms by which *A. aquaticus* deals with the pollutants it encounters, and the subsequent fate of these pollutants. These mechanisms are initially studied under the single-element assumption, and then the potential interactions between pollutants in the environment, and the manner in which this may impact upon the uptake and sequestering of these pollutants in *A. aquaticus*, are considered. Finally, consideration is given

to other stressors, and the indirect effects pollutants may have upon *A. aquaticus via* these stressors.

Freshwater as a Loose Term

A. aquaticus is unusual among benthic macroinvertebrates, as it has a significant salinity tolerance which may facilitate an extension of its range into brackish conditions (K. Lagerspetz & Mattila, 1961; Lockwood, 1959; Wolff, 1973). This raises the potential for its use as a biomonitor in both freshwater and estuarine systems. However, there is some debate about the mechanics of metal speciation in seawater, as opposed to freshwater. Although salinity is generally thought to influence the speciation of metals in water, one study found little difference for Cu, Pb or Zn between the freshwater and estuarine sections of a river, but there was significant reduction of Fe between the two sections (Hart & Davies, 1981). The oxidation characteristics of Fe have been found to differ in seawater and freshwater, and Fe has been seen to display a different pH dependency in the two water types (Hatje et al., 2003). This is attributed to rates of complexation and rates of oxygenation, rather than salinity. Care must, therefore, be taken not to freely extrapolate freshwater findings to the estuarine situation.

Ultimately, the issue of the interaction of organisms and pollutants in the environment cannot be answered solely through direct analysis of the

environmental contamination. It would appear that two approaches are possible. Firstly, determination of the physicochemical and mechanical processes that the contaminants undergo, as well as the mechanics of bioavailability, would allow for the prediction of the potential threat to aquatic biota from pollution events. However, current understanding is insufficient to accurately predict the eventual speciation and distribution of pollutants in a waterway, partly due to the sheer complexity of the problem. The alternative approach would be to develop a means of assessing the bioavailable concentrations of pollutants. Some form of bioaccumulative biomonitor is ideal for this purpose, as it allows for the determination of pollutants at the point at which they enter the biosphere, in ignorance of the processes that the pollutants have undergone up to this point. In response to this, *A. aquaticus* has been the subject of various studies investigating the species' response to a variety of priority pollutants.

Isolated Pollutant Uptake, Sequestration & Excretion

Presently, one must consider the proposed mechanisms of metal uptake in the context of isolated metal pollutants. Three potential pathways have been proposed for this sequestering of metals: ingestion (*via* the sediment), respiration (*via* the overlying and interstitial water) and surface adsorption (*via* both the water and sediment).

It is generally accepted that metals settle and accumulate in riverbed sediment, which leaves benthic organisms particularly exposed, and it is plausible that the uptake of metals by *A. aquaticus* could occur by way of an ingestion mechanism. Several authors suggest this pathway, based on measured high concentrations of PGE in the sediment, and trace concentrations in the water (Moldovan et al., 2001; Rauch & Morrison, 1999), and other studies also generally recognise ingestion as a likely route of metal uptake (Santoro et al., 2009).

However, one study found that there was a greater accumulation of Al by dead specimens than that of live specimens of *A. aquaticus*, which would seem to be in direct contradiction of the suggestion that the uptake of metals occurs by way of ingestion, and favours the theory of uptake by surface adsorption (Elangovan et al., 1999). Somewhat in keeping with this, water has been identified as the primary route for the uptake of ^{14}C-terbutryn and ^{14}C-benzo[a]pyrene (Richter & Nagel, 2007). Rather interestingly, another study found benzo[a]pyrene to have no observable effect on *A. aquaticus*, and also noted that varying the size of the organic particles made little difference to the uptake (Peeters et al., 2000).

It should be noted, then, that attempting to rule for one uptake mechanism over the other may be misguided, as it is very possible that both mechanisms occur to a significant level, under different conditions. The bioavailability of metals may vary greatly with complexation and concentration. With that in

mind, the rate of uptake will likely differ greatly with each pathway and set of environmental conditions. An interesting parallel may be drawn with findings that dietary uptake of hydrophobic pollutants increases with log K_{OW}, while aqueous uptake decreases with log K_{OW}, where K_{OW} is the octanol-water partition coefficient (Fisk et al., 1998; Qiao et al., 2000).

The mechanism by which bioaccumulation may occur has also been studied, but no solid conclusions have been drawn, due to the inherent difficulties involved in studying internal biological processes. However, two plausible theories emerge.

Metallothionein is linked to a metal capture-and-transport mechanism, and is associated with Zn regulation (Rauch & Morrison, 1999). The exact process by which this operates is unknown, but it is presumed that any binding to other metals involves Zn as an intermediate. Metallothionein has been studied in a range of species, not limited to crustaceans, and it should be noted that it has a high binding affinity for some metals, such as Zn and Cd. One theory suggests that the protein is present in invertebrates to regulate homeostasis of physiological Zn and Cu, and that it is by coincidence that it is also able to effectively regulate Cd (Talbot & Magee, 1978). There is still much debate about the exact mechanism by which metallothionein is able to protect the body against Cd toxicity, but there is consensus that it does (Klaassen et al., 1999).

In addition, it has been suggested that different metals would have different affinities to metallothionein, and would, therefore, differ in their ability to accumulate, or, indeed, the likelihood of accumulating (Berandah et al., 2010). To this end, greater accumulation of Pd and Pt compared to Rh, to which metallothioneins are known to have a lower affinity, has been observed (Moldovan et al., 2001), and an increased uptake rate of Pt (IV) over Pt (II) has been noted (Rauch & Morrison, 1999). Therefore, it would seem that *A. aquaticus*, for one reason or another, may be selectively accumulating metals.[1]

On that note, it is worth specifying that the bioconcentration factor (BCF) between *A. aquaticus* and the sediment has been seen to vary according to pollutant. For instance, one study found that the BCF for Cd and Pb were 0.4 and 0.1, respectively, while that of Pt was found to be in the range of 4.8-28.6, which may suggest that *A. aquaticus* is better suited to the biomonitoring of some pollutants over others (Rauch & Morrison, 1999). Meanwhile, another study calculated the BCF of Pd, Pt and Rh, as 150, 85 and 7, respectively (Moldovan et al., 2001). There is a clear discrepancy, in this case, between the two calculated BCF values for Pt, for which the reason is unclear. There does not appear to have been much consideration for the

[1] It should be noted that transmembrane metal-capturing proteins act as transporters to regulate the entry of metal ions into the cell, and, therefore, metallothionein is not solely responsible for the accumulation of metals.

differing contributions of water and sediment, both of which a benthic macroinvertebrate is in near-constant contact with. Since the sediment and water will likely have different concentrations and uptake mechanisms, this would justify the determination of differing BCF values for each medium. Further investigation is needed in order to solidify our knowledge of the bioconcentration of various pollutants in *A. aquaticus*, and it is of great importance for the evaluation of a biomonitoring system that the various forms of a metal, as well as field conditions are taken into account.

Alternatively, it has been suggested that metals which have not been metabolised may accumulate in the digestive system (Köhler, 2002). In support of this theory, large, globular accumulations of Cu have been found in the hepatopancreas of *A. meridianus* (B. E. Brown, 1977), and such accumulation could very well occur in other species.

It would appear that the accumulation of metals often occurs in the exoskeleton of invertebrates, or in the soft tissue directly beneath the exoskeleton. It has been suggested that accumulation of metals in *A. aquaticus* occurs through the formation of Type B granules in S-type cells (Hare, 1992). One study found metal concentrations in a moulted carapace to be higher than total body concentrations by a factor of 22 (Rauch & Morrison, 1999). Moulting of the carapace would likely remove these harmful chemicals from the body, acting as an effective means of depurating

harmful toxins; a study of the moulting habits and bioaccumulation sites in less-tolerant invertebrate species should, therefore, show some difference.

In contrast, it has been suggested that *A. aquaticus* may consume its shed cuticle (Elangovan et al., 1999), which would result in re-accumulation of the metals. A decrease in moulting frequency has been observed in the presence of bisphenol A (BPA) (Plahuta et al., 2015), and again in the presence of domestic wastewater samples (Plahuta et al., 2017), potentially due to endocrine disruption, which may also occur in heightened metal concentrations (Georgescu et al., 2011).

In one study, a number of static toxicity tests were carried out for the tolerance of *A. aquaticus* to various metal species, and it was found that the species was highly sensitive, although in varying degrees, to all metals tested (Migliore & Nicola Giudici, 1990). Similarly, although not in keeping with the majority of the current body of literature on the subject, one study found *A. aquaticus* to be highly sensitive to Cu, and that the species is among the most sensitive macroinvertebrates to Cu to be studied as of yet (Nicola Giudici et al., 1987). Further investigation is recommended.

Stable or radioisotope tracing could prove very useful in determining the ultimate fate of metals in the body of *A. aquaticus*. This would consist of labelling metals to render them detectable, and feeding them into the system *via* the suggested potential pathways. Making use of this method to

determine the pathway through which uptake of Cd occurs in an isopod, one study found the Cd uptake to primarily occur through the water, and, therefore, suggested that increasing the metal partitioning to the sediment would result in a decreased bioaccumulation of Cd in the specimen (Eimers et al., 2002). Interestingly, it has been hypothesised that tolerance to Cd in *A. aquaticus* may occur if embryos are exposed to sub-lethal concentrations, prompting the tissues to develop necessary metal-binding proteins in order to overcome future Cd toxicity (Green et al., 1986).

Synergistic & Antagonistic Effects

The majority of studies of metal pollutants have thus far focused on single metals and, as a result, have oversimplified potentially complex interactions between two or more metal species (Boyd, 2010). Consideration must be given to a scenario where a mixture of metals is present in the environment. There is much scope for further study in this area, as the examination of individual pollutants in isolation is not sufficient to offer insight into the mechanics of a real-world pollution event. One point that has been widely debated is the identification of whether a combination of metals has antagonistic or synergistic effects. This has previously been referred to as "additive", "more-than-additive" or "less-than-additive" (Pagenkopf, 1983), but for the purposes of this review, the more common terms of

"antagonistic" and "synergistic" have been adhered to describe to relationship between metals.

Antagonistic interactions may occur when two or more metals have similar properties, and compete for priority binding. This most readily occurs in the case of protein binding sites. While the sites selectively favour an element over others, it can occur that more than one element will fit the criteria for binding to a specific site. For example, one study predicted that Cd and Pb both compete for Ca^{2+} binding sites, so one would expect to see that those species will have antagonistic interactions (Van Ginneken et al., 2015).

With that in mind, there are a number of properties that may give an indication of the likelihood of correctly predicting which metal in a mixture is most likely to bioaccumulate, such as the co-ordination number (CN) of the metal, or the co-ordination geometry. Other factors include the valence state and ionic radius of the metal, as well as the charge and polarisability of the ligand. All of these factors influence the potential mechanism, and a thorough examination of the nature of the metal species may help to determine the effects of each species in a mixture. However, as of yet, we do not have a complete understanding of the process by which metallothionein selects the required metal.

That said, some exploratory work has been carried out into the accumulation of metal mixtures by *A. aquaticus*. It is apparent that Zn^{2+} is predisposed to

competition from Cu^{2+}. Also noteworthy from one paper is the authors' statement that a comprehensive understanding of the competition between biologically-necessary metals and toxic metal species is lacking (Dudev & Lim, 2013). The authors suggest that further investigation is needed in the following areas:

a) factors controlling the kinetics of the metal exchange in protein binding sites;

b) the effects of ionic strength on the process and selectivity;

c) the biological role of various metal ions;

d) thorough studies of the factors influencing selectivity of anionic binding sites.

Other factors may influence the interactions between metals. It has been tentatively established that there is a strong relationship between pH and metal contaminant entrapment within sediment (Sako et al., 2009), and it has also been suggested that selective metal binding in *A. aquaticus* is potentially linked to increased body water content (Hargeby, 1990), while others argue that it may be due to metabolic potential (Simčič & Brancelj, 2006). Additionally, the intrinsic properties of each of the elements will factor in determining which mechanism is more plausible. While the metal ion will compete with other metallic cations in the environment, certain evolutions

must have taken place to ensure that a specific metal will bind to the protein, as may be required by the creature's body (Dudev & Lim, 2013). This refers to the evolution of the cell, drawing the conclusion that metalloproteins developed selectivity for certain metals due to an abundance of those species in the primordial ocean from which the cell evolved.

One study determined that a significant percentage of interactions between Cd, Cu and Zn, in the freshwater environment, are antagonistic in type. Additionally, the point was emphasised, that where the specimen is exposed to a mixture of contaminants, the outcome is difficult to predict, and models thus far have been somewhat imprecise. The authors of that paper go one step further, and state that current scientific understanding does not yet allow for the possibility of predicting the outcome when multiple contaminants are present, and the best we can hope to achieve is to identify a probable outcome for certain types of cases (Vijver et al., 2011).

However, elucidation of the differences between isolated exposures and complex mixtures has only just begun, and a more complete understanding would be required before the biomonitor is considered suitable for use in a practical setting.

Other Stressors in the Environment

There are many factors, other than the presence of metal pollutants, which could influence the survival and health of *Asellus aquaticus*, many of which

have been investigated in-depth. Most of these parameters are physicochemical in nature, and while it is difficult to consider every possible scenario, it is of the utmost importance that at least some thought is given to natural conditions.

Temperature is one such parameter that has been studied in the context of *A. aquaticus*, and it has been determined that the survival rate of the species is reduced at high temperatures (Ieromina et al., 2014). It has also been found that the survival rate of eggs and embryos is highest at lower temperatures (Holdich & Tolba, 1981). It has been found that the optimal temperature for the embryo development of *A. aquaticus* is in the range of 14.5-18.8°C (Roshchin & Mazelev, 1979). *A. aquaticus* has been observed using defence mechanisms against high temperatures, namely behavioural avoidance reactions by way of increased turnings, or "klinokinesis", induction or increase in production of a heat shock protein associated with an increase in thermal tolerance, and the slower but longer-lasting mechanism of thermal acclimation, associated with CNS and/or endocrine effects (K. Y. Lagerspetz, 2003).

It has been proposed that the Fluctuating-Asymmetry (FA) observed when *A. aquaticus* is subject to temperature-related stress could be employed as a measure of overall environmental stress (Savage & Hogarth, 1999). Although this method would be low-cost, quick and require minimal formal training on the part of the observer, it is not clear if the sample size used in

the aforementioned study was sufficient to definitively draw a parallel between a temperature stressor and FA observed. As it is possible that other stressors may not have been fully accounted for, further investigation would need to be carried out before this method could be accepted as an indicator for general environmental health.

Dissolved oxygen levels are also known to have an influence on the growth of *A. aquaticus* (Maltby, 1995). As one would expect, this has been confirmed by a number of studies, with the observation of impaired growth of the organisms in a low oxygen environment. Growth inhibition is associated with a higher energy requirement for respiration (Ieromina et al., 2014).

On this point, it is necessary to note that other authors have held the assumption that *A. aquaticus* is tolerant of low oxygen conditions (De Smet & Das, 1981), so further investigation is recommended in order to determine the species' limits of tolerance to this parameter.

A change in the pH of a stream can have a detrimental effect on a large number of species. Acidification may also play a part in the health of *A. aquaticus*, as has been outlined in a number of studies. A reduction in the ingestion rate of *A. aquaticus* was seen as acidification increased (Costantini et al., 2005). While it has been found that *A. aquaticus* is affected by acidification, some authors note that the species is more tolerant than other crustacean species, namely *Gammarus pulex*, as well as noting that specimens

from polluted water sites may be more tolerant to acidification than specimens from clean water sites (Naylor et al., 1990).

Despite the general concern about pesticides entering the hydrosphere (Rasmussen et al., 2015), they do not seem to pose a direct threat to *A. aquaticus*. It is unclear by what mechanism the species has developed a tolerance to pesticide pollution, but a number of studies have verified this claim (Bundschuh et al., 2012; Ieromina et al., 2014; Lukančič et al., 2010). Once again, however, the literature is contradictory, as, in a study of various species' sensitivity to an insecticide, it was found that *A. aquaticus* had a tolerance almost as poor as the tested insect species, and was found to be the most sensitive of any crustacean species tested (Finnegan et al., 2018). This again emphasises the need for methodical testing of the species to a range of pollutants, under various conditions, to determine the tolerance.

While most authors believe that pesticides do not appear to harm *A. aquaticus*, the use of fungicides may limit the amount of fungal growth on leaves, thus reducing the availability of food for *A. aquaticus*, and, in turn, having an effect on the growth and reproduction of the species (Feckler et al., 2016; Gardeström et al., 2016).

Another factor to consider is the presence of other organisms in the vicinity of *A. aquaticus*, as interactions with other species may be antagonistic. The species is commonly predated upon by a range of visual predators, which, it

has been suggested, is the driving force behind the evolution of a transparent, or cryptically pigmented, carapace (Hargeby et al., 2005). It is known to be predated on by a number of species, including fish (Dallinger & Kautzky, 1985; Rask & Hiisivuori, 1985), flatworms (Bundschuh et al., 2012; Ham et al., 1995), amphibians (Verrell, 1985), and other crustacean species (Dick et al., 2002). Interestingly, it has been found that *A. aquaticus* is most frequently predated upon by perch at dawn and dusk (Persson, 1983).

There has been some suggestion that the precopulatory mate guarding mechanism of *A. aquaticus* has evolved in response to predation, in order to maximise survival and mating success (Benesh et al., 2007; Verrell, 1985). Furthermore, the fitness and survival of *A. aquaticus* is said to decrease in the presence of *Gammarus pulex*, potentially attributable to the prolonged excretion of amino acids as a chemical avoidance strategy used by *A. aquaticus* following visual or chemical contact with *G. pulex* (Blockwell et al., 1998).

A. aquaticus may also be subject to parasitism, with findings that suggest that juveniles and maturing adults exposed to parasites may have a greater survival rate than adults exposed (Hasu et al., 2006). At least one study has found that the parasite, in this case *Acanthocephalus lucii*, also contained Cd and Pb, although significantly lower than that found in the host (Sures & Taraschewski, 1995).

Use of *Asellus aquaticus* as a Biomonitor

Suitability in Principle

A biomonitor is defined as a species that exhibits a quantitative response to the presence of a pollutant in the environment. An effective biomonitor has the following qualities (Johnson et al., 1993; Usseglio-Polatera et al., 2000):

a) a measurable reaction occurs in the presence of the pollutant of interest;

b) the reaction is relatively easy to measure or observe;

c) it is abundant and widespread;

d) it can tolerate the conditions in which the measurement is to take place;

e) a change occurs in the reaction metric over a wide range of pollutant concentrations;

f) the reaction is insensitive to other factors, or can be calibrated against other factors.

A biomarker is a specific type of qualitative biomonitor that exhibits a binary response, and is, therefore, only useful in determining the presence, but not the concentration, of a pollutant (Ansari et al., 2009; Torre et al., 2002).

One could potentially suggest that many macroinvertebrates may serve as effective biomonitors of freshwater pollution, however, there are several characteristics specific to *A. aquaticus*, including some aspects of the life history of the species, that give the isopod a number of advantages over other macroinvertebrates, identifying it as a particularly suitable candidate.

With its wide geographical range and abundance, *A. aquaticus* has long been of interest to freshwater ecologists, and has frequently been utilised, alongside other macroinvertebrates, as a bioindicator of water quality, as well as in the determination of the way in which a given benthic community may respond to changes in the ecosystem over time, due to pollution (Bascombe et al., 1988; Bergfur et al., 2007; Hunting et al., 2013; Montan es et al., 1995). *A. aquaticus*, as a relatively common macroinvertebrate which can be found in most temperate freshwater systems, has been the subject of a variety of studies of metal toxicity and accumulation for several decades (Canivet et al., 2001; Green et al., 1986; Van Ginneken et al., 2015). Significantly, the organism cannot swim, and often lives quite a localised existence within the sediment of water bodies, which, in that respect, makes it an ideal candidate for spatial biomonitoring (Resh, 2008).

Application in Lab and Field

Although *Asellus aquaticus* has been proposed as a biomonitor in a number of studies, it is worth pointing out that there have been both successful and unsuccessful applications.

Previous studies have examined the use of *A. aquaticus* as a biomonitor for a number of common pollutants. The effect of Cu and As on other reactions (Na^+/K^+-ATPase, metallothionein and thiobarbituric acid reactive substance, or TBARS) has been studied, and an increase in reactivity with regard to the latter two mechanisms when these metals are in the environment was observed, indicating that *A. aquaticus* can be used as a biomarker by examining the effects of these reactions, and therefore the reactivity (Bouskill et al., 2006).

One study, however, should serve as a warning of the potential for complications in applying *A. aquaticus* as a biomonitor (Kaya et al., 2014). No significant differences in Na^+/K^+-ATPase or TBARS were noted in the presence of high levels of metals; however, the authors noted that there was an increase in total glutathione levels, which is indicative of reactive oxygen species production. They suggest that the organisms have adapted to the polluted environment by producing antioxidants to combat the increased oxidative stress. Further studies should be carried out to determine if this could lead to a reduction in bioassay effectiveness over time.

An example of a full-scale biomonitoring project with mixed results has been described, wherein a long-term study with temporal and spatial dimensions involving a number of biomonitor species, including *A. aquaticus*, failed to show statistical trends for any of the species studied. It was suggested that reduced bioavailability of the metals could be at fault (Kolaríkova et al., 2012).

One point that is worth emphasising, and could prove crucial in the implementation of any subsequent biomonitoring programme, is the assumption made in many of these studies that superposition holds, that by studying the effects of each pollutant in isolation, we can predict how a real-world situation, with many different pollutants, will affect the animal.

Firstly, as shown by at least two studies, the biomonitor responds differently when more than one pollutant is present, potentially due to the various pollutants competing for the same binding site (Charles et al., 2014; Van Ginneken et al., 2015). Secondly, complexation may play a role, as there is no reason that a mechanism that would work for a pollutant in isolation should work similarly for grouped elements. This is one of the key points of this chapter - the current way of approaching the problem is too simplistic.

There is a complex relationship between predator stress and stress due to the presence of metal pollutants, in isolation or in a mixture (Van Ginneken et al., 2018). It would appear, then, that a successful biomonitoring

programme would need to take into account the sensitivity of the biomonitor mechanism to various stressors, other than those being measured.

During the design process of a typical biomonitoring programme, the response of the organism, in terms of a measurable quantity, N, is evaluated at multiple concentrations of the pollutant, C_x. These parameters are then used to estimate the conversion function of the model:

$$N = f'(C_x) \tag{1}$$

However, if other pollutants (C_1, C_2, …) and/or other stressors (S_1, S_2, …) are present, and have an effect on the response of the biomonitor, the resulting real-world conversion function is:

$$N = f(C_x, C_1, C_2, \dots, S_1, S_2, \dots) \tag{2}$$

The estimated conversion function is, therefore, only valid under the stressor conditions under which it is evaluated. For this reason, *ex-situ* tests can only ever be considered as a crude approximation of *in-situ* conditions, unless a comprehensive range of factors, other than those of interest, have also been studied (Bloor & Banks, 2006).

For a more robust biomonitor, all factors that could significantly influence the conversion function must be identified and accounted for.

As has been explored above, the mechanism of contaminant accumulation by *A. aquaticus* is likely to be complicated, suggesting that there is a plethora of potential synergistic and/or antagonistic interactions between stressors. Some of these interactions may be unexpected, as is seen in one case where effects on an algal community were attributed to the response of the grazer community to the combination of elevated nutrient levels and a cocktail of metal contaminants (Breitburg et al., 1999).

It is likely that any specimens used for a biomonitoring programme would be more suitable if they were bred for the purpose, and placed *in-situ*, as this would ensure all specimens are of a similar age, and would help to avoid the inclusion of individuals which may have been exposed for a longer period, thus skewing the results. A study that examined the use of juvenile brown trout as potential biomonitors of metal pollution in freshwater backs up this argument, stating that it is useful to standardise the breeding of the organisms to a certain timeframe, as the accumulated pollutants would then clearly correspond to the contamination within that time period (Lamas et al., 2007).

When considering the use of *A. aquaticus* as a biomonitor, it should be noted that juvenile individuals bred from specimens which were subject to sub-lethal doses of pollutants have been found to be less sensitive than the parent generation (Nicola Giudici et al., 1986). There is some suggestion that this developed resistance has a genetic basis, but this point has been challenged

by one study, which determined that long-term isolation of a population had little effect, when compared to other populations, on the tolerance level that *A. aquaticus* had to Cd (Pascoe & Carroll, 2004).

Further incentive for the use of macroinvertebrates as part of a biomonitoring programme is that they are predated upon, and by way of this, the pollutants that have been bioaccumulated may enter into the food chain (Croteau et al., 2005; Griboff et al., 2018; Lau et al., 1998; Watras et al., 1998). It has been found that fish which feed on macroinvertebrates have a higher concentration of Cd and Zn, than piscivorous species (Amundsen et al., 1997).

The use of a species as a biomonitor is never clear-cut, as there is always debate about various properties and characteristics. For example, one paper makes the point that the most persistent compounds will be most abundant in the tissues of older organisms (Lamas et al., 2007). While this certainly makes sense in terms of bioaccumulation over a lifetime, another paper directly contradicts this statement by suggesting metal concentrations are lower in older specimens, as they may excrete the pollutant more efficiently than the juvenile specimens (Amundsen et al., 1997). Both parties make a compelling argument, and perhaps this varies with chosen species, but the point remains that there is never a single "turn-key" biomonitor species that can be used in any given scenario, and a great amount of investigation and

understanding must take place before a programme can be successfully implemented.

Some Observations

This exposition, while by no means exhaustive, has outlined much of the general understanding, thus far, regarding *Asellus aquaticus*, and, more specifically, its use as a biomonitor for metal pollutants in freshwater systems. By way of reviewing the current and past literature pertaining to the subject, a number of points have come to light, and it follows that several areas or topics have much scope for expansion.

Although metals alone pose a threat to the environment, further thought must be given to how these pollutants may be altered or accelerated as a result of other incidental factors in a real-world setting. Further studies on the interactions between metals, and the consequences of such for benthic macroinvertebrates, are greatly needed in order to expand our understanding of the ways by which a mixture of metals may impact upon biota.

Our understanding of uptake, sequestering and excretion of metals by *A. aquaticus* is minimal, and any amount of further investigation in this area would greatly improve the current state of knowledge. Even better would be expansion of the body of data pertaining to field samples, and the uptake of metals outside of a laboratory setting.

The *Gammarus* : *Asellus* ratio and the observation of Fluctuating-Asymmetry both hold great potential as techniques that could be implemented, perhaps even with a citizen science application, but are sorely in need of further validation in order to cement the theory, as there is significant argument that negates the assumptions put forward by the methods.

It would appear from the literature, that toxicity tests are a good format for the validation of the effects various pollutants have on *A. aquaticus*. However, a great number of common and exotic pollutants have yet to be tested, and there have not been enough replicates of those few that have been carried out. Too much emphasis has been put on a study being the first of its kind, and not nearly enough on replicating and validating existing results. It is only by doing this that a method may actually be rolled out for practical use.

In the case of *Asellus aquaticus*, one could make the argument that while there remains much to be understood about the species, and, in particular, the mechanism by which it sequesters metal pollutants, it has already been determined that the species is remarkably tolerant to poor water conditions and it has been ascertained that it does bioaccumulate metals. These points, as well as the wide geographical range, abundance and fast reproduction rate of the species make it, once some further validation has been successfully

carried out, an ideal candidate for use in a biomonitoring programme for the detection and quantification of metal pollution.

Chapter IV

On Thiophilicity

Portions of this chapter have been published in:

O'Callaghan, I., Fitzpatrick, D., and T. Sullivan
"Thiophilicity is a determinant of bioaccumulation in benthic fauna."
Environmental Pollution 294 (2022): 118641

Portions of this chapter have been disseminated at:

IFSA Annual Scientific Meeting, Dublin (2022)
SETAC Europe 32nd Annual Meeting, Copenhagen (2022)
Environ: 32nd Irish Environmental Researchers' Colloquium, Belfast (2022)

Our understanding of the fate of contaminants in freshwaters is incomplete. While a lot of work has studied the issue, the sheer number of potential conditions in such a complex environmental system makes broadly applicable truths hard to determine. Additionally, the large number of novel, emerging contaminants of concern make it difficult to produce a comprehensive picture of contaminant fate in freshwaters.

One thing that has been more or less ascertained is that contaminant binding to organic matter is a defining process in the aquatic environment. This is particularly true in slow-moving rivers and lakes, where sediment tends to be soft and silty with higher ratios of organic to inorganic matter (Reuter &

Perdue, 1977). The mechanism of metal contaminant binding to organic matter is generally envisaged as the capture of the metal ion by a sulfur-containing compound, which indicates that sulfur plays a key role in the transfer of metals from the water to the sediment phase, and the creation of a contaminant sink in the aquatic environment (Smith et al., 2002).

While the relative importance of this process is generally accepted, the details are largely contaminant specific, with certain classes of contaminant showing relatively little affinity to organic matter. The aforementioned increase in contaminants of concern makes an understanding of these processes difficult to obtain by pure experimentation, and stronger, broadly-applicable theoretical insights are required.

Contaminants not only bind with dead organic matter, but also the flora and fauna present in the environment, posing an important toxicity risk. While the field of environmental science offers little insight into the direct toxicity of contaminants to higher orders, the dominant hypothesis is that the primary detoxification mechanism of most organisms occurs through the action of a class of proteins called metallothionein (MT).

Metallothionein

MT is found, in its various isoforms, in such diverse taxa as fish, molluscs and mammals, and is believed to be ubiquitous across all living things

(Hamilton & Mehrle, 1986; Kojima & Kägi, 1978; Mourgaud et al., 2002; Richards, 1989; Viarengo et al., 1999). It is understood to play a fundamental role in the sequestration and detoxification of internalised metal and metalloid contaminants. This protein is believed to have the ability to distinguish between metabolically desirable and toxic compounds, thus regulating levels of biologically important minerals such as iron and zinc (Dunn et al., 1987; Good & Vasak, 1986; Jacob et al., 1998).

The theorised mechanism by which MT captures and manipulates contaminants is through the use of a series of thiol groups. These compounds contain a sulfur atom at their extremity, which forms a bond with the target metal.

The common theme between the capturing of contaminants by organic matter in the aquatic environment, and by MT within living organisms, is the hypothesised employment of sulfur or sulfur-containing compounds to perform the binding with the contaminant. This commonality would suggest that sequestration of metal and metalloid contaminants in the environment is mediated by its affinity to sulfur.

MT in Macroinvertebrates

Benthic macroinvertebrates have been shown to uptake and accumulate a range of metals from their sedimentary environment (Canivet et al., 2001;

Hare, 1992; Oberholster et al., 2012; Santoro et al., 2009). It is noted that these organisms sequester metals, which may later be made metabolically available, in the case of essential elements (eg. Cu, Fe, Zn), or remain toxically inert (Isani & Carpenè, 2014; Truchet et al., 2020). It is most commonly theorised that this de-mobilisation of metal ions is through a metallothionein (MT)-regulated mechanism (Ngu & Stillman, 2009), although other thiol-mediated processes have also been proposed (Cobbett & Goldsbrough, 2002). While the study of MT, and its various expressions, has determined the viability of this theory, there remain questions about the selectivity of the protein in the case of freshwater benthic fauna and the relative importance of this particular detoxification mechanism (Palmiter, 1998). It has been widely ascertained that MT will enable the bioaccumulation of Cu, Cd, Zn and Ag (Samuel et al., 2021; C. Wang et al., 2018; Yang et al., 2019), and there is some evidence that it can capture Platinum-group elements (Bongers et al., 1988; Moldovan et al., 2001; O'Callaghan et al., 2019; Rauch & Morrison, 1999; Wong & Stillman, 2018), and Pb (Bordon et al., 2018; Yang et al., 2019).

The Thiophilic Scale

In chemical terms, the affinity of an element or compound towards a sulfur atom is termed *thiophilicity* (Moreno-Alcántar et al., 2018; Porath et al., 1985).

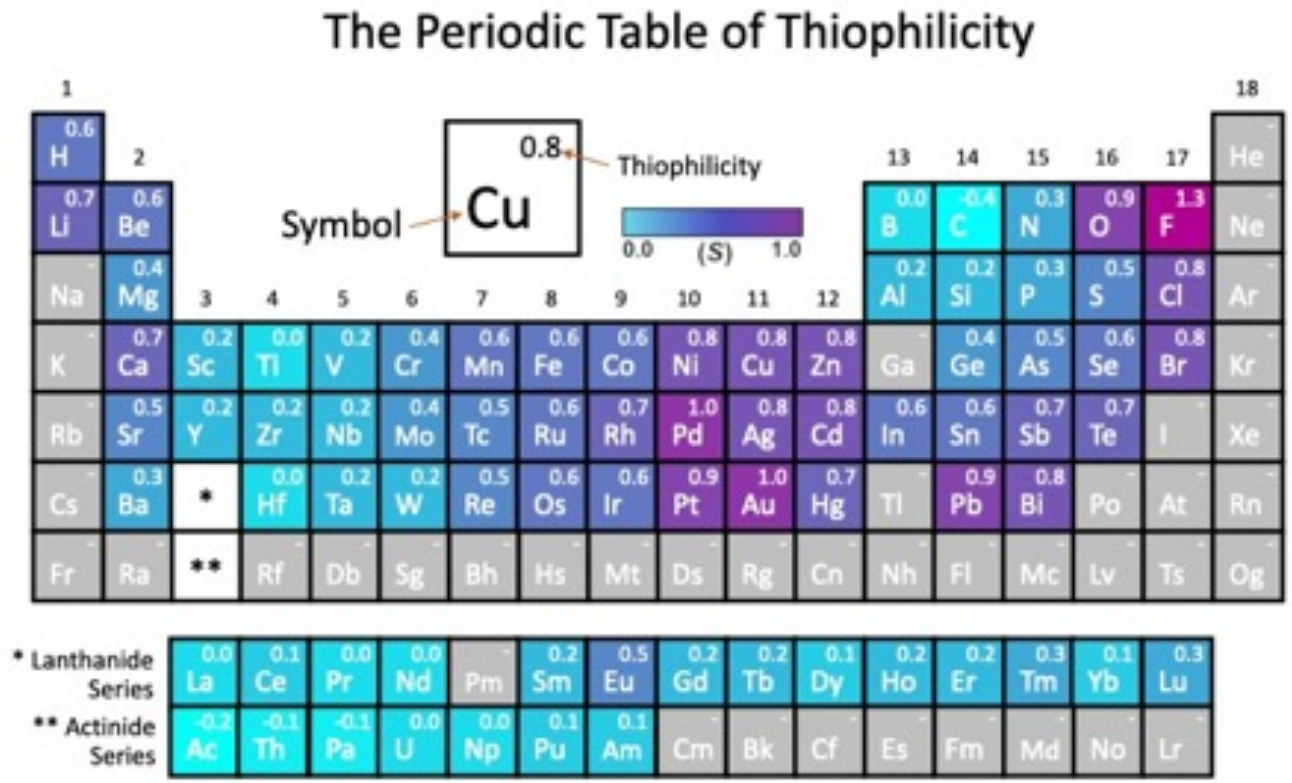


Figure 6: The Periodic Table of Thiophilicity, according to Kepp, 2016. Each element is assigned a value according to their relative affinities to S and O, with higher values denoting a higher affinity to S relative to O. Elements have been colour-coded accordingly.

Recent scholarship has proposed a scale of thiophilicity, that assigns a ranking to the majority of elements according to their relative affinity towards sulfur over oxygen (Kepp, 2016). The Thiophilic Scale (TS) is overlaid on the periodic table in Figure 6.

This scale has been employed in the field of catalysis, but never investigated in an environmental context. However, given the importance assigned to sulfur in these processes, it would seem logical to assume that the scale could give us insights into the behaviour of contaminants in the environment.

The binding of contaminants to organic matter being likely mediated by sulfur, a contaminant with a higher value on the TS should be more likely to undergo this process. Similarly, this contaminant would be more readily sequestered by MT, thus bioaccumulating faster and posing more of a risk of subsequent trophic transfer. Conversely, contaminants which score lower on the TS would be more likely to act in an inert fashion within the aquatic environment.

A disadvantage of the TS in this context is that it is only described for the elemental form. This restriction arises primarily from the lack of authorative data on bond dissociation enthalpies between S/O and arbitrary molecules, as there is nothing preventing the application of this definition of thiophilicity to molecular compounds. Most contaminants entering the environment are molecular in nature; however, it is perceived that the

elemental behaviour could reflect, whether in part or whole, the behaviour of the parent molecule. Thus, the TS should still give us a valuable indication of how the contaminant should behave.

A final observation of this hypothesis is that it suggests where the bioaccumulative amplification approach described previously would be most applicable. If the process of bioaccumulation does depend upon thiol-mediated sequestration by MT, then elements scoring higher on the TS would bioaccumulate more readily, and thus be better amplified by the method.

In this chapter, an argument is presented to support the use of the TS to predict the bioaccumulation rate of differing pollutants. A determination is made of the strength of the correlation between experimentally-derived elemental accumulation across multiple macroinvertebrate taxa, and a meta-analysis is provided of previously-published studies in this context. Ultimately, the results demonstrate that the TS strongly determines the bioaccumulation of metal contaminants in sediment-dwelling organisms.

Materials and Methods

Environmental Sampling

Samples were acquired in the field to ensure that the conclusions of this study are environmentally relevant. In this manner, disagreements regarding

the comparability of lab-based exposures and natural environmental processes (Belzunce-Segarra et al., 2015; Burkhard, 2003; Burkhard et al., 2012; Hare, 1992; Selck et al., 2012; Weisbrod et al., 2009) are conveniently side-stepped.

Sampling was carried out at two sites on the Tramore River (see Figure 7), on the periphery of Cork City, Ireland. All water, sediment and macroinvertebrate samples of *Asellus aquaticus* and *Gammarus sp.* were obtained during the month of July 2021.

Macroinvertebrate samples were obtained through kick-net sampling, using an aquatic net (1 mm mesh size, #175601), purchased from NHBS Ltd. (Devon, UK). Sterile plastic sample bottles (300 mL, NHBS Ltd., #223954) were used to take water and sediment (from the top 1-2 cm) samples, and all samples were transferred to sterile 50 mL Eppendorf tubes (DNA LoBind, #15581312), from Fisher Scientific Ireland Ltd. (Dublin, Ireland), for subsequent ICP analysis. A 50 mL water sample was taken at each site, and sediment was taken from the top 3 cm of the riverbed at each site. Macroinvertebrate specimens were identified and separated in a white plastic tray. A sufficient number of adult specimens were obtained of each macroinvertebrate species in order to ensure that there was enough biomass for analysis.

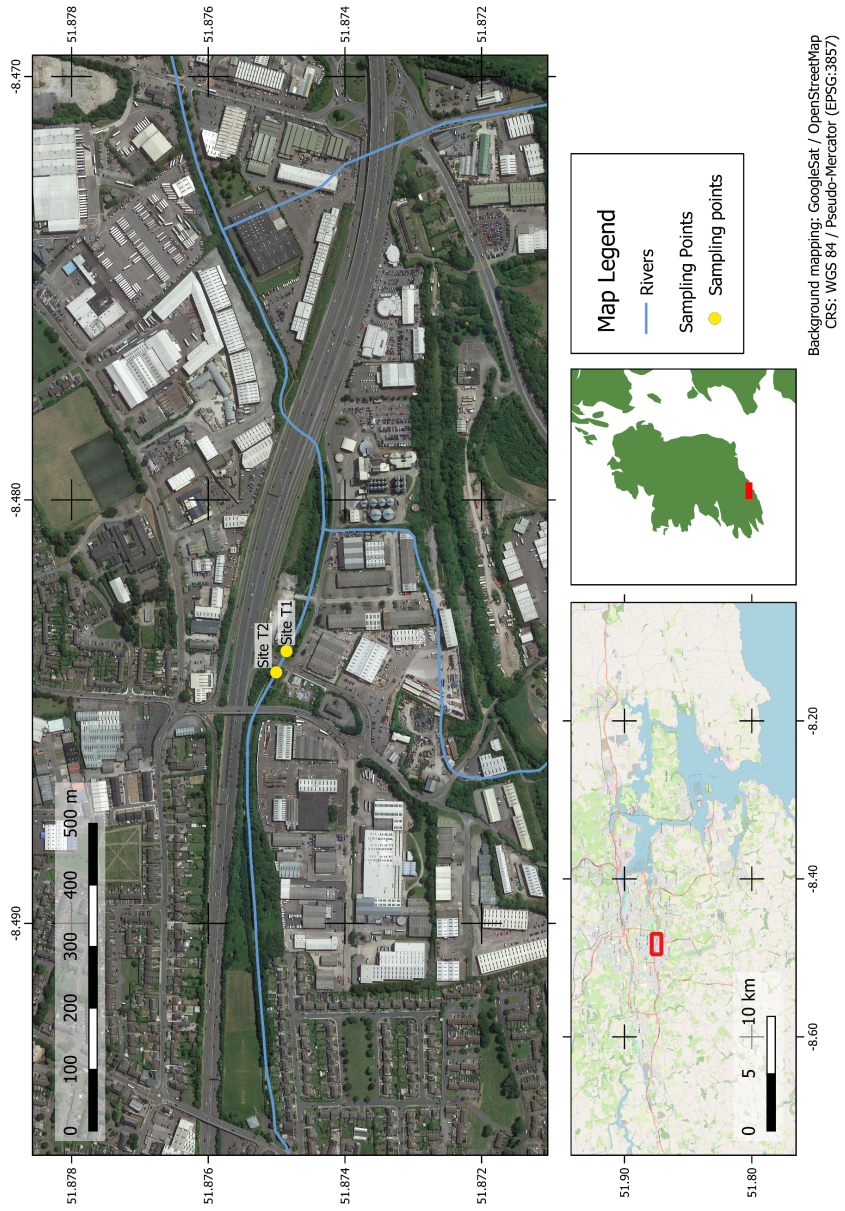


Figure 7: Map of sampling sites (yellow points) for thiophilicity study, located at 51°52'29.5"N, 8°29'00.8"W (T1) and 51°52'30.0"N, 8°29'02.6"W (T2) on the Tramore River (blue line), Cork City, Ireland.

Chemical Analysis

Solid samples (sediment and macroinvertebrate) were dried and approximately 25 mg (dry weight) of each per site were digested with 2 mL conc. HNO_3 and 1 mL HF, then heated to reflux overnight. HF content was subsequently evaporated, and the remaining solutions were diluted to 100 mL with deionised water.

In order to determine the elemental concentrations of Al, Ti, V, Cr, Mn, Fe, Co, Ni, Cu, Zn, As, Pd, Ag, Cd, Sb, W, Pt, Au, Hg and Pb in the samples, analysis was carried out using a PerkinElmer NexION 2000B ICP-MS. External calibration was carried out using serial dilutions from 10 ppm standards. Diluent consisted of a 2% HNO_3 solution, prepared using in-house distilled nitric acid and 18.2 MΩ deionised water. SLRS-6 (riverine water, Canada) was used as a certified reference material, and instrument drift was normalised by spiking laboratory blanks, standards and samples with 1 ppb of Rh, In and Ir.

Determination of Bioaccumulation Factor (BAF)

The bioaccumulation factor (BAF) is a measure of the degree of contaminant accumulation by an organism, normalised to the concentration of the contaminant in an external, environmental compartment. The BAF is typically defined as the ratio of the accumulated contaminant concentration

to the contaminant concentration in the water (DeForest et al., 2007; Mackay et al., 2013); in this work, this definition is denoted BAF_W:

$$\mathrm{BAF}_W = \frac{[\text{organism}]}{[\text{water}]} \tag{3}$$

An alternative definition, denoted BAF_S herein, considers instead the sediment concentration (DeForest et al., 2007):

$$\mathrm{BAF}_S = \frac{[\text{organism}]}{[\text{sediment}]} \tag{4}$$

Contaminant concentrations in the sediment were, in this study, consistently several orders of magnitude larger than water concentrations. Causal mediation analysis of measured water, sediment and accumulated macroinvertebrate concentrations, described below, supported the hypothesis of uptake directly from sediment to macroinvertebrate ($p < .001$), but did not support the hypothesis of uptake directly from water to macroinvertebrate ($p = .106$). For this reason, the BAF_S is employed exclusively in this chapter to quantify accumulation.

Determination of Thiophilicity

The thiophilicity (S) was determined in (Kepp, 2016), using data from (Haynes, 2014), according to the following equations:

$$\Delta D_{\mathrm{OS}}(M) = D_{\mathrm{O}}(M) - D_{\mathrm{S}}(M) \tag{5}$$

$$S(M) = 1 - \frac{\Delta D_{\mathrm{OS}}(M) - \Delta D_{\mathrm{OS}}(\mathrm{Au})}{\Delta D_{\mathrm{OS}}(\mathrm{Hf}) - \Delta D_{\mathrm{OS}}(\mathrm{Au})} \quad (6)$$

where $D_O(M)$ is the bond dissociation enthalpy of a metal-oxygen bond, $D_S(M)$ is the bond dissociation enthalpy of a metal-sulfur bond, and $D_{OS}(M)$ is the difference between these two quantities. Au and Hf were chosen as reference elements to obtain a scale that is mostly contained within the range of 0 to 1, although some exceedances of these limits occur.

Where there is a lack of experimental data to support the application of the equation for a given analyte, the estimated value for the thiophilicity determined in (Kepp, 2016) was employed here.

Statistical Analysis

Data pre-processing was carried out using Excel (Microsoft Corp.), and statistical analysis was carried out using RStudio software. A number of statistical packages were employed, namely mediation, ggplot2 and tidyverse.

Estimation of the relative contributions of direct uptake from water and uptake from sediment was carried out using the mediate function (10,000 simulations with robustSE set to TRUE) (Tingley et al., 2014). Logarithmic regressions were employed to investigate the hypothesis of a correlation between thiophilicity and accumulation, as follows:

$$ln(\mathrm{BAF}_S(M)_i) = \beta_1 S(M) + \beta_0 + \epsilon_i \quad (7)$$

where $BAF_S(M)_i$ is a single measurement datum, β_0 and β_1 are the regression coefficients associated with the relationship between BAF_S and thiophilicity, and ϵ_i is the residual.

Comparative Analysis

Data from a number of previously-published studies, outlined in Table 2, were analyzed in a similar manner to the data presented in the study to verify this phenomenon over a wider range of conditions, taxa and analytical approaches. Data collection was limited to studies that considered multiple analytes and multiple taxa and/or sites. The resulting dataset contains data on over 20 taxonomic orders and 11 elements. Where the data were not presented in numerical form, webplotdigitizer was employed to extract the values from figures (Rohatgi, 2020).

As bioaccumulation factor can be site- and species-specific, these contributions have been accounted for through normalisation. In studies considering species from different orders, BAF_S values were first normalised by taxonomic order. Normalisation of site-specific contributions was then performed using the following multivariate logarithmic regression:

$$\ln(\mathrm{BAF_S}(M)_i) = \sum_{k=2}^{6} \beta_k X_k + \beta_1 S(M) + \beta_0 + \epsilon_i \quad (8)$$

Table 2: Studies considered as part of the meta-analysis. [2]

Reference	Environment	Taxa considered	Analytes considered
Boubonari et al., 2009	Marine	*Alismatales*, *Amphipoda*, *Cardiida*, *Decapoda*, *Littorinimorpha*, *Phyllodocida*, *Ulvales*	Fe, Cu, Zn, Cd, Pb
Culioli et al., 2009	Freshwater	*Coleoptera*, *Ephemeroptera*, *Hygrophila*, *Plecoptera*, *Trichoptera*, *Tricladida*	As, Sb
Erasmus et al., 2020	Freshwater	*Decapoda*, *Diptera*, *Ephemeroptera*, *Haplotaxida*, *Hygrophila*, *Odonata*, *Trichoptera*	Cr, Ni, Cu, Zn, Cd, Pt, Pb
Farag et al., 2007	Freshwater	"Benthic macroinvertebrates"	Cu, Zn, As, Cd, Pb
Levit et al., 2020	Marine	*Amphipoda*, *Bivalvia*, *Gastropoda*, *Hirudinea*, *Oligochaeta*	Mn, Fe, Cu, Zn, Cd, Pb
Pourang, 1996	Freshwater	*Diptera*, *Haplotaxida*, *Mytilida*, *Venerida*	Mn, Cu, Zn, Pb

[2] Where possible, taxa classification is given as the order; however, where taxonomic irregularities or unspecific reporting prevented order-level identification of an order, the closest taxonomic level is given.

where β_0 and β_1 are the regression coefficients associated with the relationship between BAF_S and thiophilicity (S), X_k are dummy variables representing studies 2 through 6, β_k are the corresponding regression coefficients, and ϵ_i is the residual. This allowed for the contribution of thiophilicity to be decoupled from other contributing factors.

Results and Discussion

Correlation Between Thiophilicity and BAF_S

Calculated sediment-associated bioaccumulation factors (BAF_S) for 20 analytes are shown in Table 3. The BAF_S could not be calculated for Pd, Au or Hg due to some concentrations being below the lower limit of detection, and also could not be calculated from *Gammarus sp.* samples for a further 4 elements for the same reason.

These calculated BAF_S values showed a strong correlation (p = .012, R^2 = 0.203) with the position of the element on the TS, as seen in Figure 8. The relationship between BAF_S and the thiophilicity (S) was estimated as:

$$\mathrm{BAF}_S = e^{(2.52 \pm 0.94)\, S - (1.64 \pm 0.61)} \qquad (9)$$

This strong correlation between BAF_S and S points to the predominance of thiol-mediated processes in the sequestration and accumulation of metal contaminants.

Table 3: Determination of bioaccumulation factors from analyzed samples.[3]

		BAF_S	
Analyte	Thiophilicity (*S*)	*A. aquaticus*	*Gammarus sp.*
Al	0.2	0.0731	0.0749
Ti	0.0	0.1266	0.1876
V	0.2	0.1361	*n. d.*
Cr	0.4	0.2101	0.4789
Mn	0.6	0.7023	1.4206
Fe	0.6	0.1879	0.0735
Co	0.6	0.3778	*n. d.*
Ni	0.8	0.4410	0.7631
Cu	0.8	7.6285	11.2537
Zn	0.8	1.9318	2.1328
As	0.5	0.4641	*n. d.*
Pd	1.0	*n. d.*	*n. d.*
Ag	0.8	1.0538	5.5998
Cd	0.8	1.4695	6.7652
Sb	0.7	4.6726	4.9619
W	0.2	3.8723	8.8327
Pt	0.9	1.2910	*n. d.*
Au	1.0	*n. d.*	*n. d.*
Hg	0.7	*n. d.*	*n. d.*
Pb	0.9	0.9788	0.1663

[3] A full listing of the field data used to calculate these values of BAF_S is given in Appendix A.

The relationship was still observed when both species were stratified (*Asellus aquaticus*: $p = .017$, $R^2 = 0.324$; *Gammarus sp.*: $p = .237$, $R^2 = 0.125$), illustrated in Figure 9, with a relatively low *p*-value for *Gammarus sp.* explained by the smaller number of detected elements in samples this species. More interestingly, there was no evidence for differing relationship in BAF_S versus thiophilicity between species, shown by a high p-value and low effect size ($p = .387$, $R^2 = 0.022$), despite each species belonging to a different macroinvertebrate order.

It is known that MT is present in a wide range of flora and fauna, in which it generally performs a metal-scavenging function. Although species-to-species differences could be expected, the uniformity of the relationship between *A. aquaticus* and *Gammarus sp.* suggests that the thiol-mediated uptake mechanisms operate similarly across freshwater crustaceans. Additionally, these results suggest that differences in life history and behaviour have a less important role than the thiol-mediated process in determining the rate of accumulation.

Examination of the adherence of each element to the trend described above showed that Pb, although scoring highly on the thiophilic scale ($S = 0.9$), was not readily accumulated by either *Asellus aquaticus* or *Gammarus sp.* ($BAF_S = 0.979$ and 0.166, respectively, compared to an expected value of 1.875).

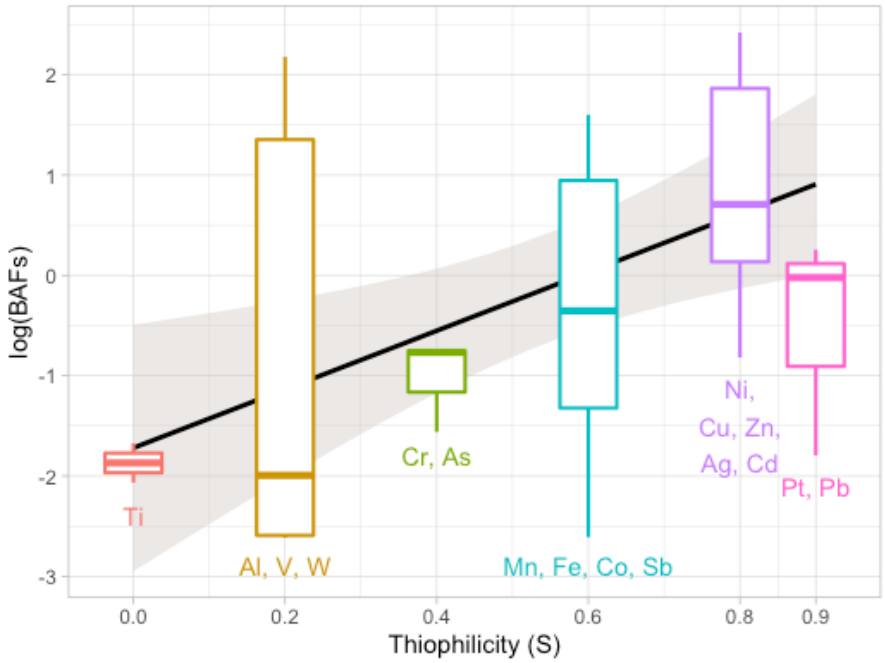


Figure 8: Correlation between position on the TS (S) and sediment-associated bioaccumulation factor (BAF_S). Different values of elemental thiophilicity are represented by horizontal position and colour. With the exception of the elements with S=0.9, S values have been rounded down to the nearest multiple of 0.2 for illustrative clarity, and elements with the same thiophilicity have been amalgamated. Pb has been excluded from the calculation of the trend line (shaded area showing 95% confidence interval; $p = .004$, $R^2 = 0.276$).

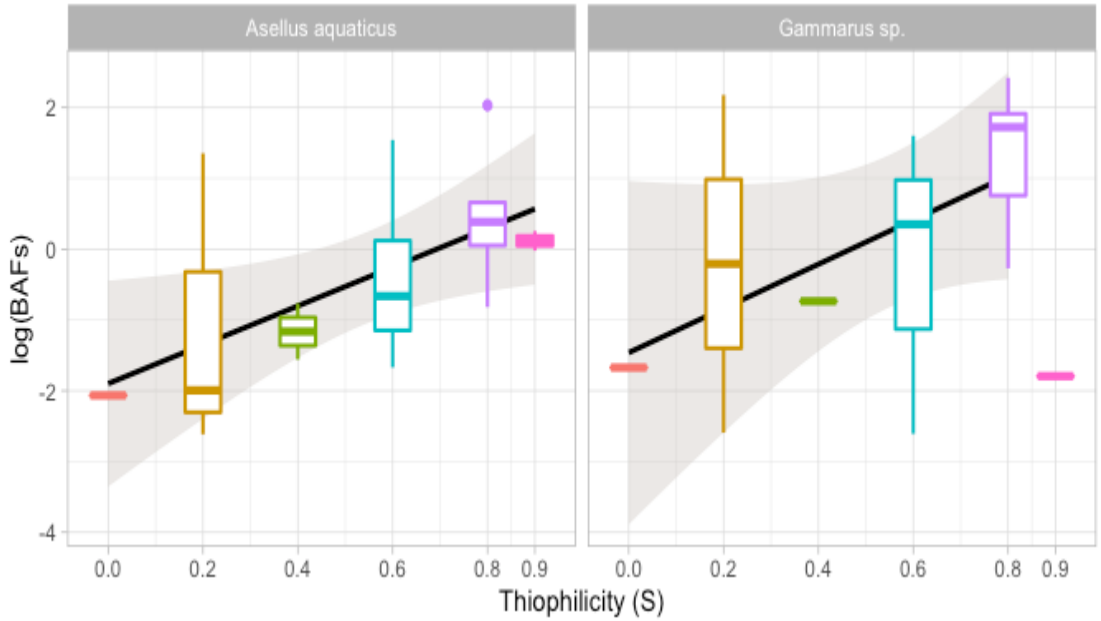


Figure 9: Correlation between position on the TS (S) and sediment-associated bioaccumulation factor (BAF_S), after stratification by species. Different values of elemental thiophilicity are represented by horizontal position and colour. Pb has been excluded from the calculation of the trend line (shaded area showing 95% confidence interval; Asellus aquaticus: $p = .020$, $R^2 = 0.332$; Gammarus sp.: $p = .094$, $R^2 = 0.255$).

Exclusion of Pb from the above analysis showed a stronger contribution of thiophilicity to the accumulation of sediment contamination (p = .004, R^2 = 0.276). This lead-free relationship is given by:

$$BAF_S = e^{(3.03 \pm 0.96)\, S - (1.81 \pm 0.60)} \qquad (10)$$

and is represented by the trend lines in Figures 8 and 9.

Comparison of Previously-Published Works

A meta-analysis was carried out using previously-published data (Boubonari et al., 2009; Culioli et al., 2009; Erasmus et al., 2020; Farag et al., 2007; Levit et al., 2020; Pourang, 1996). The studies considered spanned a wide range of sediment-dwelling taxa with differing life histories, and from both marine and freshwater environments. This aggregated data[4], shown in Figure 10, also showed a lower-than-expected accumulation of Pb with respect to its position on the TS, so this element has been omitted from the following analysis, although it is included in the accompanying figures for completeness.

[4] A full listing of the extracted data used in this meta-analysis is given in Appendix B.

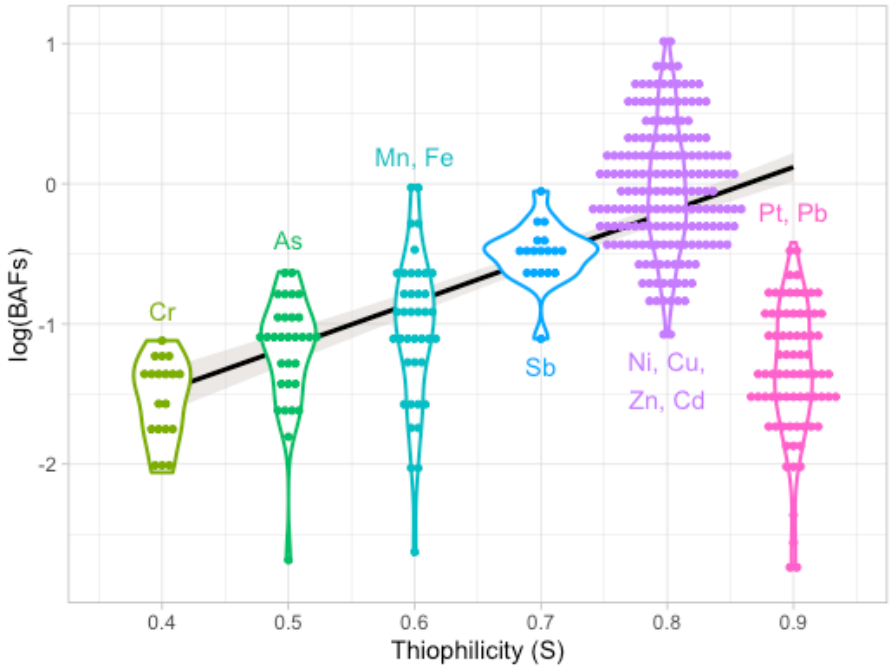


Figure 10: Correlation between position on the TS (S) and sediment-associated bioaccumulation factor (BAF_S), for a range of previously-published studies. Different values of elemental thiophilicity are represented by horizontal position and colour. Each dot represents a single data point, and the outline represents the normalised distribution of BAF_S values. Pb was omitted from the analysis and determination of the trend line (shaded area showing 95% confidence interval; $p < .001$, $R^2 = 0.409$), but is shown here for illustration.

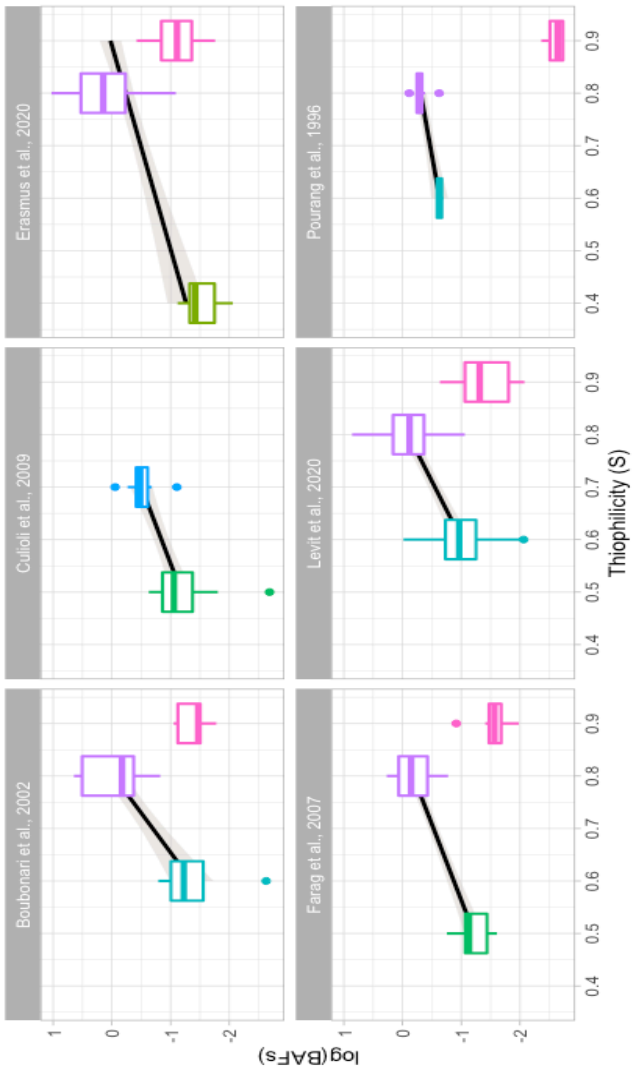


Figure 11: Correlation between position on the TS (S) and sediment-associated bioaccumulation factor (BAF_S) for a range of previously-published studies, after stratification by study. Different values of elemental thiophilicity are represented by horizontal position and colour. Pb was omitted from the analysis and determination of the trend line (shaded area showing 95% confidence interval), but is shown here for illustration. The elements included in each study are listed in Table 2.

Analysis of this data shows a similarly robust relationship between accumulation and proposed thiophilicity ($p < .001$, $R^2 = 0.409$). The estimated relationship between thiophilicity and BAF_S for this agglomerated dataset is:

$$\mathrm{BAF}_S = e^{(3.21 \pm 0.24)\, S - (2.77 \pm 0.21)} \qquad (11)$$

This relationship was found to remain significant for each individual study after stratification (Figure 11). The strength of the effect despite the inclusion of such a diverse range of taxa provides further evidence in favour of the dominance of thiol-mediated accumulation across benthic fauna. It also suggests that differences in uptake (due to, for example, differences in morphology, behaviour and life history) between species is less of a contributor to the total accumulated concentration than is frequently suggested (Cid et al., 2010; Fletcher et al., 2014; Goodyear & McNeill, 1999).

Further Discussion

The strong correlation between bioaccumulation and the thiophilicity of the element, along with the lack of a significant correlation between sediment concentrations and thiophilicity, points to the key role of a metal-sulfur bond in the bioaccumulation process within the macroinvertebrates. This provides strong evidence for the importance of a thiol-based accumulation process, supporting extant hypotheses of MT-ruled detoxification mechanisms.

The analysis presented above assumes that the elemental thiophilicity offers a suitable approximation for the probability of the thiol capturing the metallic component of a molecule. Needless to say, there may be differences between the thiophilicity of a given element and a molecule containing that element; but for the purposes of this work, the simplifying assumption is made that the elemental properties are representative. In an unspecified environment, where there is little certainty about the molecular composition of contaminants present, and where the elemental accumulation is of most concern, this assumption would appear to be justified. In the complex environment of the freshwater benthos, it would be expected that molecule-specific effects average out to produce similar behavior to this elemental approximation.

It is known that the structure and characteristics of MT can vary between species (Amiard et al., 2006; Engel & Brouwer, 1984; Mao et al., 2012; Pedersen et al., 1996), but all rely on the thiol group for the capture of the metal analyte. The consistency of the correlation between thiophilicity and accumulation supports the hypothesis that MT-regulation is a common and equally important detoxification mechanism across species.

While it is notable from the aforementioned results that a similar relationship between thiophilicity and BAF_S is seen across taxa from different orders, it is expected that the nature of this relationship would vary by species. It is likely that some species or higher taxonomic groupings may exhibit specific

effects, such as differing accumulation saturation points, wherein accumulated concentrations reach a horizontal asymptote, or independent differences in accumulation rate. Furthermore, the expression of metallothionein can also differ between species (Beil et al., 2019; Homa et al., 2010; Le Croizier et al., 2018; Pérez-Rafael et al., 2012), resulting in further element-specific effects.

The Special Case of Pb

The results presented in this chapter support the hypothesis that the accumulation of elemental contaminants in benthic fauna correlates significantly with the analyte's position on the TS. However, Pb was not found to follow this trend; despite occupying the highest position on the TS of any element considered in this chapter, the BAF_S of Pb was found to be well below the observed trend. Unfortunately, while a number of metallothionein isoforms have been characterised, the metal-detoxification role of non-mammalian MT remains poorly understood (He et al., 2019; Park et al., 2007; Rocha et al., 2018; Soazig & Marc, 2003; Vergani et al., 2005, 2007), leaving little indication of possible Pb-specific effects. Several hypotheses could be put forward to explain the seemingly inhibited response of the bioaccumulation mechanism to Pb:

- The elemental thiophilicity of Pb may not necessarily relate to the thiophilicities of the dominant compounds in which Pb is found in

the environment. Pb is expected to persist in the environment as a free ion or in a complex such as PbO, $PbSO_4$, PbS, $PbCO_3$, $Pb_3(PO_4)_2$ or as a halide (e.g. PbBrCl). It may also complex to other anions or colloids in the aqueous environment. It is possible that the form in which the element is found in the environment prevents the formation of a thiol bond.

- Species-specific metallothionein may exhibit stereochemistry not conducive to a bond with a large Pb atom. A recent study illustrated an analogous example, where Pb^{2+} showed a strong thiophilic tendency to bind with the S site of methyl thiophosphate over the corresponding O site of methyl phosphate; however, Pb^{2+} also showed an oxophilic tendency to bind with the O site of uridylyl-(5'→3')-[5']-uridylate over the corresponding S site of P-thiouridylyl-(5'→3')-[5']-uridylate. This observation was attributed to the properties of the $6s^2$ lone pair of Pb^{2+}, and its role in the Pb^{2+} coordination sphere (Sigel et al., 2018).

- It is possible that a separate Pb-specific detoxification mechanism exists that causes Pb to be excreted at a rate higher than other elements. A previous study examining the ecdysis of the crab species *Uca pugnax* found Cu and Zn concentrations in the exoskeleton replaced with Pb concentrations from the soft tissue immediately

prior to moulting of the exoskeleton, thus depurating Pb from the body (Bergey & Weis, 2007).

- The TS employs the bond dissociation enthalpy of MS as a proxy for affinity of the thiol to bind with an element. In the case of Pb, this relationship may not necessarily hold.

Thiophilicity Determines Bioaccumulation

This chapter has demonstrated that the TS acts as a suitable predictor of bioaccumulation potential. The correlation between TS and BAF_S is observed across taxa from different orders, in multiple studies addressing both freshwater and marine environments.

In the context of environmental modelling and impact prediction, this observation can inform predictions of bioavailability and the corresponding contribution to toxicological risk of hazardous substances, especially in the case of lesser-studied analytes and in situations where the feasibility of direct measurement is limited. It also strongly suggests the predominant role of thiol-mediated accumulation mechanisms, such as have been reported with metallothionein.

In the context of the bioaccumulative amplification approach, it has previously been stated that this approach selects for contaminants that are more bioavailable. As the TS predicts the bioavailability of contaminants, the

selectivity of this method can be expected to follow the TS, with the exception of Pb as outlined above.

Chapter V

Bioaccumulative Amplification in Practice

Portions of this chapter have been disseminated at:

Environ: 32nd Irish Environmental Researchers' Colloquium, Belfast (2022)

The preceding chapters have discussed the limitations of existing freshwater monitoring approaches, outlined the advantages of the bioaccumulative amplification approach, and demonstrated that the selectivity of this technique to bioavailable contaminants is predicted by the thiophilic scale. This chapter presents a practical application of the method in the field, thus performing an applied evaluation of the method's effectiveness and utility.

Methodology

Field Sampling

Sampling was carried out at sites along the Ballybrack, Riverstick, Owenabue and Garryduff Rivers, all in County Cork, Ireland (Figure 12). Samples of macroinvertebrates, sediment and water were obtained during January 2022.

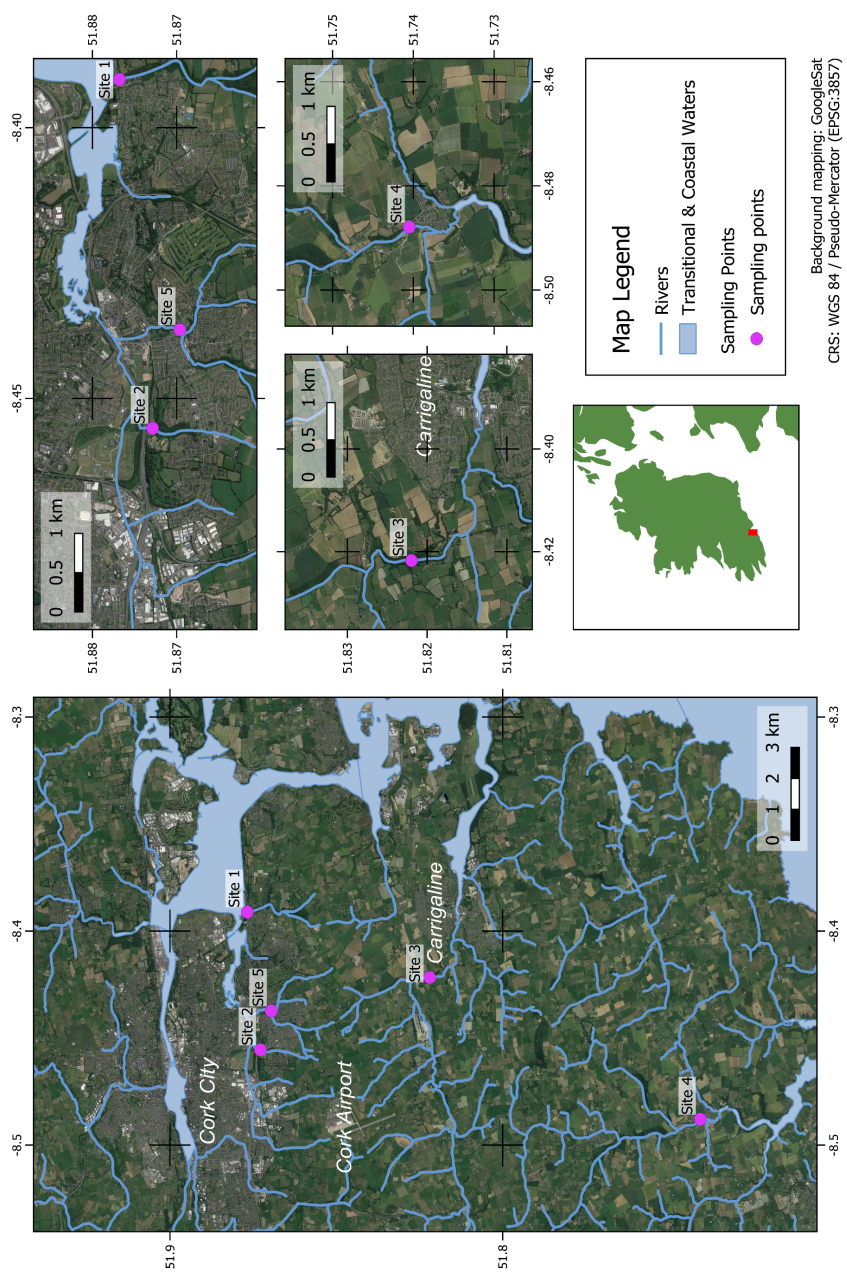


Figure 12: Map of sampling sites, shown as pink points, for field validation study. A range of freshwater sites with differing characteristics were chosen on the Garrydiff (S1: 51°52'36.4"N, 8°23'27.9"W), Tramore (S2: 51°52'22.2"N, 8°27'19.8"W), Owenabue (S3: 51°49'19.1"N, 8°25'18.2"W), Stick (S4: 51°44'25.8"N, 8°29'16.5"W) and Ballybrack (S5: 51°52'10.6"N, 8°26'14.3"W) Rivers.

Macroinvertebrate samples were obtained through kick-net sampling, using an aquatic net (1 mm mesh size, #175601), purchased from NHBS Ltd. (Devon, UK). Specimens were identified and separated in a white plastic tray and placed in sterile 50 mL Eppendorf tubes (DNA LoBind, #15581312), from Fisher Scientific Ireland Ltd. (Dublin, Ireland), for subsequent ICP analysis. Sterile plastic sample bottles (300 mL, NHBS Ltd., #223954) were used to take sediment (from the top 1-2 cm) samples, which were then transferred to sterile 50 mL Eppendorf tubes. Water samples were also taken at each sampling site.

Chemical Analysis

Dried macroinvertebrate and sediment samples were digested in 2 mL conc. HNO_3 and 1 mL HF, heated to reflux overnight. HF content was subsequently evaporated, and the remaining solutions were then diluted to 100 mL with deionised water.

Elemental concentrations of Mg, Ti, Cr, Mn, Co, Ni, Cu, Zn, As, Ba, Fe, Li, Se, Pd, Ag, Cd, Sn, Sb, W, Pt, Au, Hg, Pb and Bi in macroinvertebrate, sediment and water samples were quantified by use of a PerkinElmer NexION 2000B ICP-MS. External calibration was carried out using serial dilutions from 10 ppm standards. Diluent was made up of a 2% HNO_3 solution, prepared using in-house distilled nitric acid and 18.2 MΩ deionised water. SLRS-6 (riverine water, Canada) was used as a certified reference

material, and any instrument drift was normalised by spiking laboratory blanks, standards and samples with 1 ppb of Rh, In and Ir.

Data Analysis

Data pre-processing was carried out using Excel (Microsoft Corp.), and statistical analysis was carried out using RStudio software using ggplot2 for data visualisation.

A logarithmic regression was used to investigate the hypothesis of a correlation between thiophilicity and accumulation, as follows:

$$ln(\mathrm{BAF}_S(M)_i) = \beta_1 S(M) + \beta_0 + \epsilon_i \qquad (12)$$

where $\mathrm{BAF}_S(M)_i$ is a single measurement datum, β_0 and β_1 are the regression coefficients associated with the relationship between BAF_S and thiophilicity, and ϵ_i is the residual.

Results

Bioaccumulation of metallic contaminants was seen across all sampling sites, with most analytes detected in the macroinvertebrate samples. The amplification factor of macroinvertebrate over water matrix concentrations, BAF_W, is shown in Figure 13. The median ratio between measured water and macroinvertebrate concentrations was 31,483, with the majority (59.6%) in

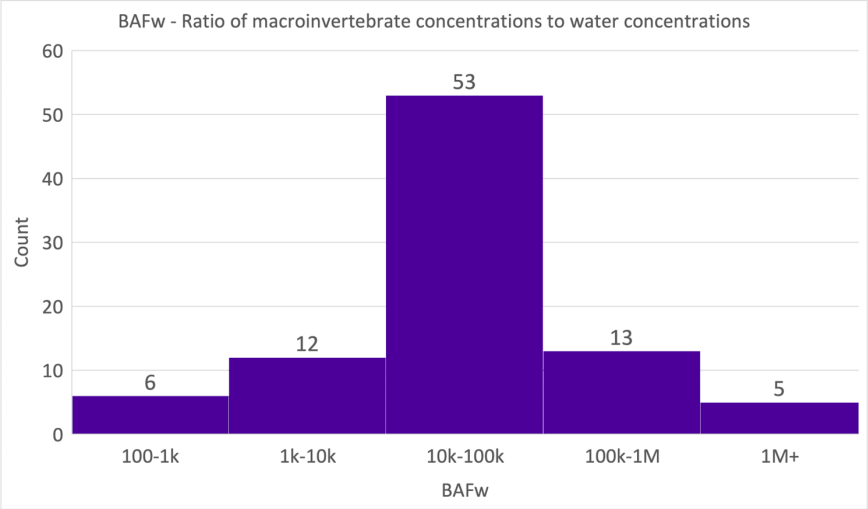


Figure 13: Histogram of BAF_W or accumulation factor from water to benthic macroinvertebrate samples. Most samples exhibted macroinvertebrate matrix concentrations exceeding water matrix concentrations by factors of 10,000-100,000. The observed values approximate a Gaussian distribution.

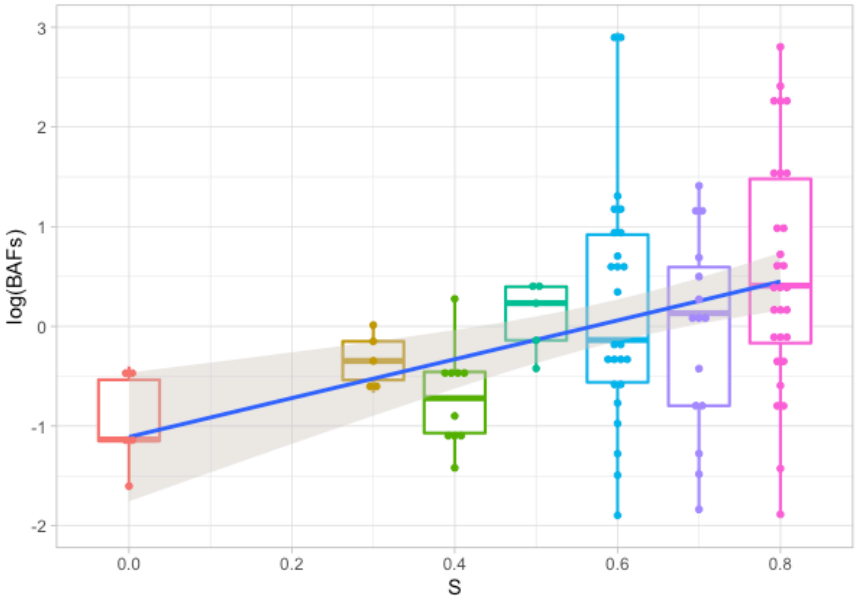


Figure 14: Correlation between position on the thiophilic scale and BAF_S from analysis of field samples (shaded area showing 95% confidence interval; $p < .001$). Different values of elemental thiophilicity are represented by horizontal position and colour.

the range of 10,000-100,000, and 79.8% of macroinvertebrate samples showing an amplification factor in excess of 10,000 over water phase analysis.

BAF_S was calculated for each analyte at each site, and these calculations also show amplification for most samples, with several notable outliers. The calculated elemental BAF_S closely matches the position of the element on the thiophilic scale, as shown in Figure 14.

Site 5 exhibited increased sediment concentrations of Pt, Pd, Ag and Sn over other sites, as demonstrated by Figure 15. Perhaps of greater note, none of these elements were detectable in the water column at any location.

Sites 1 and 2 contained significantly heightened concentrations of Ti, Cr and Fe in both sediment and macroinvertebrate samples (Figure 16).

Discussion

The undetectability of Pt, Pd, Ag and Sn in water samples from site 5, despite their strong concentrations in sediments, illustrates the discrepancy between measured concentrations in water and solid environmental matrices. This discrepancy arises because sediment concentrations, occurring through long-term accumulation processes, offer a long-term average of time-varying inputs into the environment, while concentrations within the water column

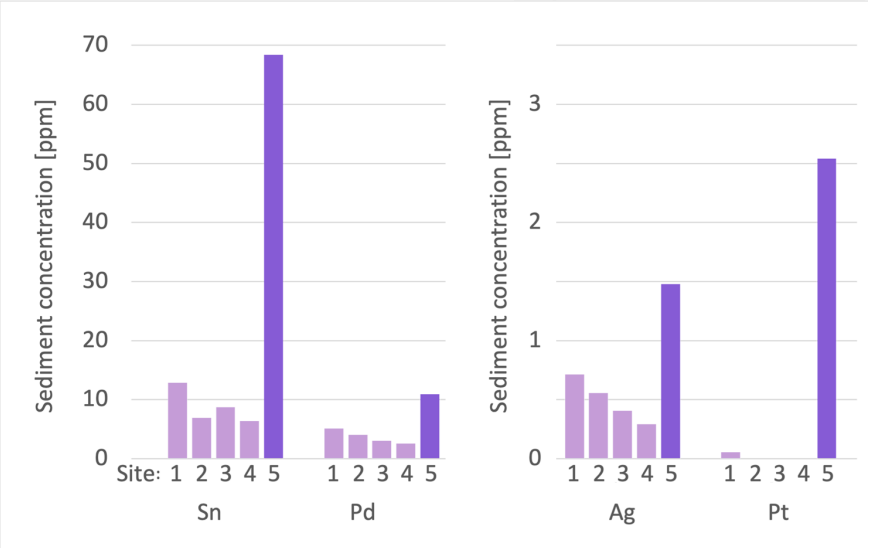


Figure 15: Increased sediment concentrations of Sn, Pd, Ag & Pt were observed at Site 5, compared to other sites. It was noted that Site 5 was located downstream of a garage and active construction site, which may have contributed to heightened concentrations of metals at this site.

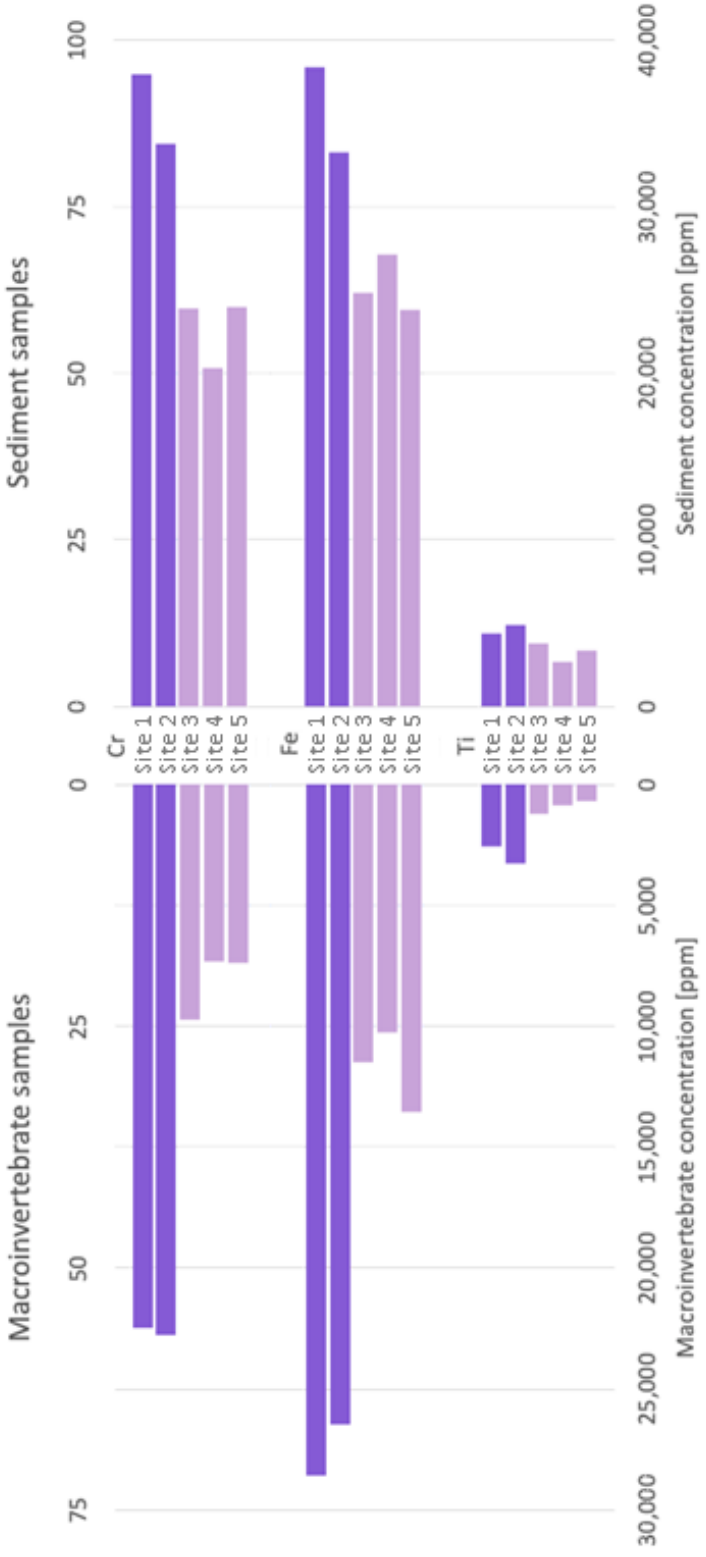


Figure 16: Increased concentrations of Cr, Fe & Ti were observed in both macroinvertebrate and sediment samples from sites 1 & 2. Cr concentrations can be read from the top axis, while Fe and Ti concentrations can be read from the bottom axis. Site 1 was located adjacent to historical mill and railway station sides, while site 2 was located adjacent to a motocross racing circuit.

are more transient. The heightened concentrations of these metals at this site may be explained by the location of a garage and active construction site upstream.

Perhaps somewhat similarly, the increased concentrations of Ti, Cr and Fe at sites 1 and 2 may be attributed to an adjacent a historical mill and railway station sites, and a motocross racing track, respectively, as the presence of these contaminants in the environment is often attributed to tire wear, wear of brake lining and motor oil leakage (Adachi & Tainosho, 2004; Apeagyei et al., 2011; Bian et al., 2015; Wik & Dave, 2009).

Comparison of macroinvertebrate samples to water phase samples show concentrations increased by many orders of magnitude in all sample pairs. These extremely high values of BAF_W once more support the use of the bioaccumulative amplification approach in the quantification of environmental contaminants.

Comparison of sediment and macroinvertebrate concentrations through the measure of BAF_S demonstrated amplification across most, but not all, samples. Once again, it was found that BAF_S was closely linked to the thiophilicity of the element. Outliers noted were Pb, as described previously; W, which is expected to persist in the environment in an insoluble form and adsorb to sediments (Gbaruko & Igwe, 2007); and PGEs, Pt & Pd. Analysis

of the dataset with these outliers removed showed a strongly significant correlation between BAF_S and S ($p < .001$).

It is observed that $S = 0.6$ marks the transition between poorly and strongly bioaccumulated analytes. Table 4 lists the percentage of analyses that showed amplification in the macroinvertebrate samples over the sediment samples for elements in the $S < 0.6$, $S = 0.6$ and $S > 0.6$ categories. These observations support the importance of thiophilicity in the bioaccumulation process identified in Chapter IV and evaluate its employment as a determining tool for field monitoring.

Au was not detected in any of the samples. Pt was only detected in macroinvertebrate and sediment samples at one of the sites, but not in any of the water samples. Additionally, concentrations of Ag, Pd & Sn were below LODs in all water samples, and Cd & W below LODs in water samples from three of the five sites.

The findings of this chapter suggest the utility of a bioaccumulative process in chemical analysis of environmental samples to overcome difficulties in detecting trace quantities of pollutant, supporting the employment of the bioaccumulative amplification approach in the field for the quantification of metallic contaminants in the environment. Macroinvertebrate concentrations far exceeded water phase concentrations, and while the

Table 4: Percentage of field analyses showing amplification of macroinvertebrate concentrations over sediment concentrations, stratified by position on the thiophilic scale (around S=0.6).

Thiophilicity	BAFs > 1	Total	% amplified in macroinvertebrate
S < 0.6	5	25	20%
S = 0.6	12	25	48%
S > 0.6	28	45	62%

accumulative advantage over sediment phase analysis depends on the analyte of interest, the processing and digestion requirements of macroinvertebrate samples are far less onerous than those of sediment samples. This investigation further supports the hypothesis that the thiophilic scale can effectively determine the accumulation potential of metallic compounds in the aquatic environment.

Chapter VI

Laboratory Evaluation of Method

Portions of this chapter have been disseminated at:

SETAC Europe 32nd Annual Meeting, Copenhagen (2022)

The previous chapter's evaluation of the bioaccumulative amplification approach in the field has demonstrated its applicability to the detection and quantification of metals and metalloid compounds in the freshwater environment. There is reason to believe that nanoscale metallic pollutants may behave differently in the benthic environment. A thorough understanding of the uptake and accumulation of metallic nanoparticles by benthic macroinvertebrates requires controlled, laboratory-based assays to evaluate the nano-specific properties of these analytes, and how they may operate in the aquatic environment.

There is little available data on this topic within the body of current published literature. The majority of studies that purport to examine these contaminants focus on a restricted subset of organisms, and do not account for unique conditions found within the hydrosphere (Batley et al., 2012; Farré et al., 2009, 2011; Gottschalk et al., 2010; Gottschalk & Nowack,

2011). Most discussion surrounds the direct toxicity of nanoparticles; mortality is typically the only notable endpoint, and the possibility of accumulation is rarely considered.

Further to this, there is no consensus as to how the metallic nanoparticle operates in the freshwater environment. There are two primary hypotheses in the literature: that the particle has a set of nano-specific properties that result in a unique behaviour pattern, and that the particle leaches metal ions, and these ions operate in much the same way that the equivalent bulk metal does. These theories have been discussed in Chapter II.

This chapter aims to experimentally investigate the bioaccumulation of metallic nanoparticles by *Asellus aquaticus*. It considers a situation where macroinvertebrates are exposed to a solution containing metallic nanoparticles, and possibly bioaccumulate the particles, or related ion leachate, as in the case of a solution of bulk metal salts. A number of dimensions are explored, with an aim to answering the following research questions:

- Is there a distinction between the bioaccumulation of bulk metal salts compared to analogous metallic nanoparticles? A nanospecific response would indicate a nanospecific mechanism, while equivalent responses to bulk salts and nanoparticles would favour the ion leachate hypothesis.

- In compounds containing different metal ion species, are synergistic or antagonistic effects observed in the parallel uptake of both species? Or are both metal ion species accumulated equally?

- Does the thiophilic scale apply to nanoparticles?

The study described in this chapter aims to address these research questions, thus providing insight into mechanisms dictating bioaccumulation of metallic nanoparticles in the freshwater environment.

Methodology

Experimental Set-up

Specimens were obtained from a site on the Tramore River (51°52'29.6"N, 8°29'01.3"W), on the periphery of Cork City, Ireland. Samples of *Asellus aquaticus* were obtained between the months of July and November 2021, inclusive.

Macroinvertebrate samples were obtained through kick-net sampling, using an aquatic net (1 mm mesh size, #175601), purchased from NHBS Ltd. (Devon, UK). Specimens were identified and separated in a white plastic tray and transported back to the lab in sterile plastic sample bottles (300 mL, NHBS Ltd., #223954) containing river water. All specimens were depurated in deionised water for 48 hours prior to exposure.

Exposure analytes of WC nanopowder (nWC) (hexagonal, 150-200 nm, Sigma Aldrich Ltd., #778346), TiO_2 nanopowder ($nTiO_2$) (mixture of rutile and anatase, <100 nm, Sigma Aldrich Ltd., #634662), bulk TiO_2 salts ($bTiO_2$) (rutile, <5 μm, Sigma Aldrich Ltd., #224227) and $BaTiO_3$ nanopowder ($nBaTiO_3$) (cubic, <100 nm, Sigma Aldrich Ltd., #467634) were suspended in deionised water and vortexed for 2 minutes, before the suspension was serially diluted to produce the exposure media. This media was placed in a series of 5 L sterile plastic tanks, with each tank containing exposure concentrations in the range of 0, 0.1, 0.5, 1 and 5 ppm. A minimum of seven adult *Asellus aquaticus* specimens were placed in each tank and allowed to accumulate the exposure analyte for two weeks.

Specimens from each assay were frozen once the two-week exposure time had come to an end, and all specimens thawed and dried once all assays had come to an end.

Physical Characterisation of Analytes

Exposure $bTiO_2$, $nTiO_2$ and $nBaTiO_3$ analytes described above were imaged under scanning electron microscope (SEM) to verify general size and morphology.

Chemical Analysis

Dried macroinvertebrate specimens were digested with 2 mL conc. HNO_3 and 1 mL HF, before being heated to reflux overnight. HF content was subsequently evaporated, and the remaining solutions were diluted to 100 mL with deionised water.

Elemental concentrations of Ti, Ba and W in both the macroinvertebrate samples and exposure solutions were determined using a PerkinElmer NexION 2000B ICP-MS. External calibration was carried out with serial dilutions from 10 ppm standards. Diluent consisted of a 2% HNO_3 solution, prepared using in-house distilled nitric acid and 18.2 MΩ deionised water. SLRS-6 (riverine water, Canada) was used as a certified reference material, and instrument drift was normalised by spiking laboratory blanks, standards and samples with 1 ppb of Rh, In and Ir.

Data Analysis

Data analysis was carried out in RStudio software and Microsoft Excel.

The significances of exposure concentration and analyte/ion were determined using a multivariate logarithmic regression, with dummy variables for the exposure analyte or ion. The regression equation is as follows:

$$log_{10}(C_{acc}) = \beta_2\, log_{10}(C_{exp}) + \beta_1 D + \beta_0 + \epsilon_i \quad (13)$$

where C_{acc} is the observed accumulated concentration, C_{exp} is the exposure concentration, D is a dummy variable representing the categorical parameter (analyte or metal ion, depending), β_0, β_1 and β_2 are the regression coefficients, and ϵ_i is the residual.

Accumulation curves were constructed according to the Hill equation:

$$C_{acc} = \frac{C_{sat}}{1+\left(\frac{\mathrm{EC}_{50}}{C_{exp}}\right)^{n}} \quad (14)$$

where C_{exp} is the exposure concentration, C_{acc} is the observed accumulated concentration, C_{sat} is the saturation concentration, EC_{50} is the 50% effective concentration (the C_{exp} that results in $C_{acc} = C_{sat}/2$) and n is the Hill coefficient. Estimates of C_{sat}, EC_{50} and n were obtained by minimizing the residuals of C_{acc} using the Excel Solver Add-In with the GRG Nonlinear Engine.

Results

Analyte characterisation

SEM imaging of exposure analytes, shown in Figure 17, demonstrated the generally spherical morphology of the nanoparticles, and the size difference between nano-scale and bulk analytes. Bulk particles were generally of the

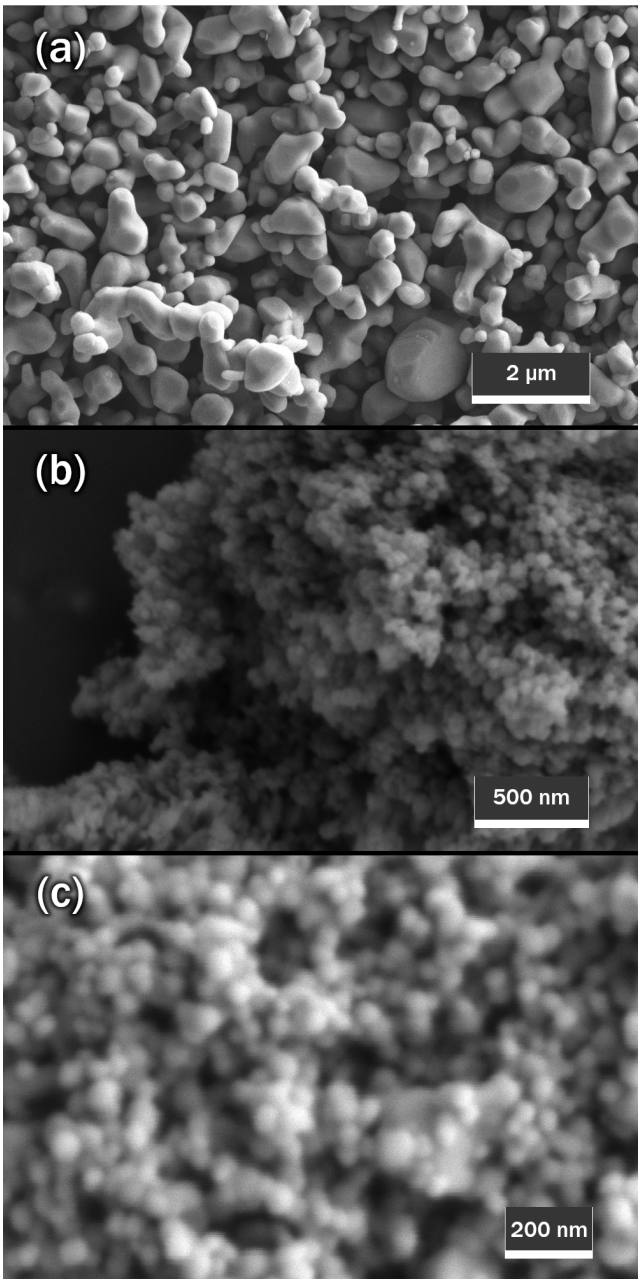


Figure 17: SEM images showing size and morphology of (a) $bTiO_2$, (b) $nTiO_2$, and (c) $nBaTiO_3$ exposure analytes. These images confirm nanoscale sizing of $nTiO_2$ and $nBaTiO_3$, and macroscale sizing of $bTiO_2$, as well as overall spherical geometry.

Table 5: Multivariate logarithmic regression of key relationships in laboratory data. In each example, the accumulated concentration is regressed on two variables, denoted a and b in the table.

Analytes	Ions	Relationship: $\log(C_{\text{acc}}) = f(a, b)$			
		a	p_a (sig.)	b	p_b (sig.)
$bTiO_2$, $nTiO_2$	Ti	$\log(C_{\text{exp}})$	< .001 **(***)**	$nTiO_2$?	< .001 **(***)**
$nTiO_2$, $nBaTiO_3$	Ti+Ba	$\log(C_{\text{exp}})$	< .001 **(***)**	$nBaTiO_3$?	.966
$nBaTiO_3$	Ti, Ba	$\log(C_{\text{exp}})$	.032 **(*)**	Ba?	.008 **(**)**

order of 1 μm in each dimension, while both nanoscale analytes were generally below 50 nm in any dimension. This imaging verifies the physical characterisation provided by the manufacturer.

Toxicity tests

No mortality was observed over the course of the 14 days in any of the assays. Additionally, no immobility or physical responses were apparent at the end of the assay periods. This would suggest that there is no acute or chronic toxicity to the isopod *Asellus aquaticus* at the concentrations tested for timescales up to 2 weeks.

Bioaccumulation assays

All exposure assays resulted in accumulated concentrations within the macroinvertebrate, with saturation of accumulated concentrations occurring in all cases.

Statistical analysis showed a significant relationship between accumulated concentrations and both exposure concentrations and exposure analyte/ion, as outlined in Table 5.

Comparison of corresponding bulk and nanopowder forms of TiO_2, shown in Figure 18, exhibited a significantly higher accumulation rate of the nanoscale form when compared to the physically larger bulk form.

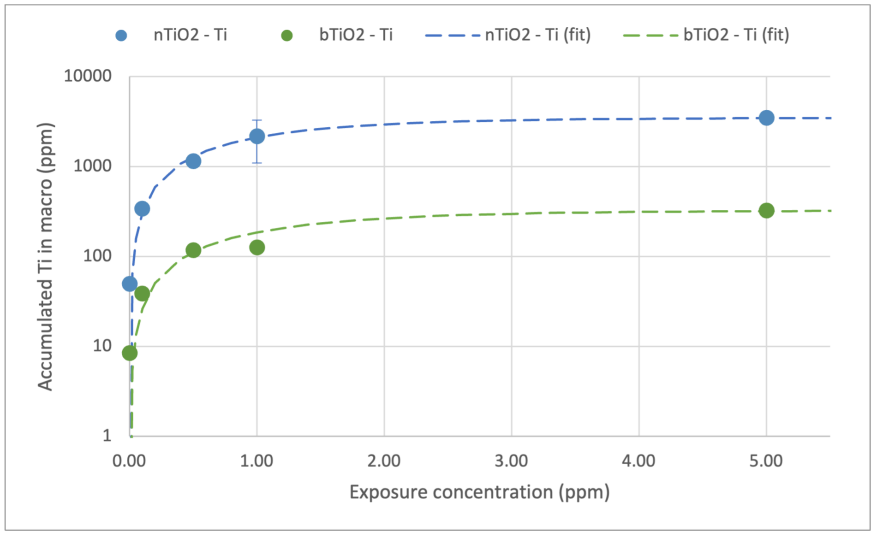


Figure 18: Comparison of bioaccumulated Ti from exposure of Asellus aquaticus to TiO_2 in nanopowder ($nTiO_2$, blue) and bulk powder ($bTiO_2$, green) forms. It was observed that the nanoscale form was more readily bioaccumulated than the bulk form.

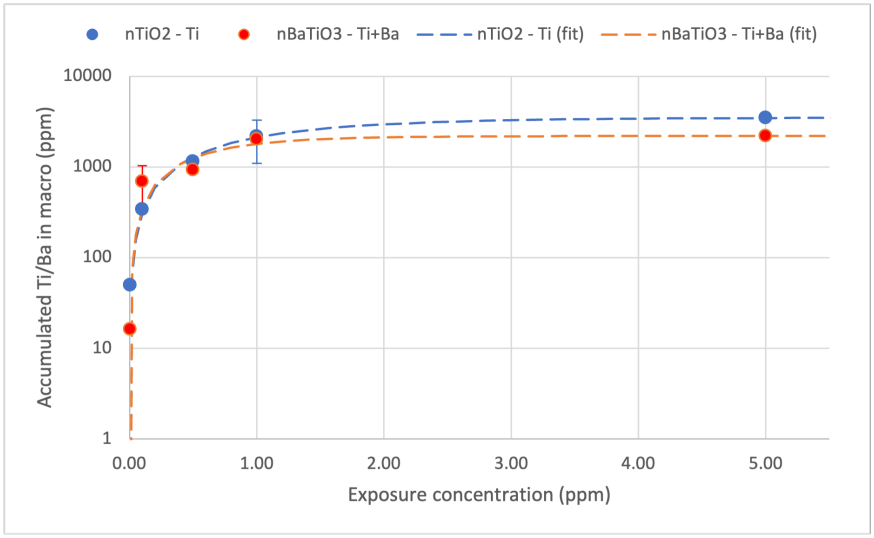


Figure 19: Comparison of bioaccumulated Ti from nanopowder TiO_2 ($nTiO_2$, blue) and combined Ba and Ti from nanopowder $BaTiO_3$ ($nBaTiO_3$, red). It was observed that overall ion bioaccumulation from both nanoscale analytes was comparable.

Accumulated concentrations of the analyte from nanoparticulate sources were in the range of an order of magnitude higher than from bulk sources.

Subsequent comparison of metal ion accumulation from nanopowders of TiO_2 and $BaTiO_3$ showed very similar accumulation responses to both analytes, as illustrated by Figure 19. A breakdown of accumulated ion by species, however, demonstrated that the Ba and Ti from $BaTiO_3$ were accumulated unevenly, with approximately 3-4 times more Ba accumulated than Ti across all exposure concentrations, as shown in Figure 20.

While nanopowder TiO_2 and $BaTiO_3$ showed a similar bioaccumulative response, nanopowder WC was accumulated at a greater rate for the same exposure concentrations (Figure 21). Accumulated concentrations of W from nWC were in the range of an order of magnitude higher than those of Ti from $nTiO_2$.

Discussion

Preferential Uptake of Nanomaterials over Bulk Analogues

Results have demonstrated the selective uptake of the nanoparticulate analyte over the analogous bulk form for TiO_2. This offers evidence in favour of the preferential uptake or sequestration of metal ions from the nanoparticulate source. These results do not, however make the distinction

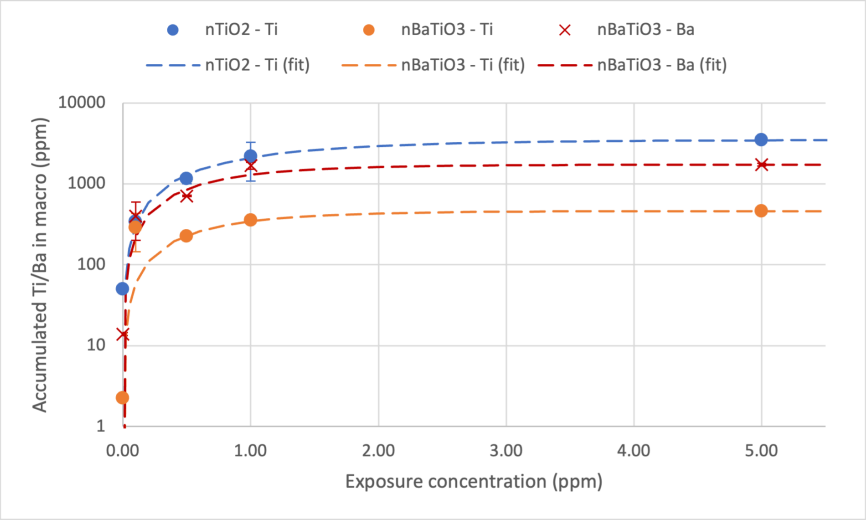


Figure 20: Comparison of bioaccumulated Ti from nanopowder TiO_2 ($nTiO_2$, blue), and Ba (red) & Ti (orange), respectively, from nanopowder $BaTiO_3$ ($nBaTiO_3$). The Ba ionic component was more readily bioaccumulated than the Ti ionic component from $nBaTiO_3$, which was less readily accumulated than that of the $nTiO_2$, despite occurring in identical concentrations.

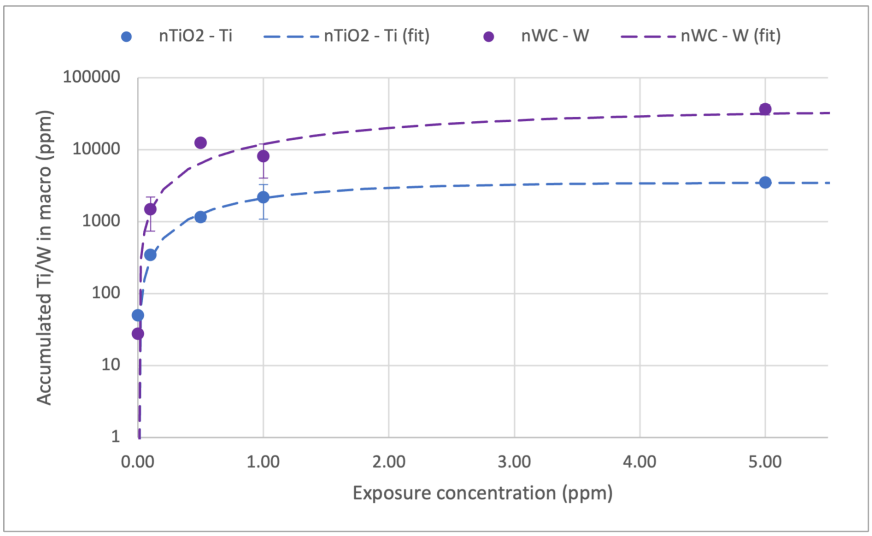


Figure 21: Comparison of bioaccumulated Ti from nanopowder TiO_2 ($nTiO_2$, blue), and W from nanopowder WC (nWC, purple). It was found that the nWC was more readily bioaccumulated than $nTiO_2$.

between mechanisms of uptake and mechanisms of accumulation. They do not, then, purport to make assumptions as to whether the nanoselectivity is at the point of uptake or at the site of contaminant entrapment. That is to say, we cannot garner, from these results alone, whether the nanoparticles are more readily ingested, or whether the bulk analogues are less so.

Heterogenous Accumulation of Polymetallic Ions

It can be seen from the results presented herein that there is a qualitatively similar pattern of accumulation across all analytes, with a similar saturation decay constant observed in all assays. Furthermore, the very similar metal ion accumulation observed in $nTiO_2$ and $nBaTiO_3$ suggests that relatively similar nanoparticle contaminants should be expected to behave similarly, with similar mechanisms of uptake and accumulation.

While the overall accumulation of metal ions from similar nanoparticle species may not appreciably change, intramolecular discrepancies in the uptake of different metal ion species from polymetallic compounds were also observed. The difference between the rates of uptake of the Ba and Ti components of $nBaTiO_3$ points to accumulation of the individual ion species being unequal. The greater accumulation of Ba over Ti, in this case, may be attributed to the greater thiophilicity of Ba (0.3) when compared to Ti (0.0). The fact that the accumulation of Ti from $nTiO_2$ closely matches the accumulation of Ba and Ti combined from $nBaTiO_3$, and not the

accumulation of Ti alone from the latter, suggests that the same endpoint is saturated by both metal ions through thiol-mediated competition between the analytes. This may be described as an antagonistic interaction between the Ba and Ti ions of $nBaTiO_3$, with the thiophilic scale ultimately determining the fate of accumulation.

Elevated Bioaccumulation of Tungsten

The decision to investigate the accumulation of nWC was informed by the unexpectedly high BAF_S found in field samples, as described in Chapter V. At 0.2, W scores low on the thiophilic scale, and therefore a high bioaccumulative potential would not be expected. This prompted further lab evaluation.

Results from these lab-based assays show nWC follows the same qualitative accumulation pattern as other analytes, with a similar saturation decay constant, but the accumulation rate of W from nWC is significantly higher than other test analytes, in agreement with the previously presented field samples. The reason for this is unclear, but one might suggest that the carbonate complex may be influencing the uptake of W, perhaps similar to the increased accumulation, seen in plants, of carbon-based nanoparticles such as MWCNTs over other nanoscale compounds (Zheng & Nowack, 2022). Perhaps this, again, supports the hypothesis that accumulation occurs

via a nano-selective process, as WC is a hard compound, insoluble in water, and is likely to be ingested intact.

Final Thoughts

Ultimately, these results have shown that aquatic contaminants are accumulated, whether in bulk or nano form, and it has been determined that, at least in the case of Ti, the nanoscale analyte may be more accumulative than the bulk analogue. Furthermore, this chapter has demonstrated that the thiophilic scale determines the uptake of contaminants when multiple analytes are present, such as in the case of polymetallic compounds, which follows an antagonistic process mediated by position on the thiophilic scale. These *ex-situ* evaluations support the applicability of the bioaccumulative amplification approach to the analysis of metallic nanoscale contaminants.

Chapter VII

Modelling the Impact of Moulting

Portions of this chapter have been published in:

O'Callaghan, I., and T. Sullivan
"Shedding the load: moulting as a cause of variability in whole-body metal concentrations."
Journal of Crustacean Biology 40 (2020): 725-733

Portions of this chapter have been disseminated at:

SETAC Europe 29th Annual Meeting, Helsinki (2019)
ESA Annual Meeting, Louisville, KY (2019)
Environ: 30th Irish Environmental Researchers' Colloquium, Online (2020)

One of the central themes of this thesis is the bioaccumulation of contaminants by benthic macroinvertebrates, such as crustaceans. There is still some debate around the extent to which crustaceans uptake and bioaccumulate metals, and consensus between reported measured metal concentrations appears to be the exception, rather than the norm (Depledge & Rainbow, 1990; O'Callaghan et al., 2019). This is compounded by the uncertainty regarding the most likely sources, uptake pathways or sites of bioaccumulation within the organism of interest (Elangovan et al., 1999; Fleming & Richards, 1982; Robinson et al., 2003; Santoro et al., 2009; Van Hattum et al., 1989). Several models have been proposed for the processes

of uptake, bioaccumulation, and excretion of various pollutants in freshwater macroinvertebrates (Awrahman et al., 2015; Rainbow & Luoma, 2011), a task made more complicated by the varying behaviour of different metal analytes and potential interactions between said metals (O'Callaghan et al., 2019). A survey of these models, however, indicates that periodic moulting of the exoskeleton, a process common to many invertebrate species (Lebrun et al., 2011), may not have been adequately accounted for with regard to metals loss from the whole organism upon renewal of the exoskeleton.

Failing to take exoskeletons into account could, therefore, be a substantial source of variability in measurement of the bioavailability of metals or in biomonitoring programmes. Previous studies have shown that the moulted exoskeleton may contain sizeable concentrations of bioaccumulated pollutants, pointing to ecdysis as being a possible pathway through which significant portions of the accumulated substance may be shed or lost from the organism (Hall, 1982; Miramand et al., 1981; Rauch & Morrison, 1999; Topcuoğlu et al., 1987). Moulting may ultimately influence survival of an organism, as periodic moulting may reduce or maintain pollutant concentrations below critical concentrations for the organism (Bergey & Weis, 2007; Bryan & Darracott, 1979). Furthermore, in the context of quantifying the accumulated concentrations, accuracy and applicability of

existing pollutant uptake and release models could be improved by consistently including moult stage as a variable.

The chapter presents a generalised description of the flow of an unspecified metal pollutant in a moulting aquatic macroinvertebrate, such as a crustacean. This conceptual description offers an illustrative, non-specific picture of the potential impact of moulting on measured accumulations, equivalent to a repeating, discontinuous depletion of total accumulated metal concentrations. The applicability of this conceptual model is demonstrated by comparing to previously published pre- and post-moult measurements of overall body concentrations of crustaceans, and the relevance of this conceptual model to the study of accumulation in biomonitor species is described. Also presented is a possible technique for reducing variability resulting from ecdysis, and the potential application of this technique both in the field and the laboratory is discussed.

Conceptualizing the Impact of Moulting

Existing Models

Common types of models used to describe the accumulation of metals in aquatic invertebrates include bioconcentration, bioaccumulation, and accumulation factors (BCF/BAF/ACF), the biotic ligand model (BLM), the

free ion activity model (FIAM), and biodynamic models (W.-X. Wang & Tan, 2019).

BCF, BAF, and ACF factors provide an intuitive and relatively uncomplicated way of estimating accumulation rates, but rely on the assumption that equilibrium will be reached across the organism-environment interface (McGeer et al., 2003; van den Brink et al., 2019). Moulting consists of dynamic changes in the organism, which violates this key assumption, reducing the contribution of moulting to a static correction term rather than a time-varying process.

BLM, as well as the related FIAM and extensions thereof, are commonly applied to studies of the total accumulated concentration ionic metals in aquatic macroinvertebrates (P. L. Brown & Markich, 2000; Di Toro et al., 2001; van den Brink et al., 2019). Both models, however, focus on the interface between the environment and the proposed metal receptor site, and ignore the internal mechanisms of translocation, transformation, and excretion (Vijver et al., 2004). The contribution of moulting is closely linked with the relative sequestration of metal pollutants in exoskeleton and soft tissue compartments, which relies on these internal mechanisms.

Biodynamic models, commonly referred to as physiologically-based pharmacokinetic (PBPK), are better suited to modelling the dynamic potential contribution of moulting to the accumulated concentrations of

contaminant (Ardestani et al., 2014; van den Brink et al., 2019). This approach models the processes of uptake, accumulation, translocation, transformation, and excretion across time, and does not rely on any steady-state assumptions. Toxicokinetic-toxicodynamic (TKTD) models, such as general unified threshold model of survival (GUTS) (Jager et al., 2011; EFSA Panel on PPR et al., 2018), are an example of a bio- dynamic approach applied to both contaminant accumulation and resultant biological effects. One of the most comprehensive static metal-accumulation biodynamic models in the literature arguably shows a relatively good correlation with observed results across a large number of studies (Luoma & Rainbow, 2005), and GUTS is considered sufficiently developed for use in risk assessment applications (EFSA Panel on PPR, 2018). These models, however, have not yet been extended to include the contribution of moulting, a correction that would have to be separately determined for each organism-analyte pair.

Choice of Approach

This chapter takes approach of describing moulting using a non-specific model that is designed to capture the essence of the problem, while remaining broadly applicable to any moulting aquatic invertebrates such as crustaceans, whose exoskeleton may act as a significant sink for contaminants, and any transition metal, metalloid, or heavy metal species. Such approach should be contrasted with the common approach of deriving a quantitative, predictive model, as described above. The aim of our model

is instead to illustrate certain contributions of the moulting process to measured concentrations that are common to all moulting aquatic invertebrates and metal analytes, without offering a prediction for the significance of these contributions in any one scenario.

The applicability of the presented model is limited to the transition, metalloid and heavy metals, as it has been observed that the accumulation of the alkali or alkaline earth metals in the exoskeleton of an aquatic crustacean may differ from that of the aforementioned elements. The accumulation of calcium, in particular, has been extensively investigated throughout the various moult stages, and has been found to undergo a series of storage and resorption processes. This is said to be linked to the use of calcium in the release of the exoskeleton and hardening of the newly developing cuticle (Greenaway, 1985). The chitinous nature of the exoskeleton, and, more specifically, the nitrogen groups therein, may play a role in the alternative behaviour of the transition metals, metalloids, and heavy metals, as it has been noted that chitinous materials show a poorer affinity towards the alkali and alkaline earth metals (Rae & Gibb, 2003). For this reason, the assumptions made in the following section apply only to the accumulation of transition metals, heavy metals, and the metalloids.

Assumptions

For the purpose of creating a concise and simplified conceptual model, it is necessary to introduce a number of assumptions. These assumptions are chosen such that they adequately isolate the impact of moulting on metals concentrations, while removing internal processes that are not mediators of the moulting process.

1) In order to reduce the process to a flow network, the assumption is made that all metal pathways are uni-directional from intake to depuration. This does not mean that there are no bi-directional pathways, but rather that bi-directional flows can be replaced by a long-term uni-directional approximation.

2) While the process of moulting may be complex and irregular, the assumption is made that each moulting event happens similarly and that the properties of each moulted exoskeleton are largely identical, in that each sequential exoskeleton is capable of accumulating metal contaminants at a fixed rate, after consideration of the growth factor. This is a simplifying assumption, and the impact of moulting is qualitatively similar under non-uniform moulting behaviour.

3) The frequency of moulting is taken to be constant, for the purposes of illustration. Again, non-constant frequency of moulting would produce qualitatively similar results.

4) Contaminant intake occurs solely through the processes of respiration, ingestion, and adsorption. The inclusion of these three pathways is intended to make the model as general as possible, and the results still hold if uptake through either ingestion or respiration does not occur, and/or if uptake through adsorption does not occur. Adsorption is defined as the uptake of metal contaminants directly from the overlying and interstitial waters in direct contact with the surface of the exoskeleton, and results in uptake of the contaminant directly into the pre-moult exoskeleton; absorption through the exoskeleton and into the body is not directly considered for the reasons explained in Assumption 1.

5) The only process of depuration included in the model is moulting. Gut contents are not taken into account, and, therefore, excretion from the alimentary tract does not reduce accumulated concentrations in the model; metal pollutants are taken to enter the system when they are assimilated from the alimentary tract into the biological tissues.

6) This model only considers the movement of metals and assumes that no internal processes of biotransformation are taking place. This is true regardless when considering the elemental concentrations, but a more complex model would be required to account for change in speciation or complexation of metals due to biological processes.

7) This conceptual system makes the assumption that the rate of translocation between the body and pre-moult exoskeleton is driven towards equilibrium by the presence of open binding sites in the destination and high concentrations at the source. The flow of translocation can therefore be approximated as proportional to the source concentrations. Other models of translocation could be considered and would result in qualitatively similar results.

8) It is furthermore assumed that the described processes are not influenced by any biological damage that may occur, and no attempt is made to incorporate mortality into the model.

The Conceptual Model

Based on the above assumptions, a simplified three-input, two-compartment model of metal accumulation in a hypothetical moulting aquatic invertebrate is presented (Figure 22). The corresponding rate diagram is shown in Figure 23. The model compartmentalises metal concentrations accumulated within (and on) the pre-moult exoskeleton (Compartment E in Figure 23), which is defined as the part of the body that is removed entirely during the moulting process, and concentrations accumulated in the remainder of the body (Compartment B in Figure 23). For the purposes of simplifying the model, the body is inclusive of all non-moulting parts (gills, legs, hepatopancreas, and other organs), but not the gut contents as explained in Assumption 5.

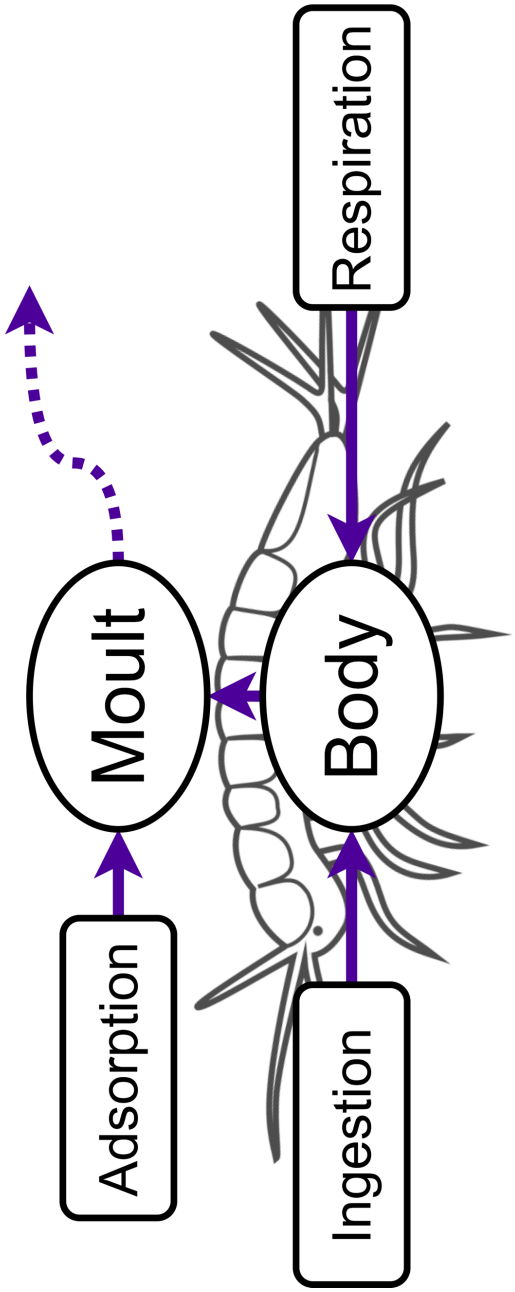


Figure 22: Schematic representation of a general overview of the major pathways of metal pollutant uptake (via ingestion, respiration and adsorption), translocation, and loss (via moulting) in a moulting aquatic organism, named Arcbie Asellus. The dashed arrow represents the elimination of accumulated pollutants at the time of moulting, which is modelled as a repeating instantaneous event, while the solid arrows represent the continuous pollutant flux.

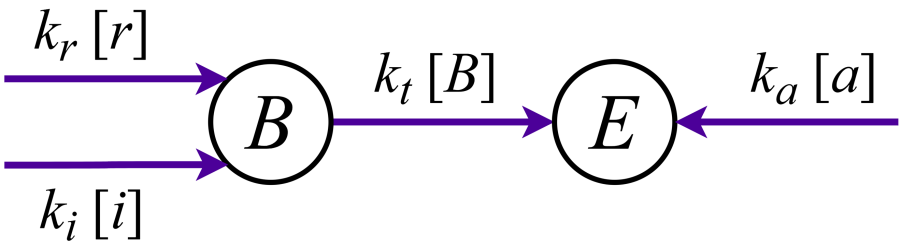


Figure 23: Rate diagram of pollutant flux into and out of the body (B) and moulting exoskeleton (E) compartments. Processes illustrated are respiration (r), ingestion (i), adsorption (a), and internal translocation (t); [r], [i], and [a] represent the concentrations from which respiration, ingestion and adsorption, respectively, occur, B the body compartment concentration. The k_X parameters represent the respective rate constants.

Contaminants may enter Compartment B through ingestion or standard respiration, where $[i]$ denotes the concentration of contaminant present in the ingestate, $[r]$ the concentration of contaminant in the water overlying the gill regions, and k_i and k_r the rate constants of the respective processes. Contaminants may enter Compartment E through surface adsorption directly from overlying and interstitial waters in contact with the exoskeleton, where $[a]$ denotes the concentration of contaminant present in these waters, and k_a the corresponding rate constant. Contaminants may also flow from Compartment B to Compartment E through the process of internal translocation or sequestration, where $[B]$ is the concentration of contaminant in Compartment B, and k_t the rate constant of translocation. The features of this flow are summarised in Assumption 7.

Moulting, or ecdysis, refers to the regular removal of the outer exoskeleton. As the exoskeleton is shed, a new exoskeleton develops beneath it (see Drach, 1967). The loss of the moulted exoskeleton cannot be modelled as a continuous flow of contaminants as it occurs suddenly and periodically, and, therefore, it is not included in the process diagram in Figure 23. Instead, the diagram describes the inter-moult movement of contaminants, and moulting is implemented externally as a periodic discontinuous removal of the contaminants within Compartment E. The moult period, or the rate at which an organism moults, will vary greatly with species and other factors. It should

be noted that occasional consumption of the organism's own moulted exoskeleton has been observed in some macroinvertebrate species (Elangovan et al., 1999), although there is consensus that metals bound within a chitinous exoskeleton are less bioavailable than other forms of analyte (F. R. Khan et al., 2010). The possibility of such an occurrence is not considered in this model but would result in qualitatively similar results.

Impact of Moulting

The conceptual two-compartment model of Figure 23 can be converted into a causal diagram describing the relationship between the variable of interest, namely the environmental concentration of bioavailable metal, and the measured metal concentration. This diagram is shown in Figure 24. The effect of environmental concentration on measured concentration occurs through the mediation variables of body and exoskeleton concentration. The hypothesis that the measured whole-body concentration is an accurate estimator for the bioavailable environmental concentration, given an acceptable measurement error, is, therefore, weakened by the direct effect of moult stage on exoskeleton concentration.

It can be directly observed from Figure 24 that the effect of the moult event on the overall accumulated metal concentration depends greatly on the ratio

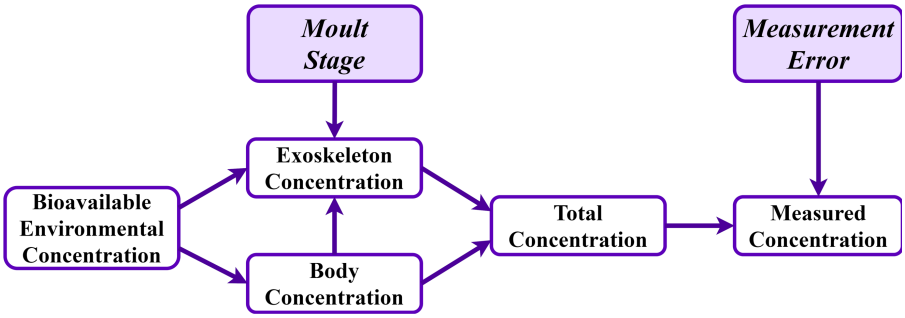


Figure 24: Causal diagram showing the connection between bioavailable environmental metal concentrations and measured whole-body metal concentrations, showing the influence of moult stage on the exoskeleton concentration mediator. In this diagram, moult stage and measurement error are two potential causes of in the typical bioaccumulation study.

of exoskeleton metal concentration to body metal concentration. If a simplifying assumption is made that the moult stage of different organisms is uncorrelated, then sampling more organisms should reduce, but not eliminate, the influence of moulting.

Derivation of Key Equations

Differential Rate Equations

The key aspects of the model are described by the following pair of differential rate equations, which describe the change in inter-moult concentrations of metal contaminant in each compartment.

$$\frac{d[B]}{dt} = k_i[i] + k_r[r] - k_t[B] \tag{15}$$

$$\frac{d[E]}{dt} = k_t[B] + k_a[a] \tag{16}$$

Growth Factor

The growth aspect is one of significant variability, as growth may indicate linear growth, lateral growth, or increasing thickness of the exoskeleton. Growth rate will vary considerably with species, as well as with the life stage of the organism. Differences in growth rate are accounted for through use of a growth factor, G. Equations 15 and 16 can, hence, be extended to account for growth by dividing each k_x term by G.

Closed-Form Expressions

Equations 15 and 16 can be solved for instantaneous compartment concentrations, assuming all concentrations are 0 at time $t = 0$ and ignoring the effects of moulting. This produces the following closed-form expressions:

$$[B](t) = \left({}^{U}/_{k_t}\right)(1 - e^{-t/\tau}) \tag{17}$$

$$[E](t) = (U + k_a[a])t - U\tau(1 - e^{-t/\tau}) \tag{18}$$

where the uptake rate is given by $U = k_i[i] + k_r[r]$, and the process time constant is $\tau = G/k_t$.

Note that the concentrations in Compartment B can be modelled as a first-order system, where the concentration approaches an equilibrium value of U/k_t, while the concentration in Compartment E increases indefinitely as the loss due to moulting is not yet accounted for.

Steady-State Equations

Steady-state is reached when $t \gg \tau$ in all the above equations. This results in expressions for the final, steady-state accumulated concentration in Compartment B in an environmental equilibrium.

$$[B] = {}^{U}/_{k_t} \tag{19}$$

As moulting happens periodically, the steady-state equivalent in the case of the Compartment E has the appearance of a sawtooth pattern, rather than a fixed value. The period of the concentration in Compartment E is equal to the moulting period, T_M, while the peak concentration is given by:

$$[E]_{\mathrm{MAX}} = (U + k_a[a])T_M \tag{20}$$

The variance of the corresponding error due to moulting is therefore given by:

$$\sigma^2 = \frac{([E]_{\mathrm{MAX}})^2}{12} \tag{21}$$

More explicit derivation of the above equations is presented in Appendix F4.

Simulation

Objectives

The conceptual model is designed to offer insights into the contribution of moulting to whole-body concentrations in the general case. The following simulation is intended to provide an example of how the model can describe the impact of moulting in an existing experimental study. Its specificity to a particular organism and metal pollutant should not be taken to be a

statement about the limitations of the conceptual model, but rather an indication of how the generalised model can be applied to a specific case. The implementation of the model employed in the following sections is described in full in Appendix F8.

Simulation Parameters

The simulation parameters shown in Table 6 were derived from studies of the uptake of vanadium by the caridean shrimp *Lysmata seticaudata* (Risso, 1816) (Miramand et al., 1981). The measurements extracted from Miramand et al. (1981) is available in Appendix E1. Further details of how these parameters were derived are presented in Appendix F5 and compared with the cited measurements in Appendix F1.

Simulation Results

Figure 25 shows the bioaccumulated concentrations of metal contaminant in Compartment B, when the environmental conditions are in equilibrium. The black dashed lines indicate the steady-state values.

As expected of a first-order system, the concentration in Compartment B reaches steady-state at a speed dictated by the rate of internal translocation of the contaminant. Once the internal concentration reaches steady-state, there is no significant change in contaminant concentration without a corresponding change in the environmental conditions.

Table 6: Model settings producing simulated results presented in the following figures. Full derivation of these figures is supplied in Appendix F5.

Parameter	Symbol	Value
Initial concentration in:		
Compartment B	$[B](0)$	0 ppm
Compartment E	$[E](0)$	0 ppm
Concentration acquired by way of:		
Respiration	$[r]$	0.10 ppm
Ingestion	$[i]$	0.07 ppm
Surface adsorption	$[a]$	0.10 ppm
Rate of uptake via:		
Respiration	k_r	0.70 day^{-1}
Ingestion	k_i	0.90 day^{-1}
Surface adsorption	k_a	0.09 day^{-1}
Rate of translocation from B to E	k_t	0.13 day^{-1}
Moult period	T_M	21 days
Growth factor	G	1

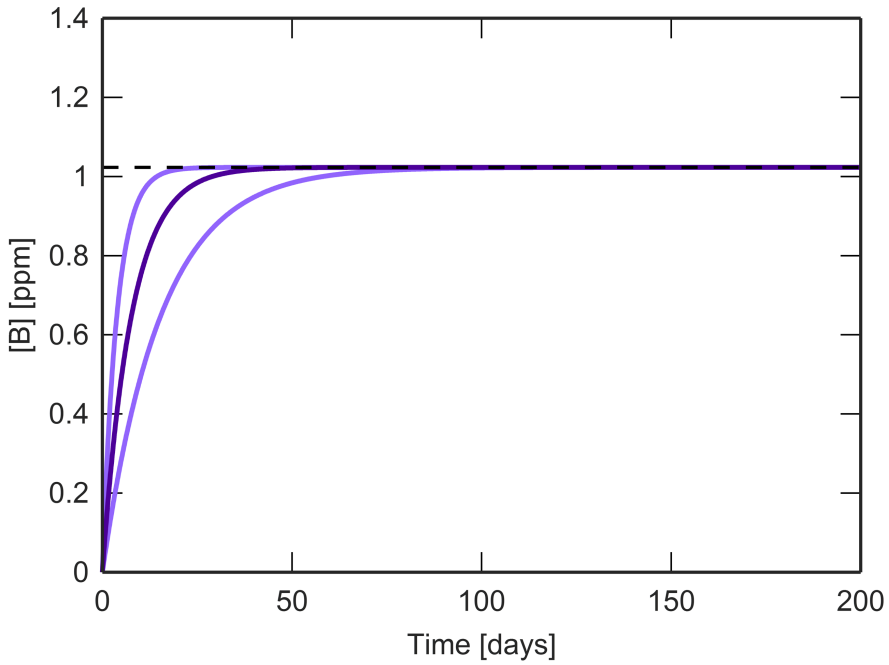


Figure 25: Simulation of theoretical concentration of a metal pollutant in Compartment B (the body of the organism, excluding the moulting exoskeleton) versus time, from application of the described parameters. The dashed black line represents the equilibrium value given by Equation 19 (see text). The lighter lines represent the effects of different values of k_t for the same equilibrium value.

Figure 26 shows the bioaccumulated concentration of the contaminant in Compartment E. Moulting forces the pre-moult exoskeleton concentration to 0 every T_M days. This produces a periodic pattern with increasing amplitude, approaching a saw-tooth pattern as Compartment B reaches steady-state.

The total concentration of contaminant in the organism as a whole is shown in Figure 27. The lower black dashed line shows the steady-state concentration for Compartment B, whereas the upper black dashed line includes the peak concentration for Compartment E. Despite the concentration in Compartment B reaching steady-state, the influence of moulting is still significant. This results in a time variation in the overall concentration.

Discussion

Contribution of Moulting

Studies measuring the bioaccumulation of metals in freshwater macroinvertebrates typically rely on the assumption that the accumulated concentrations of metals are relatively time-invariant. Many models of pollutant uptake likewise rely on the steady-state assumption. In both cases, individual measurements of total accumulated pollutant concentrations provide an accurate quantification of the time-averaged accumulation flux.

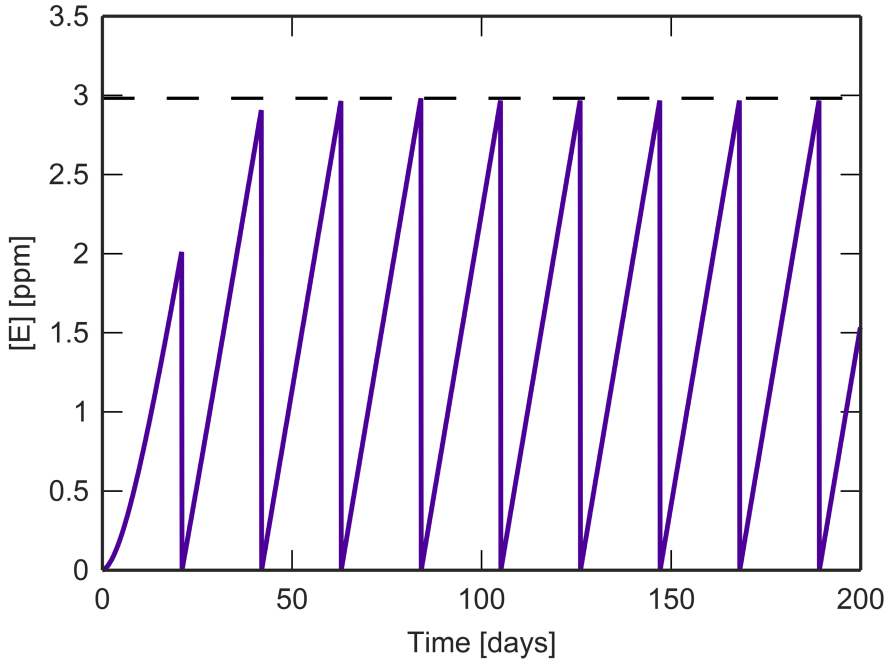


Figure 26: Simulation of concentration of a metal pollutant in Compartment E (the moulting exoskeleton of the organism) versus time, from application of the described parameters. Unlike with the concentration in the body compartment, B (see Figure 23), the concentration does not reach an equilibrium state, but oscillates between 0 (complete absence, due to moulting) and a maximum value. The equilibrium maximum value is given by Equation 20 (see text), and is denoted here by the dashed black line.

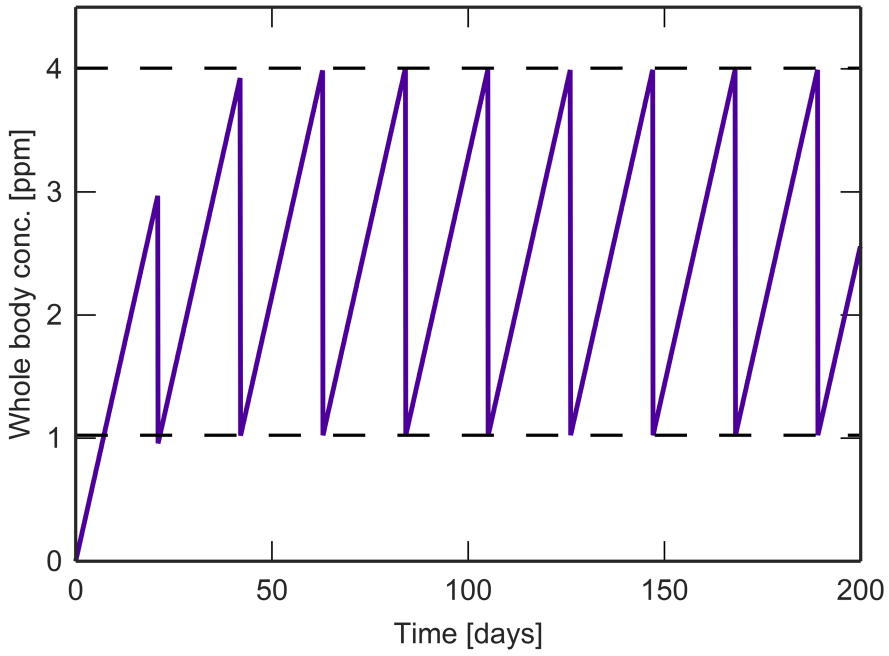


Figure 27: Simulation of overall concentration of a metal pollutant in the organism versus time. The overall concentration is a mass-weighted combination of the concentrations in the body and moulting exoskeleton compartments, B and E. This simulation represents the evolution of the actual measured whole-body concentration over time, where the variation in the concentration beyond day 200 is entirely due to contaminant loss through moulting. The equilibrium minimum and maximum are given by the dashed black lines, and are derived from Equations 19 and 20 (see text) after accounting for body mass.

The contribution of the conceptual model presented herein is to explain how periodic processes, exemplified by moulting, can produce fluctuations in the total accumulated whole-body concentrations. The *L. seticaudata* example demonstrates the significant effect this can have on the measured whole-body concentration. Seeing as discontinuous loss occurs during each moult, steady-state is not reached; the internal concentrations settle into a periodic oscillation, with the total concentration varying between minimum and maximum values. The error introduced by the continuous approximation is described in Appendix F7, and illustrated in Appendices F2 and F3. From an experimental perspective, this introduces a source of variability in the measurements, as the measured value depends not only on the mean total concentration, but also on the moult stage at the time at which the measurement is taken.

Validity of Simulated Example

Example parameters, listed in Table 6 were used for the purposes of demonstrating the effects of moulting on the measured whole-body concentration. This raises the question of whether the chosen parameters produce results that fairly represent realistic pollutant accumulations. This can only be answered through comparison with measured concentrations. The model predicts that approximately 74% of the accumulated metal contaminant concentration is lost during the process of moulting. Table 7 presents published measurements of analyte concentrations accumulated

within the exoskeleton of various species, expressed as a percentage of whole-body accumulated concentrations. In cases where data extraction and/or post-processing was required to obtain the values given in Table 7, further details are given in Appendices E4-E7. It must be emphasised, when interpreting these figures, that most of the cited studies do not account for the effects of moulting on overall concentrations described. Therefore, by assuming steady-state whole-body concentrations it would be expected that the measured values presented herein represent approximately half of the exoskeleton concentration at the time of moulting. Under these same assumptions, the exoskeleton would contribute approximately 37% of the whole-body concentration using the model parameters presented herein.

As is to be expected and considering the wide range of biological species, analytes, and environmental or experimental conditions, there is a broad variation in reported exoskeleton concentrations. Despite this variation, it is clear that such concentrations are a significant fraction of the whole-body accumulated concentration. Our model would, therefore, be correct in attributing a significant role to the contribution of moulting to whole-body pollutant concentrations.

Table 7: Studies investigating the contribution of the exoskeleton compartment of organisms to overall measured whole-body accumulated concentrations.[5]

Reference	Species	Analyte	% in E
Bergey & Weis, 2007	*Minuca pugnax* (Smith, 1870) (as *Uca pugnax*)	Cu	20.0
		Pb	62.1
		Zn	24.6
Bertine & Goldberg, 1972	*Ensis ensis* (Linnaeus, 1758)	Ag	91.0
		Co	75.0
		Fe	87.0
		Hg	68.0
		Sb	43.0
		Se	61.0
		Zn	79.0
Eriksson & Baden, 1998	*Nephrops norvegicus* (Linnaeus, 1758)	Mn	73.8
Guary & Fowler, 1990	*Carcinus maenas* (Linnaeus, 1758)	Am	73.8
		Pu	67.0
Hennig, 1984	*Palaemon pacificus* (Stimpson, 1860)	Cu	84.7
		Fe	78.9
		Sr	89.0
		Zn	77.0
Keteles & Fleeger, 2001	*Palaemonetes pugio* (Holthuis, 1949)	Cd	41.1
		Cu	13.9
		Zn	72.5
Miramand et al., 1981	*Carcinus maenas* (Linnaeus, 1758)	V	90.0
	Lysmata seticaudata (Risso, 1816)	V	58.0
Reinecke et al., 2003	*Potamonautes perlatus* (H. Milne Edwards, 1837)	Cd	22.8
		Pb	27.2

[5] Where relevant, data taken before the depuration period was preferred. Sample 8 in Eriksson & Baden (1998) was excluded as the authors determined that this measurement was an outlier.

If the results of the model are valid, the question then arises as to whether the mechanisms described in the model are also valid. (Hall, 1982) presented measurements of the accumulated concentrations of nickel in the cladoceran *Daphnia magna* (Straus, 1820), reproduced in Appendices E2 and E3. Figure 28 shows the measured soft-tissue and exoskeleton concentrations in individuals that have not moulted. It shows that the soft-tissue concentrations rapidly reach steady-state, while the exoskeleton concentrations continue to increase in the absence of moulting. A corresponding fit of the model is shown, with a value of $p < .001$ for both datasets. *In-vivo* measurements of whole-body nickel concentrations of one individual over time are shown in Figure 29. A moulting event occurred between $t = 20$ h and $t = 49$ h, depleting the whole-body concentration. Our model correctly describes the effects due to this moulting behaviour. These results indicate that our description of the processes that result in depuration *via* moulting is likely valid. Further details of the derivation of these parameters is given in Appendix F6.

Reducing Variability due to Moulting

Figure 27 shows how accumulated concentrations can fluctuate through time. For most of the moult period it is unclear at what point in the period the organism lies. In the context of crustaceans, however, it is usually

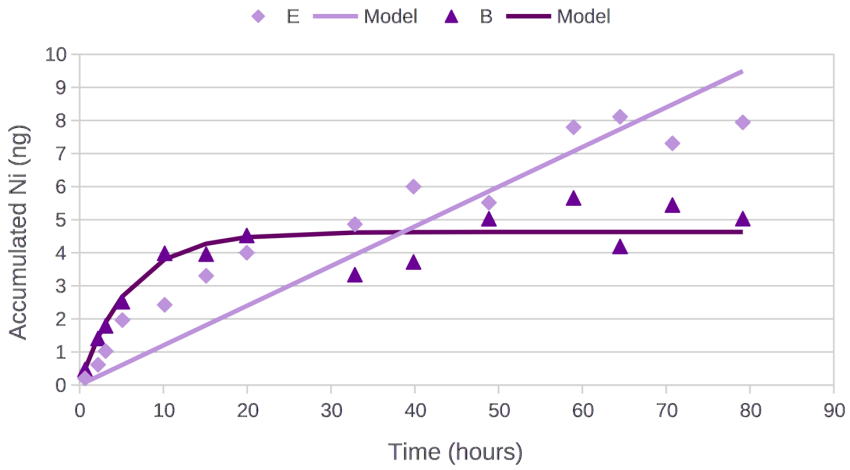


Figure 28: Accumulated concentrations of nickel in the soft-tissue (B) and exoskeleton (E) of multiple Daphnia magna individuals (from Hall, 1982). The corresponding fit of the model qualitatively matches the behaviour seen, where B saturates, but E continues to accumulate indefinitely in the absence of moulting. Hall (1982) also observed indefinite accumulation in the filtering appendages, which contain parts of exoskeleton and soft tissue, so have not been included in this figure.

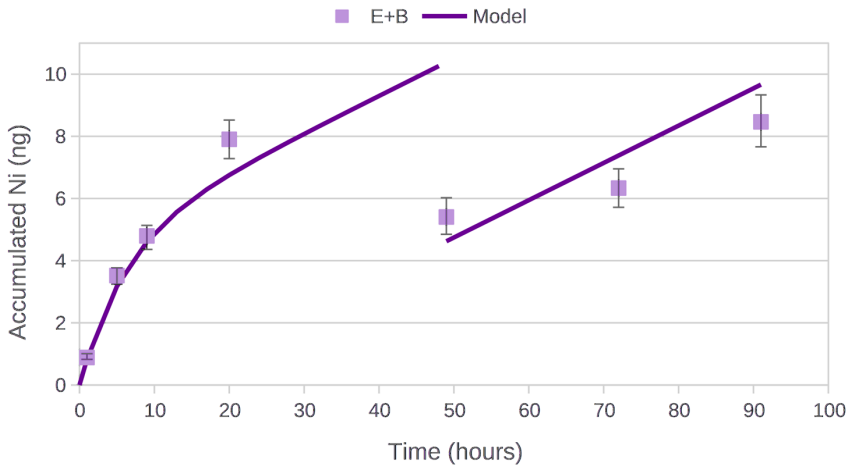


Figure 29: Accumulated concentrations, across time, of nickel in an individual specimen of Daphnia magna (from Hall, 1982). A moulting event occurred between t = 20 h and t = 49 h. A fit of the model, accounting for a moulting event just before t = 49 h, accurately describes the observed behaviour, despite the relative simplicity of the model.

relatively easy to identify if the organism is immediately at a pre-moult or post-moult stage (Buchholz, 1982; Drach, 1967). The pre-moult stage is often, depending on the species, associated with visual changes to the exoskeleton, such as changing colour or texture (Drach, 1967). The post-moult stage is, at the very least, signalled by the appearance of a shed cuticle. Both these stages correspond to the maximum and minimum exoskeleton concentrations, respectively. In the context of bioaccumulation studies, it is therefore proposed that sampling could be undertaken synchronously with moulting (moult-synchronous sampling) to ensure the robustness of the measurement by reducing the variability due to exoskeleton concentration fluctuations. This would take the form of ensuring only specimens which are immediately pre-moult or post-moult are sampled.

In the context of *ex-situ* studies, implementation of moult- synchronous sampling quite simply takes the form of delaying sampling until the desired moult stage has been reached for each organism. Implementation for *in-situ* studies, however, is less straightforward due to the requirement that samples be taken when the site is visited. In a case such as this, one could acquire the organisms as normal, retaining them in a suitable tank until the desired moult stage has been reached. This approach assumes that minimal depuration through other means occurs between acquisition and moulting.

An argument could be put forward that the variability due to moulting could be reduced by sampling multiple specimens. This argument relies on the

assumption that the moult stage of each specimen is uncorrelated; however, moulting can be induced or accelerated by environmental stressors (Fowler et al., 1971; Nugegoda & Rainbow, 1987), therefore, it could happen that specimens in similar conditions can moult together. For this reason, performing measurements on multiple specimens held in the same conditions may not be sufficient to overcome the effects of moulting on accumulated concentrations.

Even ignoring the possibility of correlated moult stage within the population under study, moult-synchronous sampling can offer a more efficient approach to the determination of mean total bioaccumulated concentrations. Both increased sampling size and moult-synchronous sampling aim to reduce the measurement error in the overall measured accumulated concentration due to moulting. Equation 21 quantifies the variance of the measurement error due to moulting. In the example of Figure 29, this corresponds to a mean error variance of $\sigma^2 = 14$ pp. If measurements were only made within the first post-moult day, this would reduce the mean error variance of a single measurement to $\sigma^2 = 0.14$ ppb. In lay terms, the resulting increase in statistical accuracy corresponds to that which would be obtained by increasing the number of specimens by a factor of 100. Figure 30 shows the reduction of measurement error variance due to moulting from

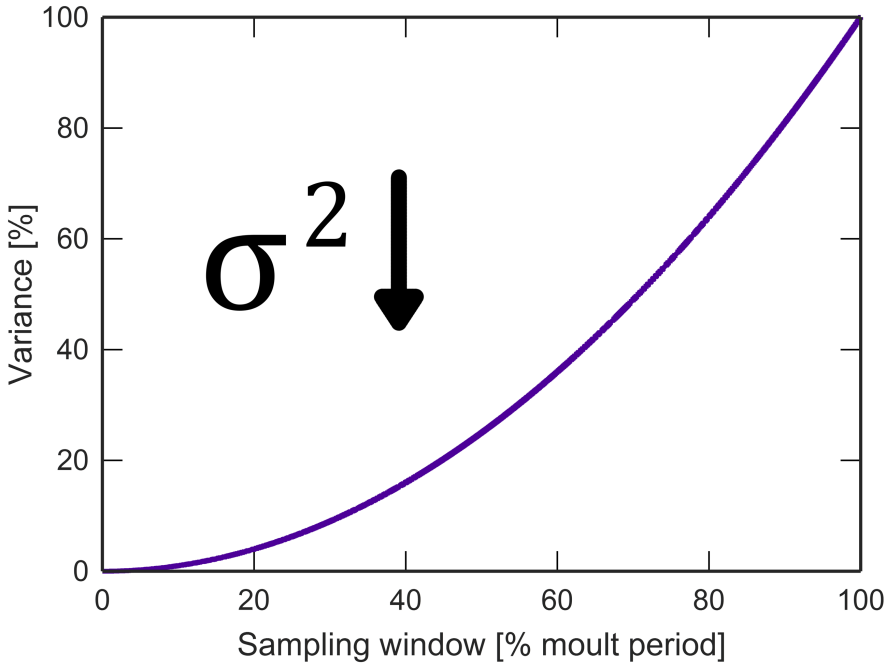


Figure 30: Proportional decrease in moult-induced measurement error with increasing accuracy of moult-synchronous sampling, where a "100%" sampling window is equivalent to ignoring moult stage when sampling. Using a sampling window of 10% of the moult period, for example, would reduce the variance by a factor of 100, for the same sample size.

restricting the sampling window. Moult-synchronous sampling is, therefore, a more efficient means of reducing the measurement error due to pollutant loss during moulting than simply increasing the sampling size.

Chapter VIII

In Conclusion

This body of work has endeavoured to identify, investigate and evaluate the bioaccumulative amplification approach to quantification of environmental contaminants, which offers advantages over existing approaches to monitoring contaminants in the freshwater environment. This thesis has presented an account of these activities, alongside relevant investigations into adjacent topics.

An overview was delivered in the first instance, outlining the prevalence of freshwater contamination and the growing threat of emerging classes of contaminants. The non-uniform threat of contaminants to freshwater biota and the ubiquitous process of bioaccumulation was described, culminating in an exposition of the utility of biomonitoring to determine the ecological impact of environmental pollutants.

An example biomonitor was then discussed, in the form of the benthic isopod *Asellus aquaticus*. Chapter III provided evidence for the suitability of this species as a candidate biomonitoring test organism; it was found to be

more suitable for the study of long-term bioaccumulation than many commonly employed biomonitors due to its relative tolerance to many aquatic contaminants and extreme environmental conditions.

Chapter IV provides new, fundamental insights into bioaccumulative processes. Clear evidence is presented for the influence of thiophilicity on bioaccumulation. These findings support the hypothesised function of the metallothionein protein in the regulation of metal bioaccumulation. The contaminant-specific accumulation seen in studies to date is explained by this dependence on thiophilicity, which is observed in existing bioaccumulation datasets. These results are mirrored across varying taxa and environmental conditions, in both marine and freshwater systems. The thiophilic scale can, therefore, act as a metric for the ecological relevance of a given contaminant.

The bioaccumulative amplification approach is, in Chapter V, evaluated in a field study. Comparison of sediment and benthic macroinvertebrate samples further validated the relationship between bioaccumulation and thiophilicity. Furthermore, this study found significant amplification of concentrations within the macroinvertebrate samples when compared to direct measurement of the water phase. It was practically demonstrated that this approach offers higher overall sensitivity, and the ability to detect and quantify a long-term average of the ecologically relevant fraction of aquatic

contaminants. The primary trade-off of this method is the introduction of a relatively straightforward digestion step prior to chemical analysis.

A subsequent lab-based application of the approach to nanomaterials was described in Chapter VI. Nano-scale contaminants were found to accumulate more than their bulk counterparts; however, the rate of saturation was similar for both bulk and nano-scale analytes. Similar monometallic and polymetallic nano-scale compounds showed similar overall metal ion uptake. Both metals from the polymetallic compound were accumulated, with an imbalance dictated by the metals' relative thiophilicities. It was demonstrated that the approach can be applied in both field and lab environments, and to both bulk and nano-scale contaminants.

The model of accumulation employed to this point, and employed in the vast majority of published bioaccumulation studies, assumes that bioaccumulation is the result of an input-only flow of contaminants into the organism. All crustaceans, however, undergo regular processes of ecdysis, a possible output pathway for accumulated contaminant concentrations. Furthermore, this pathway would be a discontinuous process, one which could not be modelled as a constant-rate mechanism like the input. Finally, Chapter VII presents a new perspective on accumulative contaminant flows, where ecdysis is incorporated as an essential aspect. It is shown that the presence of ecdysis can introduce an error term into the experimental evaluation of accumulated concentrations, and analysis of bioaccumulation

assays demonstrates that this error can be significant. These results demonstrate the necessity of considering the impact of ecdysis, and a technique for minimising this error in practice is described.

Taken as a whole, this work contributes to our understanding of the fate of metal contaminants in the benthic environment and our ability to detect and respond to them. The primary contribution of this thesis is the description of a fundamental relationship between bioaccumulation of contaminants and their position on the thiophilic scale, which offers new insight into the ecological fate of contaminants. This is accompanied by an evaluation of the effectiveness of the bioaccumulative amplification approach to quantification of ecologically-relevant freshwater contamination. This approach is found to be substantially more sensitive than the direct measurement of contaminants in the water phase, while also directly quantifying the bioavailable and ecologically relevant fraction of aquatic pollutants.

References

Adachi, K., & Tainosho, Y. (2004). Characterization of heavy metal particles embedded in tire dust. *Environment International*, *30*(8), 1009–1017.

Adams, J., Greenwood, P., Pollitt, R., & Yonow, T. (1985). Loading constraints and sexual size dimorphism in Asellus aquaticus. *Behaviour*, 277–287.

Adcock, J. A. (1979). Energetics of a population of the isopod Asellus aquaticus: Life history and production. *Freshwater Biology*, *9*, 343–355.

Adriaenssens, V., Goethals, P. L., & De Pauw, N. (2006). Fuzzy knowledge-based models for prediction of Asellus and Gammarus in watercourses in Flanders (Belgium). *Ecological Modelling*, *195*, 3–10.

Ali, D., Alarifi, S., Kumar, S., Ahamed, M., & Siddiqui, M. A. (2012). Oxidative stress and genotoxic effect of zinc oxide nanoparticles in freshwater snail Lymnaea luteola L. *Aquatic Toxicology*, *124*, 83–90.

Allen, H. E., Hall, R. H., & Brisbin, T. D. (1980). Metal speciation. Effects on aquatic toxicity. *Environmental Science & Technology*, *14*, 441–443.

Ambrosone, A., Mattera, L., Marchesano, V., Quarta, A., Susha, A. S., Tino, A., Rogach, A. L., & Tortiglione, C. (2012). Mechanisms underlying toxicity induced by CdTe quantum dots determined in an invertebrate model organism. *Biomaterials*, *33*(7), 1991–2000.

Amiard, J.-C., Amiard-Triquet, C., Barka, S., Pellerin, J., & Rainbow, P. (2006). Metallothioneins in aquatic invertebrates: Their role in metal

detoxification and their use as biomarkers. *Aquatic Toxicology*, *76*, 160–202.

Amundsen, P.-A., Staldvik, F. J., Lukin, A. A., Kashulin, N. A., Popova, O. A., & Reshetnikov, Y. S. (1997). Heavy metal contamination in freshwater fish from the border region between Norway and Russia. *Science of the Total Environment*, *201*, 211–224.

Angel, B. M., Vallotton, P., & Apte, S. C. (2015). On the mechanism of nanoparticulate CeO2 toxicity to freshwater algae. *Aquatic Toxicology*, *168*, 90–97.

Ansari, R. A., Kaur, M., Ahmad, F., Rahman, S., Rashid, H., Islam, F., & Raisuddin, S. (2009). Genotoxic and oxidative stress-inducing effects of deltamethrin in the eryth- rocytes of a freshwater biomarker fish species. *Channa Punctata Bloch. Environmental Toxicology*, *24*(5), 429–436.

Apeagyei, E., Bank, M. S., & Spengler, J. D. (2011). Distribution of heavy metals in road dust along an urban-rural gradient in Massachusetts. *Atmospheric Environment*, *45*(13), 2310–2323.

Ardestani, M. M., Straalen, N. M., & Gestel, C. A. (2014). Uptake and elimination kinetics of metals in soil invertebrates: A review. *Environmental Pollution*, *193*, 277–295.

Aston, R. J., & Milner, A. G. P. (1980). A comparison of populations of the isopod Asellus aquaticus above and below power stations in organically polluted reaches of the River Trent. *Freshwater Biology*, *10*, 1–14.

Atkinson, C. A., Jolley, D. F., & Simpson, S. L. (2007). Effect of overlying water pH, dissolved oxygen, salinity and sediment disturbances on metal release and sequestration from metal contaminated marine sediments. *Chemosphere*, *69*, 1428–1437.

Awrahman, Z. A., Rainbow, P. S., Smith, B. D., Khan, F. R., Bury, N. R., & Fialkowski, W. (2015). Bioaccumulation of arsenic and silver by the caddisfly larvae Hydropsyche siltalai and H. pellucidula: A biodynamic modeling approach. *Aquatic Toxicology*, *161*, 196–207.

Bascombe, A. D., Ellis, J. B., Revitt, D. M., & Shutes, R. B. E. (1988). Macroinvertebrate biomonitoring and water quality management within urban catchments. *Hydrological Processes and Water Management in Urban Areas (Proceedings of the Duisberg Symposium)*.

Batley, G. E., Kirby, J. K., & McLaughlin, M. J. (2012). Fate and Risks of Nanomaterials in Aquatic and Terrestrial Environments. *Accounts of Chemical Research*, *46*(3), 854–862. https://doi.org/10.1021/ar2003368

Beil, A., Jurt, S., Walser, R., Schönhut, T., Güntert, P., Palacios, Ò., Atrian, S., Capdevila, M., Dallinger, R., & Zerbe, O. (2019). The solution structure and dynamics of Cd-metallothionein from Helix pomatia reveal optimization for binding Cd over Zn. *Biochemistry*, *58*, 4570–4581.

Belzunce-Segarra, M. J., Simpson, S. L., Amato, E. D., Spadaro, D. A., Hamilton, I. L., Jarolimek, C. V., & Jolley, D. F. (2015). The mismatch between bioaccumulation in field and laboratory environments: Interpreting the

differences for metals in benthic bivalves. *Environmental Pollution*, *204*, 48–57.

Benesh, D. P., Valtonen, E. T., & Jormalainen, V. (2007). Reduced survival associated with precopulatory mate guarding in male Asellus aquaticus (Isopoda). *Annales Zoologici Fennici*, 425 434.

Berandah, F. E., Kong, Y. C., & Ismail, A. (2010). Bioaccumulation and distribution of heavy metals (Cd, Cu, Fe, Ni, Pb and Zn) in the different tissues of Chicoreus capucinus lamarck (Mollusca: Muricidae) collected from Sungai Janggut, Kuala Langat, Malaysia. *Environment Asia*, *3*, 65 71.

Bergey, L. L., & Weis, J. S. (2007). Molting as a mechanism of depuration of metals in the fiddler crab, Uca pugnax. *Marine Environmental Research*, *64*, 556–562.

Bergfur, J., Johnson, R. K., Sandin, L., Goedkoop, W., & Nygren, K. (2007). Effects of nutrient enrichment on boreal streams: Invertebrates, fungi and leaf-litter breakdown. *Freshwater Biology*, *52*, 1618 1633.

Bhuvaneshwari, M., Bairoliya, S., Parashar, A., Chandrasekaran, N., & Mukherjee, A. (2016). Differential toxicity of Al2O3 particles on Gram-positive and Gram-negative sediment bacterial isolates from freshwater. *Environmental Science and Pollution Research*, *23*(12), 12095–12106.

Bian, B., Lin, C., & Wu, H. S. (2015). Contamination and risk assessment of metals in road-deposited sediments in a medium-sized city of China. *Ecotoxicology and Environmental Safety*, *112*, 87–95.

Bifari, E. N., Bahadar Khan, S., Alamry, K. A., Asiri, A. M., & Akhtar, K. (2016). Cellulose acetate based nanocomposites for biomedical applications: A review. *Current Pharmaceutical Design*, *22*(20), 3007–3019.

Blockwell, S. J., Taylor, E. J., Jones, I., & Pascoe, D. (1998). The influence of fresh water pollutants and interaction with Asellus aquaticus (L.) on the feeding activity of Gammarus pulex (L.). *Archives of Environmental Contamination and Toxicology*, *34*, 41 47.

Bloor, M. C., & Banks, C. J. (2006). An evaluation of mixed species in-situ and ex-situ feeding assays: The altered response of Asellus aquaticus and Gammarus pulex. *Environment International*, *32*, 22 27.

Bobori, D., Dimitriadi, A., Karasiali, S., Tsoumaki-Tsouroufli, P., Mastora, M., Kastrinaki, G., Feidantsis, K., Printzi, A., Koumoundouros, G., & Kaloyianni, M. (2020). Common mechanisms activated in the tissues of aquatic and terrestrial animal models after TiO2 nanoparticles exposure. *Environment International*, *138*, 105611.

Bonada, N., Prat, N., Resh, V. H., & Statzner, B. (2006). Developments in aquatic insect biomonitoring: A comparative analysis of recent approaches. *Annual Review of Entomology*, *51*, 495–523.

Bone, A. J., Colman, B. P., Gondikas, A. P., Newton, K. M., Harrold, K. H., Cory, R. M., Unrine, J. M., Klaine, S. J., Matson, C. W., & Giulio, R. T. D. (2012). Biotic and abiotic interactions in aquatic microcosms determine fate and toxicity of Ag nanoparticles: Part 2–toxicity and Ag speciation. *Environmental Science & Technology*, *46*(13), 6925–6933.

Bongers, J., Richardson, D. E., & Bell, J. U. (1988). Platinum (II) binding to metallothioneins. *Journal of Inorganic Biochemistry*, *34*, 55–62.

Bordon, I. C., Emerenciano, A. K., Melo, J. R. C., Silva, J. R. M. C., Favaro, D. I. T., Gusso-Choueri, P. K., Campos, B. G., & Souza Abessa, D. M. (2018). Implications on the Pb bioaccumulation and metallothionein levels due to dietary and waterborne exposures: The Callinectes danae case. *Ecotoxicology and Environmental Safety*, *162*, 415–422.

Boubonari, T., Kevrekidis, T., & Malea, P. M. (2009). Pb and Cd) concentration patterns in components of a macrophyte-based coastal lagoon ecosystem. *Hydrobiologia*, *635*, 27–36.

Bouskill, N. J., Handy, R. D., Ford, T. E., & Galloway, T. S. (2006). Differentiating copper and arsenic toxicity using biochemical biomarkers in Asellus aquaticus and Dreissena polymorpha. *Ecotoxicology and Environmental Safety*, *65*, 342–349.

Boyd, R. S. (2010). Heavy metal pollutants and chemical ecology: Exploring new frontiers. *Journal of Chemical Ecology*, *36*, 46 58.

Breitburg, D. L., Sanders, J. G., Gilmour, C. C., Hatfield, C. A., Osman, R. W., Riedel, G. F., Seitzinger, S. P., & Seitzinger, S. P. (1999). Variability in responses to nutrients and trace elements, and transmission of stressor effects through an estuarine food web. *Limnology and Oceanography*, *44*, 837 863.

Brodie, J. E., Kroon, F. J., Schaffelke, B., Wolanski, E. C., Lewis, S. E., Devlin, M. J., Bohnet, I. C., Bainbridge, Z. T., Waterhouse, J., & Davis, A. M.

(2012). Terrestrial pollutant runoff to the Great Barrier Reef: An update of issues, priorities and management responses. *Marine Pollution Bulletin*, *65*(4–9), 81–100.

Brown, B. E. (1977). Uptake of copper and lead by a metaltolerant isopod Asellus meridianus Rac. *Freshwater Biology*, *7*, 235 244.

Brown, P. L., & Markich, S. J. (2000). Evaluation of the free ion activity model of metal- organism interaction: Extension of the conceptual model. *Aquatic Toxicolgy*, *51*, 177 194.

Bryan, G. W., & Darracott, A. (1979). Bioaccumulation of marine pollutants. *Philosophical Transactions of the Royal Society of London B: Biological Sciences*, *286*, 483–505.

Buchholz, F. (1982). Drach's molt staging system adapted for euphausiids. *Marine Biology*, *66*, 301–305.

Bundschuh, M., Appeltauer, A., Dabrunz, A., & Schulz, R. (2012). Combined effect of invertebrate predation and sublethal pesticide exposure on the behavior and survival of Asellus aquaticus (Crustacea; Isopoda). *Archives of Environmental Contamination and Toxicology*, *63*, 77 85.

Burkhard, L. P. (2003). Factors influencing the design of bioaccumulation factor and biotasediment accumulation factor field studies. *Environmental Toxicology and Chemistry: An International Journal*, *22*, 351–360.

Burkhard, L. P., Cowan-Ellsberry, C., Embry, M. R., Hoke, R. A., & Kidd, K. A. (2012). Bioaccumulation data from laboratory and field studies: Are

they comparable? *Integrated Environmental Assessment and Management*, *8*, 13–16.

Buzier, R., Tusseau-Vuillemin, M.-H., Keirsbulck, M., & Mouchel, J.-M. (2011). Inputs of total and labile trace metals from wastewater treatment plants effluents to the Seine River. *Physics and Chemistry of the Earth, Parts A/B/C*, *36*, 500–505.

Callender, E. (2003). Heavy metals in the environment – historical trends. *Treatise on Geochemistry*, *9*, 67–105.

Campbel, P. G. C., & Stokes, P. M. (1985). Acidification and toxicity of metals to aquatic biota. *Canadian Journal of Fisheries and Aquatic Sciences*, *42*, 2034 2049.

Canivet, V., Chambon, P., & Gibert, J. (2001). Toxicity and bioaccumulation of arsenic and chromium in epigean and hypogean freshwater macroinvertebrates. *Archives of Environmental Contamination and Toxicology*, *40*, 345 354.

Cao, Y., Bark, A. W., & Williams, W. P. (1996). Measuring the responses of macro- invertebrate communities to water pollution: A comparison of multivariate approaches, biotic and diversity indices. *Hydrobiologia*, *341*, 1 19.

Cardinale, B. J., Bier, R., & Kwan, C. (2012). Effects of TiO2 nanoparticles on the growth and metabolism of three species of freshwater algae. *Journal of Nanoparticle Research*, *14*(8), 913.

Chambers, M. R. (1977). A comparison of the population ecology of Asellus aquaticus (L.) and Asellus meridianus Rac. In the reed beds of the Tjeukemeer. *Hydrobiologia*, *53*, 147–154.

Charles, J., Crini, G., Degiorgi, F., Sancey, B., Morin-Crini, N., & Badot, P.-M. (2014). Unexpected toxic interactions in the freshwater amphipod Gammarus pulex (L.) exposed to binary copper and nickel mixtures. *Environmental Science and Pollution Research*, *21*, 1099–1111.

Chen, L. Q., Kang, B., & Ling, J. (2013). Cytotoxicity of cuprous oxide nanoparticles to fish blood cells: Hemolysis and internalization. *Journal of Nanoparticle Research*, *15*(3), 1507.

Chen, Z., Sheng, X., Wang, J., & Wen, Y. (2018). Silver nanoparticles or free silver ions work? An enantioselective phytotoxicity study with a chiral tool. *Science of the Total Environment*, *610*, 77–83.

Cherchi, C., & Gu, A. Z. (2010). Impact of titanium dioxide nanomaterials on nitrogen fixation rate and intracellular nitrogen storage in Anabaena variabilis. *Environmental Science & Technology*, *44*(21), 8302–8307.

Cid, N., Ibáñez, C., Palanques, A., & Prat, N. (2010). Patterns of metal bioaccumulation in two filter-feeding macroinvertebrates: Exposure distribution, inter-species differences and variability across developmental stages. *Science of the Total Environment*, *408*, 2795–2806.

Cobbett, C., & Goldsbrough, P. (2002). Phytochelatins and metallothioneins: Roles in heavy metal detoxification and homeostasis. *Annual Review of Plant Biology*, *53*, 159–182.

Costantini, M. L., Mancinelli, G., Mandrone, S., & Rossi, L. (2005). Combined effects of acidification and competition on the feeding preference of a freshwater macroinvertebrate, Asellus aquaticus (Crustacea: Isopoda): A laboratory experiment. *Marine and Freshwater Research*, *56*, 997–1004.

Courtney, L. A., & Clements, W. H. (2000). Sensitivity to acidic pH in benthic invertebrate assemblages with different histories of exposure to metals. *Journal of the North American Benthological Society*, *19*, 112 127.

Croteau, M.-N., Luoma, S. N., & Stewart, A. R. (2005). Trophic transfer of metals along freshwater food webs: Evidence of cadmium biomagnification in nature. *Limnology and Oceanography*, *50*, 1511–1519.

Culioli, J.-L., Fouquoire, A., Calendini, S., Mori, C., & Orsini, A. (2009). Trophic transfer of arsenic and antimony in a freshwater ecosystem: A field study. *Aquatic Toxicology*, *94*, 286–293.

Dalai, S., Pakrashi, S., Chakravarty, S., Hussain, S., Chandrasekaran, N., & Mukherjee, A. (2014). Studies on interfacial interactions of TiO2 nanoparticles with bacterial cells under light and dark conditions. *Bulletin of Materials Science*, *37*(3), 371–381.

Dallinger, R., & Kautzky, H. (1985). The importance of contaminated food for the uptake of heavy metals by rainbow trout (Salmo gairdneri): A field study. *Oecologia*, *67*, 82 89.

De Jonge, M., Vijver, B., Blust, R., & Bervoets, L. (2008). Responses of aquatic organisms to metal pollution in a lowland river in Flanders: A

comparison of diatoms and macroinvertebrates. *Science of the Total Environment*, *407*, 615 629.

De Lange, H. J., Sperber, V., & Peeters, E. T. H. M. (2006). Avoidance of polycyclic aromatic hydrocarbon-contaminated sediments by the freshwater invertebrates Gam- marus pulex and asellus aquaticus. *Environmental Toxicology & Chemistry*, *25*, 452.

De Smet, W. H. O., & Das, A. M. L. (1981). *Of a sellus aquaticus (L.*

DeForest, D. K., Brix, K. V., & Adams, W. J. (2007). Assessing metal bioaccumulation in aquatic environments: The inverse relationship between bioaccumulation factors, trophic transfer factors and exposure concentration. *Aquatic Toxicology*, *84*, 236–246.

Depledge, M. H., & Rainbow, P. S. (1990). Models of regulation and accumulation of trace metals in marine invertebrates. *Comparative Biochemistry and Physiology C*, *97*, 1–7.

Deryabin, D. G., Efremova, L. V., Vasilchenko, A. S., Saidakova, E. V., Sizova, E. A., Troshin, P. A., Zhilenkov, A. V., & Khakina, E. A. (2015). A zeta potential value determines the aggregate's size of penta-substituted [60] fullerene derivatives in aqueous suspension whereas positive charge is required for toxicity against bacterial cells. *Journal of Nanobiotechnology*, *13*(1), 50.

Di Lascio, A., Rossi, L., & Letizia Costantini, M. (2011). Different temperature tolerance of northern and southern European populations of a

freshwater Isopod Crustacean species (Asellus aquaticus L.) *Fundamental and Applied Limnology*, *179*, 193 201.

Di Toro, D. M., Allen, H. E., Bergman, H. L., Meyer, J. S., Paquin, P. R., & Santore, R. C. (2001). Biotic ligand model of the acute toxicity of metals. 1. Technical basis. *Environmental Toxicology and Chemistry*, *20*, 2383–2396.

Dick, J. T., Platvoet, D., & Kelly, D. W. (2002). Predatory impact of the freshwater invader Dikerogammarus villosus (Crustacea: Amphipoda). *Canadian Journal of Fisheries and Aquatic Sciences*, *59*, 1078 1084.

Ding, X., Pu, Y., Tang, M., & Zhang, T. (2022). Environmental and health effects of graphene-family nanomaterials: Potential release pathways, transformation, environmental fate and health risks. *NanoToday*, *42*, 101379.

Donaldson, K., & Poland, C. A. (2013). Nanotoxicity: Challenging the myth of nano-specific toxicity. *Current Opinion in Biotechnology*, *24*(4), 724–734.

Drach, P. (1967). Sur la méthode de détermination des stades d'intermue et son application générale aux crustacés. *Vie et Milieu, Série A: Biologie marine*, *18*, 595–610.

Dudev, T., & Lim, C. (2013). Competition among metal ions for protein binding sites: Determinants of metal ion selectivity in proteins. *Chemical Reviews*, *114*, 538 556.

Dunn, M. A., Blalock, T. L., & Cousins, R. J. (1987). Metallothionein. *Experimental Biology and Medicine*, *185*(2).

Eimers, M. C., Evans, R. D., & Welbourn, P. M. (2002). Partitioning and bioaccumulation of cadmium in artificial sediment systems: Application of a stable isotope tracer technique. *Chemosphere*, *46*, 543 551.

Ekvall, M. T., Hedberg, J., Odnevall Wallinder, I., Hansson, L.-A., & Cedervall, T. (2018). Long-term effects of tungsten carbide (WC) nanoparticles in pelagic and benthic aquatic ecosystems. *Nanotoxicology*, *12*, 79 89.

El Gawad, S. S. I. A. (2009). The mollusk gastropod Lanistes carinatus (Olivier, 1804) as a biomonitor for some trace metals in the nile river. *International Journal of Zoological Research*, *5*, 115 125.

Elangovan, R., Ballance, S., White, K., McCrohan, C., & Powell, J. (1999). Accumulation of aluminium by the freshwater crustacean Asellus aquaticus in neutral water. *Environmental Pollution*, *106*, 257 263.

Engel, D. W., & Brouwer, M. (1984). Trace metal-binding proteins in marine molluscs and crustaceans. *Marine Environmental Research*, *13*, 177–194.

Erasmus, J., Malherbe, W., Zimmermann, S., Lorenz, A., Nachev, M., Wepener, V., Sures, B., & Smit, N. (2020). Metal accumulation in riverine macroinvertebrates from a platinum mining region. *Science of the Total Environment*, *703*, 134738.

European Commission. (2000). Directive 2000/60/EC of the European Parliament and of the Council of 23 October 2000 establishing a framework for Community action in the field of water policy. *OJ*, *L 327*, 1–73.

European Commission. (2008). Directive 2008/105/EC of the European Parliament and of the Council of 16 December 2008 on environmental quality standards in the field of water policy, amending and subsequently re- pealing Council Directives 82/176/EEC, 83/513/EEC, 84/156/EEC, 84/491/EEC, 86/280/EEC and amending Directive 2000/60/EC of the European Parliament and of the Council. *OJ*, *L 348*, 84.

Fahmy, S. R., & Sayed, D. A. (2017). Toxicological perturbations of zinc oxide nanoparticles in the Coelatura aegyptiaca mussel. *Toxicology and Industrial Health*, *33*(7), 564–575.

Falfushynska, H., Gnatyshyna, L., Yurchak, I., Sokolova, I., & Stoliar, O. (2015). The effects of zinc nanooxide on cellular stress responses of the freshwater mussels Unio tumidus are modulated by elevated temperature and organic pollutants. *Aquatic Toxicology*, *162*, 82–93.

Farag, A. M., Nimick, D. A., Kimball, B. A., Church, S. E., Harper, D. D., & Brumbaugh, W. G. (2007). Concentrations of metals in water, sediment, biofilm, benthic macroinvertebrates, and fish in the Boulder River watershed, Montana, and the role of colloids in metal uptake. *Archives of Environmental Contamination and Toxicology*, *52*, 397–409.

Fard, J. K., Jafari, S., & Eghbal, M. A. (2015). A Review of Molecular Mechanisms Involved in Toxicity of Nanoparticles. *Advanced Pharmaceutical Bulletin*, *5*(4), 447–454.

Farré, M., Gadja-Schrantz, K., Kantiani, L., & Barceló, D. (2009). Ecotoxicity and analysis of nanomaterials in the aquatic environment. *Analytical and Bioanalytical Chemistry*, *393*, 81–95.

Farré, M., Sanchís, J., & Barceló, D. (2011). Analysis and assessment of the occurrence, the fate and the behavior of nanomaterials in the environment. *TrAC Trends in Analytical Chemistry*, *30*(3), 517–527.

Feckler, A., Goedkoop, W., Zubrod, J. P., Schulz, R., & Bundschuh, M. (2016). Exposure pathway-dependent effects of the fungicide epoxiconazole on a decomposer-detritivore system. *Science of the Total Environment*, *571*, 992 1000.

Feng, L. J., Li, J. W., Xu, E. G., Sun, X. D., Zhu, F. P., Ding, Z., Tian, H., Dong, S. S., Xia, P. F., & Yuan, X. Z. (2019). Short-term exposure to positively charged polystyrene nanoparticles causes oxidative stress and membrane destruction in cyanobacteria. *Environmental Science: Nano*, *6*(10), 3072–3079.

Feurtet-Mazel, A., Mornet, S., Charron, L., Mesmer-Dudons, N., Maury-Brachet, R., & Baudrimont, M. (2016). Biosynthesis of gold nanoparticles by the living freshwater diatom Eolimna minima, a species developed in river biofilms. *Environmental Science and Pollution Research*, *23*(5), 4334–4339.

Finnegan, M. C., Emburey, S., Hommen, U., Baxter, L. R., Hoekstra, P. F., Hanson, M. L., Thompson, H., & Hamer, M. (2018). A freshwater mesocosm study into the effects of the neonicotinoid insecticide

thiamethoxam at multiple trophic levels. *Environmental Pollution*, *242*, 1444 1457.

Fisk, A. T., Norstrom, R. J., Cymbalisty, C. D., & Muir, D. C. (1998). Dietary accumulation and depuration of hydrophobic organochlorines: Bioaccumulation parameters and their relationship with the octanol/water partition coefficient. *Environmental Toxicology & Chemistry*, *17*, 951 961.

Fleeger, J. W., Carman, K. R., & Nisbet, R. M. (2003). Indirect effects of contaminants in aquatic ecosystems. *Science of the Total Environment*, *317*, 207 233.

Fleming, T. P., & Richards, K. S. (1982). Uptake and surface adsorption of zinc by the freshwater tubificid oligochaete Tubifex tubifex. *Comparative Biochemistry and Physiology C*, *71*, 69–75.

Flessas, C., Couillard, Y., Pinel-Alloul, B., St-Cyr, L., & Campbell, P. G. (2000). Metal concentrations in two freshwater gastropods (Mollusca) in the St. Lawrence River and relationships with environmental contam- ination. *Canadian Journal of Fisheries and Aquatic Sciences*, *57*, 126–137.

Fletcher, D. E., Lindell, A. H., Stillings, G. K., Mills, G. L., Blas, S. A., & McArthur, J. V. (2014). Spatial and taxonomic variation in trace element bioaccumulation in two herbivores from a coal combustion waste contaminated stream. *Ecotoxicology and Environmental Safety*, *101*, 196–204.

Förstner, U., & Prosi, F. (1979). *Biological Aspects of Freshwater Pollution*. Elsevier.

Fowler, S. W., Small, L. F., & Kečkeš, S. (1971). Effects of temperature and size on molting of euphausiid crustaceans. *Marine Biology*, *11*, 45–51.

Fu, L., Hamzeh, M., Dodard, S., Zhao, Y. H., & Sunahara, G. I. (2015). Effects of TiO2 nanoparticles on ROS production and growth inhibition using freshwater green algae pre-exposed to UV irradiation. *Environmental Toxicology and Pharmacology*, *39*(3), 1074–1080.

Fuller, N., Ford, A. T., Nagorskaya, L. L., Gudkov, D. I., & Smith, J. T. (2018). Reproduction in the freshwater crustacean Asellus aquaticus along a gradient of radionuclide contamination at Chernobyl. *Science of the Total Environment*, *628*, 11 17.

Gangadoo, S., Owen, S., Rajapaksha, P., Plaisted, K., Cheeseman, S., Haddara, H., Truong, V. K., Ngo, S. T., Vu, V. V., Cozzolino, D., Elbourne, A., Crawford, R., Latham, K., & Chapman, J. (2020). *Nano-plastics and their analytical characterisation and fate in the marine environment: From Source to Sea. Science of The Total Environment, p.138792.*

Gao, J., Wang, Y., Folta, K. M., Krishna, V., Bai, W., Indeglia, P., Georgieva, A., Nakamura, H., Koopman, B., & Moudgil, B. (2011). Polyhydroxy fullerenes (fullerols or fullerenols): Beneficial effects on growth and lifespan in diverse biological models. *PLoS One*, *6*(5).

Gardeström, J., Ermold, M., Goedkoop, W., & McKie, B. G. (2016). Disturbance history influences stressor impacts: Effects of a fungicide and nutrients on microbial diversity and litter decomposition. *Freshwater Biology*, *61*, 2171 2184.

Garner, K. L., Qin, Y., Cucurachi, S., Suh, S., & Keller, A. A. (2018). Linking Exposure and Kinetic Bioaccumulation Models for Metallic Engineered Nanomaterials in Freshwater Ecosystems. *Sustainable Chemistry & Engineering*, *6*(10), 12684–12694.

Gbaruko, B. C., & Igwe, J. C. (2007). Tungsten: Occurrence, Chemistry, Environmental and Health Exposure Issues. *Global Journal of Environmental Research*, *1*(1), 27–32.

Georgescu, B., Georgescu, C., Dărăban, S., Bouaru, A., & Paşcalău, S. (2011). Heavy metals acting as endocrine disrupters. *Scientific Papers: Animal Science and Biotechnologies*, *44*, 89–93.

Gerhardt, A. (1993). Review of impact of heavy metals on stream invertebrates with special emphasis on acid conditions. *Water, Air, & Soil Pollution*, *66*, 289 314.

Good, M., & Vasak, M. (1986). Iron(II)-substituted metallothionein: Evidence for the existence of iron-thiolate clusters. *Biochemistry*, *25*, 8353–8356.

Goodyear, K., & McNeill, S. (1999). Bioaccumulation of heavy metals by aquatic macroinvertebrates of different feeding guilds: A review. *Science of the Total Environment*, *229*, 1–19.

Gottschalk, F., & Nowack, B. (2011). The release of engineered nanomaterials to the environment. *Journal of Environmental Monitoring*, *5*.

Gottschalk, F., Sonderer, T., Scholz, R. W., & Nowack, B. (2010). Possibilities and limitations of modeling environmental exposure to engineered

nanomaterials by probabilistic material flow analysis. *Environmental Toxicology and Chemistry*, *29*(5), 1036–1048.

Gottschalk, F., Sun, T., & Nowack, B. (2013). Environmental concentrations of engineered nanomaterials: Review of modeling and analytical studies. *Environmental Pollution*, *181*, 287–300.

Graça, M. A. S., Maltby, L., & Calow, P. (1993). Importance of fungi in the diet of Gammarus pulex and Asellus aquaticus. *Oecologia*, *96*, 304 309.

Graça, M. A. S., Maltby, L., & Calow, P. (1994). Comparative ecology of Gammarus pulex (L.) and Asellus aquaticus (L.) I: population dynamics and microdistribution. *Hydrobiologia*, *281*, 155 162.

Green, D. W., Williams, K. A., & Pascoe, D. (1986). The acute and chronic toxicity of cadmium to different life history stages of the freshwater crustaceanAsellus aquaticus (L.) *Archives of Environmental Contamination and Toxicology*, *15*, 465–471.

Greenaway, P. (1985). Calcium balance and moulting in the Crustacea. *Biological Reviews*, *60*, 425–454.

Griboff, J., Horacek, M., Wunderlin, D. A., & Monferran, M. V. (2018). Bioaccumulation and trophic transfer of metals, As and Se through a freshwater food web affected by antrophic pollution in Córdoba, Argentina. *Ecotoxicology and Environmental Safety*, *148*, 275–284.

Hall, T. M. (1982). Free ionic nickel accumulation and localization in the freshwater zooplankter, Daphnia magna. *Limnology and Oceanography*, *27*, 718–727.

Hallouin, T., Bruen, M., Christie, M., Bullock, C., & Kelly-Quinn, M. (2018). Challenges in Using Hydrology and Water Quality Models for Assessing Freshwater Ecosystem Services: A Review. *Geosciences*, *8*(2), 45.

Ham, L., Quinn, R., & Pascoe, D. (1995). Effects of cadmium on the predator-prey interaction between the turbellarian Dendrocoelum lacteum (Müller, 1774) and the isopod crustacean Asellus aquaticus (L.) *Archives of Environmental Contamination and Toxicology*, *29*, 358 365.

Hamilton, S. J., & Mehrle, P. M. (1986). Metallothionein in Fish: Review of Its Importance in Assessing Stress from Metal Contaminants. *Transactions of the Americal Fisheries Society*, *115*(4), 596–609.

Hare, L. (1992). Aquatic insects and trace metals: Bioavailability, bioaccumulation, and toxicity. *Critical Reviews in Toxicology*, *22*, 327 369.

Hargeby, A. (1990). Effects of pH, humic substances and animal interactions on survival and physiological status of Asellus aquaticus (L.) and Gammarus pulex (L.) *Oecologia*, *82*, 348 354.

Hargeby, A., Stoltz, J., & Johansson, J. (2005). Locally differentiated cryptic pigmentation in the freshwater isopod Asellus aquaticus. *Journal Evolutionary Biology*, *18*, 713 721.

Hart, B. T., & Davies, S. H. (1981). Trace metal speciation in the freshwater and estuarine regions of the Yarra River, Victoria. *Estuarine, Coastal and Shelf Science*, *12*, 353 374.

Hasu, T., Tellervo Valtonen, E., & Jokela, J. (2006). Costs of parasite resistance for female survival and parental care in a freshwater isopod. *Oikos*, *114*, 322 328.

Hatje, V., Payne, T. E., Hill, D. M., McOrist, G., Birch, G. F., & Szymczak, R. (2003). Kinetics of trace element uptake and release by particles in estuarine waters: Effects of pH, salinity, and particle loading. *Environment International*, *29*, 619 629.

Hayes, A. W., & Sahu, S. C. (2020). Genotoxicity of engineered nanomaterials found in the human environment. *Current Opinion in Toxicology*, *19*, 68–71.

Haynes, W. M. (2014). *CRC Handbook of Chemistry and Physics*. CRC press.

He, Y., Wang, L., Ma, W., Lu, X., Li, Y., & Liu, J. (2019). Secretory expression, immunoaffinity purification and metal-binding ability of recombinant metallothionein (ShMT) from freshwater crab Sinopotamon henanense. *Ecotoxicology and Environmental Safety*, *169*, 457–463.

Holdich, D. M., & Tolba, M. R. (1981). The effect of temperature and water quality on the in vitro development and survival of Asellus aquaticus (Crustacea: Isopoda) eggs. *Hydrobiologia*, *78*, 227 236.

Homa, J., Klimek, M., Kruk, J., Cocquerelle, C., Vandenbulcke, F., & Plytycz, B. (2010). Metal-specific effects on metallothionein gene induction and riboflavin content in coelomocytes of Allolobophora chlorotica. *Ecotoxicology and Environmental Safety*, *73*, 1937–1943.

Hunting, E. R., Mulder, C., Kraak, M. H. S., Breure, A. M., & Admiraal, W. (2013). Effects of copper on invertebrate–sediment interactions. *Environmental Pollution*, *180*, 131–135.

Ieromina, O., Peijnenburg, W., De Snoo, G. R., & Vijver, M. G. (2014). Population responses of Daphnia magna, Chydorus sphaericus and Asellus aquaticus in pesticide contaminated ditches around bulb fields. *Environmental Pollution*, *192*, 196–203.

Intrchom, W., Thakkar, M., Hamilton, R. F., Holian, A., & Mitra, S. (2018). Effect of Carbon Nanotube-Metal Hybrid Particle Exposure to Freshwater Algae Chlamydomonas reinhardtii. *Scientific Reports*, *8*(1), 1–11.

Isani, G., & Carpenè, E. (2014). Metallothioneins, unconventional proteins from unconventional animals: A long journey from nematodes to mammals. *Biomolecules*, *4*, 435–457.

Jacob, C., Maret, W., & Vallee, B. L. (1998). Control of zinc transfer between thionein, metallothionein, and zinc proteins. *PNAS*, *95*(7).

Jager, T., Albert, A., Preuss, T. G., & Ashauer, R. (2011). General Unified Threshold Model of Survival – a toxicokinetic-toxicodynamic framework for ecotoxicology. *Environmental Science & Technology*, *45*, 2529–2540.

Jaiswal, D., & Pandey, J. (2020). Benthic hypoxia in anthropogenically-impacted rivers provides positive feedback enhancing the level of bioavailable metals at sediment-water interface. *Environmental Pollution*, *258*, 113643.

Javed, M. (2005). Heavy Metal Contamination of Freshwater Fish and Bed Sediments in the River Ravi Stretch and Related Tributaries. *Pakistan Journal of Biological Sciences*, *8*, 1337–1341.

Jeevanandam, J., Barhoum, A., Chan, Y. S., Dufresne, A., & Danquah, M. K. (2018). Review on nanoparticles and nanostructured materials: History, sources, toxicity and regulations. *Beilstein Journal of Nanotechnology*, *9*(1), 1050–1074.

Johnson, R. K., Wiederholm, T., & Rosenberg, D. M. (1993). Freshwater biomonitoring using individual organisms, populations, and species assemblages of benthic macroinvertebrates. In D. M. Rosenberg & V. H. Resh (Eds.), *Freshwater biomonitoring and benthic macroinvertebrates* (pp. 40–158). Chapman & Hall.

Kadukova, J. (2016). Surface sorption and nanoparticle production as a silver detoxification mechanism of the freshwater alga Parachlorella kessleri. *Bioresource Technology*, *216*, 406–413.

Kar, D., Sur, P., Mandai, S. K., Saha, T., & Kole, R. K. (2008). Assessment of heavy metal pollution in surface water. *International Journal of Environmental Science and Technology*, *5*, 119 124.

Karbalaei, S., Hanachi, P., Walker, T. R., & Cole, M. (2018). Occurrence, sources, human health impacts and mitigation of microplastic pollution. *Environmental Science and Pollution Research*, *25*(36), 36046–36063.

Kaya, H., Akbulut, M., Selvi, K., Ileri, B., & Duysak, M. (2014). Heavy metal accumulation, biomarker responses and sensitivity to oxidative stress in

Isopoda asellus aquaticus from saricay creek (canakkale-Turkey). *Ekoloji Dergisi*, *23*.

Keeler, B. L., Polasky, S., Brauman, K. A., Johnson, K. A., Finlay, J. C., O'Neill, A., Kovacs, K., & Dalzell, B. (2012). Linking water quality and well-being for improved assessment and valuation of ecosystem services. *Sustainability Science*, *109*(45).

Kepp, K. P. (2016). A quantitative scale of oxophilicity and thiophilicity. *Inorganic Chemistry*, *55*, 9461–9470.

Ketelaars, H. A., & Frantzen, N. M. (1995). One decade of benthic macroinvertebrate biomonitoring in the River Meuse. *Netherlands Journal of Aquatic Ecology*, *29*, 121 133.

Khan, F. R., Bury, N. R., & Hogstrand, C. (2010). Cadmium bound to metal rich granules and exoskeleton from Gammarus pulex causes increased gut lipid peroxidation in zebrafish following single dietary exposure. *Aquatic Toxicology*, *96*, 124–129.

Khan, I., Saeed, K., & Khan, I. (2019). Nanoparticles: Properties, applications and toxicities. *Arabian Journal of Chemistry*, *12*(7), 908–931.

Khan, R., Inam, M. A., Park, D. R., Khan, S., Akram, M., & Yeom, I. T. (2019). The Removal of CuO Nanoparticles from Water by Conventional Treatment C/F/S: The Effect of pH and Natural Organic Matter. *Molecules*, *24*(5), 914.

Kiffney, P. M., & Clements, W. H. (1996). Size-dependent response of macroinvertebrates to metals in experimental streams. *Environmental Toxicology & Chemistry*, *15*, 1352 1356.

Klaassen, C. D., Liu, J., & Choudhuri, S. (1999). Metallothionein: An intracellular protein to protect against cadmium toxicity. *Annual Review of Pharmacology and Toxicology*, *39*, 267 294.

Klavinš, M., Briede, A., Rodinov, V., Kokorite, I., Parele, E., & Klavina, I. (2000). Heavy metals in rivers of Latvia. *Science of the Total Environment*, *262*, 175–183.

Kleiven, M., Macken, A., & Oughton, D. H. (2019). Growth inhibition in Raphidocelis subcapita–Evidence of nanospecific toxicity of silver nanoparticles. *Chemosphere*, *221*, 785–792.

Koehle-Divo, V., Cossu-Leguille, C., Pain-Devin, S., Simonin, C., Bertrand, C., Sohm, B., Mouneyrac, C., Devin, S., & Giambérini, L. (2018). Genotoxicity and physiological effects of CeO2 NPs on a freshwater bivalve (Corbicula fluminea). *Aquatic Toxicology*, *198*, 141–148.

Köhler, H.-R. (2002). Localization of metals in cells of saprophagous soil arthropods (Isopoda, Diplopoda, Collembola). *Microscopy Research and Technique*, *56*, 393 401.

Koiter, A. J., Owens, P. N., Petticrew, E. L., & Lobb, D. A. (2013). The behavioural characteristics of sediment properties and their implications for sediment fingerprinting as an approach for identifying sediment sources in river basins. *Earth-Science Reviews*, *125*, 24–42.

Kojima, Y., & Kägi, J. H. R. (1978). Metallothionein. *Trends in Biochemical Sciences*, *3*(2), 90–93.

Kolaríkova, K., Stuchlík, E., Liska, M., Horecký, J., Tatosova, J., Hardekopf, D., Lapsanska, N., Horicka, Z., Hovorka, J., Mihaljevic, M., Fuksa, J. K., & Tümpling, W. (2012). Long-term changes in the bioaccumulation of as, Cd, Pb, and Hg in macroinvertebrates from the elbe river (Czech Republic). *Water, Air, & Soil Pollution, 223*, 3511 3526.

Kulacki, K. J., & Cardinale, B. J. (2012). Effects of nano-titanium dioxide on freshwater algal population dynamics. *PLoS One*, *7*(10).

Kuppusamy, M. R., & Giridhar, V. V. (2006). Factor analysis of water quality characteristics including trace metal speciation in the coastal environmental system of Chennai Ennore. *Environment International, 32*, 174 179.

Lagerspetz, K., & Mattila, M. (1961). Salinity reactions of some fresh-and brackish-water crustaceans. *The Biological Bulletin, 120*, 44 53.

Lagerspetz, K. Y. (2003). Thermal acclimation without heat shock, and motor responses to a sudden temperature change in Asellus aquaticus. *Journal of Thermal Biology, 28*, 421 427.

Lamas, S., Fernandez, J. A., Aboal, J. R., & Carballeira, A. (2007). Testing the use of juvenile Salmo trutta L. as biomonitors of heavy metal pollution in freshwater. *Chemosphere*, *67*, 221 228.

Lau, S., Mohamed, M., Yen, A. T. C., & Su'Ut, S. (1998). Accumulation of heavy metals in freshwater molluscs. *Science of the Total Environment*, *214*, 113–121.

Le Croizier, G., Lacroix, C., Artigaud, S., Le Floch, S., Raffray, J., Penicaud, V., Coquillé, V., Autier, J., Rouget, M.-L., & Le Bayon, N. (2018). Significance of metallothioneins in differential cadmium accumulation kinetics between two marine fish species. *Environmental Pollution*, *236*, 462–476.

Lebrun, J. D., Perret, M., Uher, E., Tusseau-Vuillemin, M. H., & Gourlay-Francé, C. (2011). *Waterborne nickel bioaccumulation in Gammarus pulex: Comparison of mechanistic models and influence of water cat*.

Lehutso, R. F., Tancu, Y., Maity, A., & Thwala, M. (2020). Aquatic toxicity of transformed and product-released engineered nanomaterials: An overview of the current state of knowledge. *Process Safety and Environmental Protection*, *138*, 39–56.

Levit, R., Shigaeva, T., & Kudryavtseva, V. (2020). Heavy Metals in Macrozoobenthos and Sediments of the Coastal Zone of the Eastern Gulf of Finland. *Russian Journal of General Chemistry*, *90*, 2700–2707.

Li, K., Qian, J., Wang, P., Wang, C., Liu, J., Tian, X., Lu, B., & Shen, M. (2017). Crystalline phase-dependent eco-toxicity of titania nanoparticles to freshwater biofilms. *Environmental Pollution*, *231*, 1433–1441.

Liang, D., Wang, X., Liu, S., Zhu, Y., Wang, Y., Fan, W., & Dong, Z. (2020). Factors determining the toxicity of engineered nanomaterials to

Tetrahymena thermophila in freshwater: The critical role of organic matter. *Environmental Science: Nano*.

Lin, L., Xu, M., Mu, H., Wang, W., Sun, J., He, J., Qiu, J. W., & Luan, T. (2019). Quantitative proteomic analysis to understand the mechanisms of zinc oxide nanoparticle toxicity to Daphnia pulex (Crustacea: Daphniidae): Comparing with bulk zinc oxide and zinc salt. *Environmental Science & Technology*, *53*(9), 5436–5444.

Liu, B., Ai, S., Zhang, W., Huang, D., & Zhang, Y. (2017). Assessment of the bioavailability, bioaccessibility and transfer of heavy metals in the soil-grain-human systems near a mining and smelting area in NW China. *Science of the Total Environment*, *609*, 822–829.

Liu, X., Jin, X., Cao, B., & Tang, C. Y. (2014). Bactericidal activity of silver nanoparticles in environmentally relevant freshwater matrices: Influences of organic matter and chelating agent. *Journal of Environmental Chemical Engineering*, *2*(1), 525–531.

Liu, Y., Wang, Z., Wang, S., Fang, H., Ye, N., & Wang, D. (2019). Ecotoxicological effects on Scenedesmus obliquus and Danio rerio Co-exposed to polystyrene nano-plastic particles and natural acidic organic polymer. *Environmental Toxicology and Pharmacology*, *67*, 21–28.

Lockwood, A. P. M. (1959). The osmotic and ionic regulation of Asellus aquaticus (L.) *Journal of Experimental Biology, 36*, 546 555.

Lukančič, S., Žibrat, U., Mezek, T., Jerebic, A., Simčič, T., & Brancelj, A. (2010). Effects of exposing two non-target crustacean species, Asellus aquaticus

L., and Gammarus fossarum Koch., to atrazine and imidacloprid. *Bulletin of environmental contamination and toxicology*, *84*(85).

Luoma, S. N., & Rainbow, P. S. (2005). Why Is metal bioaccumulation so variable? Biodynamics as a unifying concept. *Environmental Science & Technology*, *39*, 1921–1931.

Lv, J., Zhang, S., Luo, L., Zhang, J., Yang, K., & Christie, P. (2014). Accumulation, speciation and uptake pathway of ZnO nanoparticles in maize. *Environmental Science: Nano*, *2*, 68–77.

Ma, T., Gong, S., & Tian, B. (2017). Effects of sediment-associated CuO nanoparticles on Cu bioaccumulation and oxidative stress responses in freshwater snail Bellamya aeruginosa. *Science of the Total Environment*, *580*, 797–804.

Maceda-Veiga, A., Monroy, M., & Sostoa, A. (2012). Metal bioaccumulation in the Mediterranean barbel (Barbus meridionalis) in a Mediterranean River receiving effluents from urban and industrial wastewater treatment plants. *Ecotoxicology and Environmental Safety*, *76*, 93–101.

Mackay, D., Arnot, J. A., Gobas, F. A., & Powell, D. E. (2013). Mathematical relationships between metrics of chemical bioaccumulation in fish. *Environmental Toxicology and Chemistry*, *32*, 1459–1466.

MacNeil, C., Dick, J. T., Bigsby, E., Elwood, R. W., Ian Montgomery, W., Gibbins, C. N., & Kelly, D. W. (2002). The validity of the Gammarus:Asellus ratio as an index of organic pollution: Abiotic and biotic influences. *Water Research, 36*, 75 84.

Malakar, A., Kanel, S. R., Ray, C., Snow, D. D., & Nadagouda, M. N. (2021). Nanomaterials in the environment, human exposure pathway, and health effects: A review. *Science of the Total Environment*, *759*, 143470.

Maltby, L. (1991). Pollution as a Probe of Life-History Adaptation in Asellus aquaticus (Isopoda). *Oikos*, *61*(11).

Maltby, L. (1995). Sensitivity of the crustaceans Gammarus pulex (L.) and Asellus aquaticus (L.) to short-term exposure to hypoxia and unionized ammonia: Observations and possible mechanisms. *Water Research, 29*, 781 787.

Mantoura, R. F. C., Dickson, A., & Riley, J. P. (1978). The complexation of metals with humic materials in natural waters. *Estuarine and Coastal Marine Science, 6*, 387 408.

Mao, H., Wang, D.-H., & Yang, W.-X. (2012). The involvement of metallothionein in the development of aquatic invertebrate. *Aquatic Toxicology*, *110*, 208–213.

Markert, B. (2007). Definitions and principles for bioindication and biomonitoring of trace metals in the environment. *Journal of Trace Elements in Medicine and Biology*, *21*, 77–82.

Markert, B., Wappelhorst, O., Weckert, V., Herpin, U., Siewers, U., Friese, K., & Breulmann, G. (1999). The use of bioindicators for monitoring the heavy-metal status of the environment. *Journal of Radioanalytical and Nuclear Chemistry*, *240*, 425 429.

Martin, T. R., & Holdich, D. M. (1986). The acute lethal toxicity of heavy metals to peracarid crustaceans (with particular reference to fresh-water asellids and gammarids). *Water Research*, *20*, 1137–1147.

McGeer, J. C., Brix, K. V., Skeaff, J. M., DeForest, D. K., Brigham, S. I., Adams, W. J., & Green, A. (2003). Inverse relationship between bioconcentration factor and exposure concentration for metals: Implications for hazard assessment of metals in the aquatic environment. *Environmental Toxicology and Chemistry*, *22*, 1017–1037.

Meylan, S., Behra, R., & Sigg, L. (2003). Accumulation of copper and zinc in periphyton in response to dynamic variations of metal speciation in freshwater. *Environmental Science & Technology, 37*, 5204 5212.

Meylan, S., Behra, R., & Sigg, L. (2004). Influence of metal speciation in natural freshwater on bioaccumulation of copper and zinc in periphyton: A microcosm study. *Environmental science & technology*, *38*, 3104–3111.

Miao, A. J., Luo, Z., Chen, C. S., Chin, W. C., Santschi, P. H., & Quigg, A. (2010). Intracellular uptake: A possible mechanism for silver engineered nanoparticle toxicity to a freshwater alga Ochromonas danica. *PLoS One*, *5*(12).

Migliore, L., & Nicola Giudici, M. (1990). Toxicity of heavy metals to Asellus aquaticus (L.)(Crustacea, Isopoda). *Hydrobiologia*, *203*, 155 164.

Miramand, P., Guary, J. C., & Fowler, S. W. (1981). Uptake, assimilation, and excretion of vanadium in the shrimp, Lysmata seticaudata (Risso), and

the crab, Carcinus maenas (L). *Journal of Experimental Marine Biology and Ecology*, *49*, 267–287.

Moldovan, M., Rauch, S., Gomez, M., Antonia Palacios, M., & Morrison, G. M. (2001). Bioaccumulation of palladium, platinum and rhodium from urban particulates and sediments by the freshwater isopod Asellus aquaticus. *Water Research, 35*, 4175 4183.

Montan es, J. C., Van Hattum, B., & Deneer, J. (1995). Bioconcentration of chlorpyrifos by the freshwater isopod Asellus aquaticus (L.) in outdoor experimental ditches. *Environmental Pollution, 88*, 137 146.

Moore, J. W. (1975). The Role of Algae in the Diet of Asellus aquaticus L. and Gammarus pulex L. *Journal of Animal Ecology*, *44*, 719–730.

Moreno-Alcántar, G., Romo-Islas, G., Flores-Alamo, M., & Torrens, H. (2018). Aurophilicity vs. Thiophilicity: Directing the crystalline supramolecular arrangement in luminescent gold compounds. *New Journal of Chemistry*, *42*, 7845–7852.

Mourgaud, Y., Martinez, É., Geffard, A., Andral, B., Stanisiere, J.-Y., & Amiard, J.-C. (2002). Metallothionein concentration in the mussel Mytilus galloprovincialis as a biomarker of response to metal contamination: Validation in the field. *Biomarkers*, *7*(6).

Munk, M., Brandão, H. M., Yéprémian, C., Couté, A., Ladeira, L. O., Raposo, N. R., & Brayner, R. (2017). Effect of multi-walled carbon nanotubes on metabolism and morphology of filamentous green microalgae. *Archives of Environmental Contamination and Toxicology*, *73*(4), 649–658.

Naylor, C., Pindar, L., & Calow, P. (1990). Inter-and intraspecific variation in sensitivity to toxins; the effects of acidity and zinc on the freshwater crustaceans Asellus aquaticus (L.) and Gammarus pulex (L). *Water Research, 24*, 757 762.

Ngu, T. T., & Stillman, M. J. (2009). Metal-binding mechanisms in metallothioneins. *Dalton Transactions*, 5425–5433.

Nicola Giudici, M., Migliore, L., Gambardella, C., & Marotta, A. (1988). Effect of chronic exposure to cadmium and copper on Asellus aquaticus (L.)(Crustacea, Isopoda. *Hydrobiologia*, *157*, 265 269.

Nicola Giudici, M., Migliore, L., & Guarino, S. M. (1986). Effects of cadmium on the life cycle of Asellus aquaticus (L.) and Proasellus coxalis Dollf.(Crustacea, Isopoda). *Environmental Technology, 7*, 45 54.

Nicola Giudici, M., Migliore, L., & Guarino, S. M. (1987). Sensitivity of asellus aqua- ticus (L.) and proasellus coxalis dollf.(Crustacea, Isopoda) to copper. *Hydrobiologia*, *146*, 63 69.

Noguera-Oviedo, K., & Aga, D. S. (2016). Lessons learned from more than two decades of research on emerging contaminants in the environment. *Journal of Hazardous Materials*, *316*, 242–251.

Nriagu, J. O. (1990). Global metal pollution: Poisoning the biosphere? *Environment: Science and Policy for Sustainable Development*, *32*, 7–33.

Nugegoda, D., & Rainbow, P. S. (1987). The effect of temperature on zinc regulation by the decapod crustacean Palaemon elegans Rathke. *Ophelia*, *27*, 17–30.

Oberholster, P. J., Myburgh, J. G., Ashton, P. J., Coetzee, J. J., & Botha, A.-M. (2012). Bioaccumulation of aluminium and iron in the food chain of Lake Loskop, South Africa. *Ecotoxicology and Environmental Safety*, *75*, 134–141.

Obst, M., Oppermann-Sanio, F. B., Luftmann, H., & Steinbüchel, A. (2002). Isolation of Cyanophycin-degrading Bacteria, Cloning and Characterization of an Extracellular Cyanophycinase Gene (cphE) from Pseudomonas Anguilliseptica Strain BI the cphE Gene from P. Anguilliseptica BI encodes a Cyanophycin-Hydrolyzing Enzyme. *Journal of Biological Chemistry*, *277*(28), 25096–25105.

O'Callaghan, I., Harrison, S., Fitzpatrick, D., & Sullivan, T. (2019). The freshwater isopod Asellus aquaticus as a model biomonitor of environmental pollution: A review. *Chemosphere*, *235*, 498–509.

O'Callaghan, I., & Sullivan, T. (2020). Shedding the load: Moulting as a cause of variability in whole-body metal concentrations. *Journal of Crustacean Biology*, *40*(6), 725–733.

O'Callaghan, I., & Sullivan, T. (2021). *Legacy Sediment Contamination* (An Fóram Uisce ESR Report, p. 75) [Policy Report]. An Fóram Uisce. https://thewaterforum.ie/app/uploads/2021/10/WaterForum_LegacySedimentContamination_Report_Final.pdf

Økland, K. A. (1978). Life history and growth of Asellus aquaticus (L.) in relation to environment in a eutrophic lake in Norway. *Hydrobiologia*, *59*, 243 259.

Pagenkopf, G. K. (1983). Gill surface interaction model for trace-metal toxicity to fishes: Role of complexation, pH, and water hardness. *Environmental Science & Technology, 17*, 342 347.

Pagnanelli, F., Esposito, A., Toro, L., & Veglio, F. (2003). Metal speciation and pH effect on Pb, Cu, Zn and Cd biosorption onto Sphaerotilus natans: Langmuir-type empirical model. *Water Research, 37*, 627 633.

Palma, P., Ledo, L., & Alvarenga, P. (2015). Assessment of trace element pollution and its environmental risk to freshwater sediments influenced by anthropogenic contributions: The case study of Alqueva reservoir (Guadiana Basin). *Catena*, *128*, 174 184.

Palmer, M. A., Covich, A. P., Lake, S., Biro, P., Brooks, J. J., Cole, J., Dahm, C., Gilbert, J., Goedkoop, W., Martens, K., Verhoeven, J., & van de Bund, W. J. (2000). Linkages between Aquatic Sediment Biota and Life Above Sediments as Potential Drivers of Biodiversity and Ecological Processes: A disruption or intensification of the direct and indirect chemical, physical, or biological interactions between aquatic sediment biota and biota living above the sediments may accelerate biodiversity loss and contribute to the degradation of aquatic and riparian habitats. *BioScience*, *50*(12), 1062–1075.

Palmiter, R. D. (1998). The elusive function of metallothioneins. *Proceedings of the National Academy of Sciences*, *95*, 8428–8430.

Park, H., Ahn, I.-Y., Choi, H. J., Pyo, S. H., & Lee, H. E. (2007). Cloning, expression and characterization of metallothionein from the Antarctic clam Laternula elliptica. *Protein Expression and Purification*, *52*, 82–88.

Pascoe, D., & Carroll, K. (2004). Comparison of cadmium toxicity to Asellus aquaticus (L.) populations following 17 years isolation in pond and laboratory cultures. *Bulletin of Environmental Contamination and Toxicology, 73*, 167 173.

Pedersen, S. N., Pedersen, K. L., Højrup, P., Depledge, M. H., & Knudsen, J. (1996). Primary structures of decapod crustacean metallothioneins with special emphasis on freshwater and semi-terrestrial species. *Biochemical Journal*, *319*, 999–1003.

Peeters, E. T., De Jager, T. J., Beijer, J. A., & Koelmans, A. A. (2000). Effects of benzo (a) pyrene and size of organic matter particles on bioaccumulation and growth of Asellus aquaticus. *Archives of Environmental Contamination and Toxicology, 39*, 307 314.

Peijnenburg, W. J. G. M., Posthuma, L. H. J. P., Eijsackers, H. J. P., & Allen, H. E. (1997). A conceptual framework for implementation of bioavailability of metals for environmental management purposes. *Ecotoxicology and Environmental Safety*, *37*, 163–172.

Pérez-Rafael, S., Mezger, A., Lieb, B., Dallinger, R., Capdevila, M., Palacios, Ò., & Atrian, S. (2012). The metal binding abilities of Megathura crenulata metallothionein (McMT) in the frame of Gastropoda MTs. *Journal of Inorganic Biochemistry*, *108*, 84–90.

Persson, L. (1983). Food consumption and competition between age classes in a perch Perca fluviatilis population in a shallow eutrophic lake. *Oikos*, *197e207*.

Pham, T. L. (2019). Effect of Silver Nanoparticles on Tropical Freshwater and Marine Microalgae. *Journal of Chemistry*.

Phillips, D. J. (1977). The use of biological indicator organisms to monitor trace metal pollution in marine and estuarine environments – a review. *Environmental Pollution*, *13*, 281–317.

Piccinno, F., Gottschalk, F., Seeger, S., & Nowack, B. (2012). Industrial production quantities and uses of ten engineered nanomaterials in Europe and the world. *Journal of Nanoparticle Research*, *14*(9), 1109.

Pinto da Costa, J. (2016). (Nano)plastics in the environment – Sources, fates and effects. *Science of the Total Environment*, *566–567*, 15–26.

Plahuta, M., Tisler, T., Pintar, A., & Toman, M. J. (2015). Adverse effects of bisphenol A on water louse (Asellus aquaticus). *Ecotoxicology and Environmental Safety*, *117*, 81 88.

Plahuta, M., Tisler, T., Toman, M. J., & Pintar, A. (2017). Toxic and endocrine disrupting effects of wastewater treatment plant influents and effluents on a freshwater isopod Asellus aquaticus (Isopoda, Crustacea). *Chemosphere*, *174*, 342 353.

Plant Protection Products, E. F. S. A. P., Residues, Ockleford, C., Adriaanse, P., Berny, P., Brock, T., Duquesne, S., Grilli, S., Hernandez-Jerez, A. F., Hougaard Bennekou, S., Klein, M., Kuhl, T., Laskowski, R., Machera,

K., Pelkonen, O., Pieper, S., Smith, R. H., Stemmer, M., Sundh, I., … Teodorovic, I. (2018). Scientific Opinion on the state of the art of Toxicokinetic/Toxicodynamic (TKTD) effect models for regulatory risk assessment of pesticides for aquatic organisms. *EFSA Journal*, *16*, 05377.

Porath, J., Maisano, F., & Belew, M. (1985). Thiophilic adsorption-a new method for protein fractionation. *FEBS Letters*, *185*, 306–310.

Pourang, N. (1996). Heavy metal concentrations in surficial sediments and benthic macroinvertebrates from Anzali wetland, Iran. *Hydrobiologia*, *331*, 53–61.

Poynton, H. C., Lazorchak, J. M., Impellitteri, C. A., Blalock, B. J., Rogers, K., Allen, H. J., Loguinov, A., Heckman, J. L., & Govindasmawy, S. (2012). Toxicogenomic responses of nanotoxicity in Daphnia magna exposed to silver nitrate and coated silver nanoparticles. *Environmental Science & Technology*, *46*(11), 6288–6296.

Pueyo, M., Rauret, G., Lück, D., Yli-Halla, M., Muntau, H., Quevauviller, P., & López-Sánchez, J. F. (2001). Certification of the extractable contents of Cd, Cr, Cu, Ni, Pb and Zn in a freshwater sediment following a collaboratively tested and optimized three-step sequential extraction procedure. *Journal of Environmental Monitoring*, *3*, 243–250.

Qian, H., Zhu, K., Lu, H., Lavoie, M., Chen, S., Zhou, Z., Deng, Z., Chen, J., & Fu, Z. (2016). Contrasting silver nanoparticle toxicity and detoxification strategies in Microcystis aeruginosa and Chlorella vulgaris: New insights

from proteomic and physiological analyses. *Science of the Total Environment*, *572*, 1213–1221.

Qiao, P., Gobas, F., & Farrell, A. P. (2000). Relative contributions of aqueous and dietary uptake of hydrophobic chemicals to the body burden in juvenile rainbow trout. *Archives of Environmental Contamination and Toxicology, 39*, 369 377.

Rae, I. B., & Gibb, S. W. (2003). Removal of metals from aqueous solu- tions using natural chitinous materials. *Water Science & Technology*, *47*, 189–196.

Rainbow, P. S. (1995). Biomonitoring of heavy metal availability in the marine environment. *Marine Pollution Bulletin, 31*, 183 192.

Rainbow, P. S. (2006). Trace metal bioaccumulation: Models, metabolic availability and toxicity. *Environment International*, *33*(4), 576–582.

Rainbow, P. S., & Luoma, S. N. (2011). Metal toxicity, uptake and bioaccumulation in aquatic invertebrates – modelling zinc in crustaceans. *Aquatic Toxicology*, *105*, 455–465.

Rask, M., & Hiisivuori, C. (1985). The predation on Asellus aquaticus (L.) by perch, Perca fluviatilis (L.), in a small forest lake. *Hydrobiologia*, *121*, 27 33.

Rasmussen, J. J., Wiberg-Larsen, P., Baattrup-Pedersen, A., Cedergreen, N., McKnight, U. S., Kreuger, J., Jacobsen, D., Kristensen, E. A., & Friberg, N. (2015). The legacy of pesticide pollution: An overlooked factor in current risk assessments of freshwater systems. *Water Research, 84*, 25 32.

Rauch, S., & Morrison, G. M. (1999). Platinum uptake by the freshwater isopod Asellus Aquaticus in urban rivers. *Science of the Total Environment, 235*, 261 268.

Resh, V. H. (2008). Which group is best? Attributes of different biological assemblages used in freshwater biomonitoring programs. *Environmental Monitoring and Assessment*, *138*, 131–138.

Reuter, J. H., & Perdue, E. M. (1977). Importance of heavy metal-organic matter interactions in natural waters. *Geochimica Er Cosmochimica Acta*, *41*(2), 325–334.

Revel, M., Châtel, A., & Mouneyrac, C. (2017). Omics tools: New challenges in aquatic nanotoxicology? *Aquatic Toxicology*, *193*, 72–85.

Richards, M. P. (1989). Recent Developments in Trace Element Metabolism and Function: Role of Metallothionein in Copper and Zinc Metabolism. *The Journal of Nutrition*, *119*(7), 1062–1070.

Richardson, G. M., Garrett, R., Mitchell, I., Mah-Poulson, M., & Hackbarth, T. (2001). Critical review on natural global and regional emis- sions of six trace metals to the atmosphere. Final Report. *Prepared for the International Lead Zinc Research Organisation, the International Copper Association, and the Nickel Producers Environmental Research Association*, *ttps://www.echa.europa.eu/documents/10162/13630/ vrar_appendix_p2_en.pdf].*

Richter, S., & Nagel, R. (2007). Bioconcentration, biomagnification and metabolism of 14C-terbutryn and 14C-benzo [a] pyrene in Gammarus fossarum and Asellus aquaticus. *Chemosphere*, *66*, 603 610.

Robinson, K. A., Baird, D. J., & Wrona, F. J. (2003). Surface metal adsorp- tion on zooplankton carapaces: Implications for exposure and effects in consumer organisms. *Environmental Pollution*, *122*, 159–167.

Rocha, T. L., Bilbao, E., Cardoso, C., Soto, M., & Bebianno, M. J. (2018). Changes in metallothionein transcription levels in the mussel Mytilus galloprovincialis exposed to CdTe quantum dots. *Ecotoxicology*, *27*, 402–410.

Rohatgi, A. (2020). *WebPlotDigitizer, Version 4.2*. URL https://automeris.io/WebPlotDigitizer.

Rosado, D., Usero, J., & Morillo, J. (2016). Ability of 3 extraction methods (BCR, Tessier and protease K) to estimate bioavailable metals in sediments from Huelva estuary (Southwestern Spain). *Marine Pollution Bulletin*, *102*(1), 65–71.

Roshchin, V. E., & Mazelev, K. L. (1979). The influence of constant temperature on the embryonic growth of Asellus aquaticus L.(Crustacea)[Translation from: Vestsi Akademii Navuk Belorusskoi SSR. *Seriya Biyal*, *1979*(1), 128 130.

Rossi, L., & Fano, A. E. (1979). Role of fungi in the trophic niche of the congeneric detritivorous Asellus aquaticus and A. coxalis (Isopoda). *Oikos*, 32(3), 380-385.

Ruchter, N., Zimmermann, S., & Sures, B. (2015). *Field Studies on PGE in Aquatic Ecosystems*. Springer.

Ryan, P. A. (1991). Environmental effects of sediment on New Zealand streams: A review. *New Zealand Journal of Marine and Freshwater Research*, *25*(2), 207–221.

Sahu, C., & Basti, S. (2021). Trace metal pollution in the environment: A review. *International Journal of Environmental Science and Technology*, *18*, 211–224.

Sakan, S. M., ĐorCevic, D. S., Manojlovic, D. D., & Predrag, P. S. (2009). Assessment of heavy metal pollutants accumulation in the Tisza river sediments. *Journal of Environmental Management, 90*, 3382 3390.

Sako, A., Lopes, L., & Roychoudhury, A. N. (2009). Adsorption and surface complexation modeling of palladium, rhodium and platinum in surficial semi-arid soils and sediment. *Applied Geochemistry*, *24*, 86 95.

Saleem, M., Iqbal, J., & Shah, M. H. (2015). Geochemical speciation, anthropogenic contamination, risk assessment and source identification of selected metals in freshwater sediments—A case study from Mangla Lake, Pakistan. *Environmental Nanotechnology, Monitoring & Management*, *4*, 27–36.

Salt, D. E., Blaylock, M., Kumar, N. P., Dushenkov, V., Ensley, B. D., Chet, I., & Raskin, I. (1995). Phytoremediation: A novel strategy for the removal of toxic metals from the environment using plants. *Nature Biotechnology*, *13*(468).

Samuel, M. S., Datta, S., Khandge, R. S., & Selvarajan, E. (2021). A state of the art review on characterization of heavy metal binding metallothioneins proteins and their widespread applications. *Science of the Total Environment*, 145829.

Santoro, A., Blo, G., Mastrolitti, S., & Fagioli, F. (2009). Bioaccumulation of heavy metals by aquatic macroinvertebrates along the Basento River in the South of Italy. *Water, Air, & Soil Pollution*, *201*, 19–31.

Savage, A., & Hogarth, P. J. (1999). An analysis of temperature-induced fluctuating asymmetry in Asellus aquaticus (Linn). *Hydrobiologia*, *411*, 139 143.

Sedlakova-Kadukova, J., & Pristas, P. (2019). Study of Mechanisms Used by Algae to Decrease The Silver Toxicity in Aquatic Environment. *Inżynieria Mineralna*, *21*.

Selck, H., Drouillard, K., Eisenreich, K., Koelmans, A. A., Palmqvist, A., Ruus, A., Salvito, D., Schultz, I., Stewart, R., & Weisbrod, A. (2012). Explaining differences between bioaccumulation measurements in laboratory and field data through use of a probabilistic modeling approach. *Integrated Environmental Assessment and Management*, *8*, 42–63.

Sendra, M., Yeste, M. P., Gatica, J. M., Moreno-Garrido, I., & Blasco, J. (2017). Direct and indirect effects of silver nanoparticles on freshwater and marine microalgae (Chlamydomonas reinhardtii and Phaeodactylum tricornutum). *Chemosphere*, *179*, 279–289.

Shen, M., Zhang, Y., Zhu, Y., Song, B., Zeng, G., Hu, D., Wen, X., & Ren, X. (2019). Recent advances in toxicological research of nanoplastics in the environment: A review. *Environmental Pollution*, *252*, 511–521.

Sigel, A., Operschall, B. P., Sigel, R. K., & Sigel, H. (2018). Metal ion complexes of nucleoside phosphorothioates reflecting the ambivalent properties of lead (II). *New Journal of Chemistry*, *42*, 7551–7559.

Simčič, T., & Brancelj, A. (2006). Effects of pH on electron transport system (ETS) activity and oxygen consumption in Gammarus fossarum, Asellus aquaticus and Niphargus sphagnicolus. *Freshwater Biology*, *51*, 686–694.

Sket, B. (1994). Distribution of Asellus aquaticus (Crustacea: Isopoda: Asellidae) and its hypogean populations at different geographic scales, with a note on Proasellus istrianus. *Hydrobiologia*, *287*, 39 47.

Smith, D. S., Bell, R. A., & Kramer, J. R. (2002). Metal speciation in natural waters with emphasis on reduced sulfur groups as strong metal binding sites. *Comparative Biochemistry and Physiology Part C: Toxicology & Pharmacology*, *133*(1–2), 65–74.

Soazig, L., & Marc, L. (2003). Potential use of the levels of the mRNA of a specific metallothionein isoform (MT-20) in mussel (Mytilus edulis) as a biomarker of cadmium contamination. *Marine Pollution Bulletin*, *46*, 1450–1455.

Späth, R., Flemming, H.-C., & Wuertz, S. (1998). Sorption properties of biofilms. *Water Science & Technology*, *37*, 207–210.

Stead-Dexter, K., & Ward, N. I. (2004). Mobility of heavy metals within freshwater sediments affected by motorway stormwater. *Science of the Total Environment*, *334*, 271–277.

Steel, E. A. (1961). Some observations on the life history of Asellus aquaticus (L.) and Asellus meridianus Racovitza (Crustacea: Isopoda). *Proceedings of the Zoological Society of London*, *137*, 71–87.

Suedel, B., Boraczek, J., & Peddicord, R. (1994). Trophic transfer and biomagnification potential of contaminants in aquatic ecosystems. *Reviews of Environmental Contamination and Toxicology*, *136*, 21–89.

Sumi, N., & Chitra, K. C. (2019). Cytogenotoxic effects of fullerene C60 in the freshwater teleostean fish, Anabas testudineus (Bloch, 1792). *Mutation Research/Genetic Toxicology and Environmental Mutagenesis*, *847*, 503104.

Sures, B., & Taraschewski, H. (1995). Cadmium concentrations in two adult acanthocephalans, Pomphorhynchus laevis andAcanthocephalus lucii, as compared with their fish hosts and cadmium and lead levels in larvae ofA. lucii as compared with their crustacean host. *Parasitology Research*, *81*, 494–497.

Swartwout, M. C., Keating, F., & Frimpong, E. A. (2016). A survey of macroinvertebrates colonizing bluehead chub nests in a Virginia stream. *Journal of Freshwater Ecology*, *31*, 147–152.

Sworobowicz, L., Grabowski, M., Mamos, T., Burzynski, A., Kilikowska, A., Sell, J., & Wysocka, A. (2015). Revisiting the phylogeography of Asellus

aquaticus in Europe: Insights into cryptic diversity and spatiotemporal diversification. *Freshwater Biology*, *60*, 1824 1840.

Taheran, M., Naghdi, M., Brar, S. K., Verma, M., & Surampalli, R. Y. (2018). Emerging contaminants: Here today, there tomorrow! *Environmental Nanotechnology, Monitoring & Management*, *10*, 122–126.

Talbot, V., & Magee, R. J. (1978). Naturally-occurring heavy metal binding proteins in invertebrates. *Archives of Environmental Contamination and Toxicology, 7*, 73 81.

Tao, X., Li, C., Zhang, B., & He, Y. (2016). Effects of aqueous stable fullerene nanocrystals (nC60) on the food conversion from Daphnia magna to Danio rerio in a simplified freshwater food chain. *Chemosphere*, *145*, 157–162.

Taylor, C., Matzke, M., Kroll, A., Read, D. S., Svendsen, C., & Crossley, A. (2016). Toxic interactions of different silver forms with freshwater green algae and cyanobacteria and their effects on mechanistic endpoints and the production of extracellular polymeric substances. *Environmental Science: Nano*, *3*(2), 396–408.

ter Halle, A., & Ghiglione, J. F. (2021). Nanoplastics: A Complex, Polluting Terra Incognita. *Environmental Science & Technology*, *55*(21), 14466–14469.

Tessier, A., Campbell, P. G. C., & Bisson, M. (1979). Sequential extraction procedure for the speciation of particulate trace metals. *Analytical Chemistry*, *51*(7), 844–851.

Thevenon, F., Graham, N. D., Chiaradia, M., Arpagaus, P., Wildi, W., & Poté, J. (2011). Local to regional scale industrial heavy metal pollution recorded in sediments of large freshwater lakes in central Europe (lakes Geneva and Lucerne) over the last centuries. *Science of the Total Environment*, *412*, 239–247.

Thorp, J. H., & Bergey, E. (1981). Field experiments on responses of a freshwater, benthic macroinvertebrate community to vertebrate predators. *Ecology*, *62*, 365–375.

Tingley, D., Yamamoto, T., Hirose, K., Keele, L., & Imai, K. (2014). Mediation: R package for causal mediation analysis. *Journal of Statistical Software*, *59*, 1–38.

Tipping, E., Rey-Castro, C., Bryan, S. E., & Hamilton-Taylor, J. (2002). Al (III) and Fe (III) binding by humic substances in freshwaters, and implications for trace metal speciation. *Geochimica et Cosmochimica Acta*, *66*, 3211 3224.

Tolba, M. R., & Holdich, D. M. (1981). The effect of water quality on the size and fecundity of Asellus aquaticus (Crustacea: Isopoda). *Aquatic Toxicology*, *1*, 101 112.

Topcuoğlu, S., Birol, E., & Ünlü, M. Y. (1987). Factors affecting the accumulation and elimination of silver (110mAg) in marine isopods. *Marine Environmental Research*, *21*, 189–198.

Torre, F. R., Ferrari, L., & Salibian, A. (2002). Freshwater pollution biomarker: Response of brain acetylcholinesterase activity in two fish species. *Comparative Biochemistry and Physiology Part C: Toxicology & Pharmacology*, *131*, 271 280.

Truchet, D. M., Buzzi, N. S., Simonetti, P., & Marcovecchio, J. E. (2020). Uptake and detoxification of trace metals in estuarine crabs: Insights into the role of metallothioneins. *Environmental Science and Pollution Research*, *27*, 31905–31917.

Tuccillo, M. E. (2006). Size fractionation of metals in runoff from residential and highway storm sewers. *Science of the Total Environment, 355*, 288 300.

Turk S, S. Ş., Sket B. (1996). Comparison between some epigean and hypogean populations of Asellus aquaticus (Crustacea: Isopoda): Asellidae. *Hydrobiologia*, *337*, 161–170.

Turk-Prevorcnik, S., & Blejec, A. (1998). Asellus aquaticus infernus, new subspecies (Isopoda: Asellota: Asellidae), from Romanian hypogean waters. *Journal of Crustacean Biology*, *18*, 763 773.

Ure, A. M. (1996). Single extraction schemes for soil analysis and related applications. *Science of the Total Environment*, *178*, 3–10.

U.S. Environmental Protection Agency. (2005). *Contaminated Sediment Remediation Guidance for Hazardous Waste Sites* (EPA-540-R-05-012).

Usseglio-Polatera, P., Bournaud, M., Richoux, P., & Tachet, H. (2000). *Biomonitoring through biological traits of benthic macroinvertebrates: How to use*

species trait databases? Assessing the Ecological Integrity of Running Waters Springer.

van den Brink, N. W., Kokalj, A. J., Silva, P. V., Lahive, E., Norrfors, K., Baccaro, M., Khodaparast, Z., Loureiro, S., Drobne, D., Cornelis, G., & Lofts, S. (2019). Tools and rules for modelling uptake and bio-accumulation of nanomaterials in invertebrate organisms. *Environmental Science: Nano*, *6*, 1985–2001.

Van Ginneken, M., Blust, R., & Bervoets, L. (2018). Combined effects of metal mixtures and predator stress on the freshwater isopod Asellus aquaticus. *Aquatic Toxicology*, *200*, 148 157.

Van Ginneken, M., De Jonge, M., Bervoets, L., & Blust, R. (2015). Uptake and toxicity of Cd, Cu and Pb mixtures in the isopod Asellus aquaticus from waterborne exposure. *Science of the Total Environment, 537*, 170 179.

Van Hattum, B., De Voogt, P., Bosch, L., Van Straalen, N. M., Joosse, E. N. G., & Govers, H. (1989). Bioaccumulation of cadmium by the freshwater isopod Asellus aquaticus (L.) from aqueous and dietary sources. *Environmental Pollution*, *62*, 129–151.

Veglio, F., & Beolchini, F. (1997). Removal of metals by biosorption: A review. *Hydrometallurgy*, *44*, 301 316.

Vergani, L., Grattarola, M., Borghi, C., Dondero, F., & Viarengo, A. (2005). Fish and molluscan metallothioneins: A structural and functional comparison. *The FEBS Journal*, *272*, 6014–6023.

Vergani, L., Grattarola, M., Grasselli, E., Dondero, F., & Viarengo, A. (2007). Molecular characterization and function analysis of MT-10 and MT-20 metallothionein isoforms from Mytilus galloprovincialis. *Archives of Biochemistry and Biophysics*, *465*, 247–253.

Verovnik, R., Sket, B., & Trontelj, P. (2005). The colonization of Europe by the freshwater crustacean Asellus aquaticus (Crustacea: Isopoda) proceeded from ancient refugia and was directed by habitat connectivity. *Molecular Ecology*, *14*, 4355 4369.

Verrell, P. A. (1985). Predation and the evolution of precopula in the isopod Asellus aquaticus. *Behaviour,* 95(3), 198–202.

Viarengo, A., Burlando, B., Cavaletto, M., Marchi, B., Ponzano, E., & Blasco, J. (1999). Role of metallothionein against oxidative stress in the musselMytilus galloprovincialis. *Comparative Physiology*, *277*(6), 1612–1619.

Vicari, T., Dagostim, A. C., Klingelfus, T., Galvan, G. L., Monteiro, P. S., Silva Pereira, L., Assis, H. C. S., & Cestari, M. M. (2018). Co-exposure to titanium dioxide nanoparticles (NpTiO2) and lead at environmentally relevant concentrations in the Neotropical fish species Hoplias intermedius. *Toxicology Reports*, *5*, 1032–1043.

Vijver, M. G., Elliott, E. G., Peijnenburg, W. J., & De Snoo, G. R. (2011). Response predictions for organisms water-exposed to metal mixtures: A meta-analysis. *Environmental Toxicology & Chemistry*, *30*, 1482 1487.

Vijver, M. G., Van Gestel, C. A., Lanno, R. P., Van Straalen, N. M., & Peijnenburg, W. J. (2004). Internal metal sequestration and its eco-toxicological relevance: A review. *Environmental Science & Technology*, *38*, 4705–4712.

Wang, C., Shu, F., Hong, Y., Wang, J., Peng, K., Sheng, J., Wu, D., Hu, B., Shi, J., & Jian, S. (2018). Analysis of the structure and activity of the promoter regions of the metallothionein genes of the freshwater pearl mussel Hyriopsis schlegelii. *Bioscience, Biotechnology, and Biochemistry*, *82*, 780–791.

Wang, J.-X., Xu, D.-M., Fu, R.-B., & Chen, J.-P. (2021). Bioavailability assessment of heavy metals using various multi-element extractants in an indigenous zinc smelting contaminated site, southwestern china. *International Journal of Environmental Research and Public Health*, *18*(16), 8560.

Wang, K., Li, Q., Zhou, Q., & Dong, Y. (2021). The Influence of Anisotropic Sediment Layer on Dissolved Oxygen Transfer in Turbulent Flows. *Water Resources Research*, *57*(2), e2020WR027932.

Wang, W.-X., & Tan, Q.-G. (2019). Applications of dynamic models in predicting the bioaccumulation, transport and toxicity of trace metals in aquatic organisms. *Environmental Pollution*, *252*, 1561–1573.

Warren, L. A., & Haack, E. A. (2001). Biogeochemical controls on metal behaviour in freshwater environments. *Earth-Science Reviews*, *54*, 261 320.

Watras, C., Back, R., Halvorsen, S., Hudson, R., Morrison, K., & Wente, S. (1998). Bioaccumulation of mercury in pelagic freshwater food webs. *Science of the Total Environment*, *219*, 83–208.

Weisbrod, A. V., Woodburn, K. B., Koelmans, A. A., Parkerton, T. F., McElroy, A. E., & Borgå, K. (2009). Evaluation of bioaccumulation using in vivo laboratory and field studies. *Integrated Environmental Assessment and Management: An International Journal*, *5*, 598–623.

Weltje, L. (2006). Effects of endocrine disrupting compounds and temperature on the moulting frequency of the freshwater isopod Asellus aquaticus L. (Isopoda: Asellota). *Acta Biologica Benrodis*, *13*, 105–115.

Whitehurst, I. (1991). The Gammarus:Asellus ratio as an index of organic pollution. *Water Research*, *25*, 333–339.

Wik, A., & Dave, G. (2009). Occurrence and effects of tire wear particles in the environment – A critical review and an initial risk assessment. *Environmental Pollution*, *157*(1), 1–11.

Williams, W. D. (1962). Notes on the ecological similarities of asellus aquaticus (L.) and A. meridianus rac. (Crust., Isopoda). *Hydrobiologia*, *20*, 1–30.

Wolff, W. J. (1973). The distribution of Asellus aquaticus (L.) and Proasellus meridianus (Rac.) in the southwestern part of The Netherlands. *Hydrobiologia*, *42*(4), 381–392.

Wong, D. L., & Stillman, M. J. (2018). Metallothionein: An aggressive scavenger—The metabolism of rhodium (II) tetraacetate (Rh2 (CH3CO2) 4. *ACS Omega*, *3*, 16314–16327.

Wormington, A. M., Coral, J., Alloy, M. M., Delmarè, C. L., Mansfield, C. M., Klaine, S. J., Bisesi, J. H., & Roberts, A. P. (2017). Effect of natural

organic matter on the photo-induced toxicity of titanium dioxide nanoparticles. *Environmental Toxicology and Chemistry*, *36*(6), 1661–1666.

Wu, D., Ma, Y., Cao, Y., & Zhang, T. (2020). Mitochondrial toxicity of nanomaterials. *Science of The Total Environment*, *702*, 134994.

Yang, H. Z., Gu, W. J., Chen, W., Hwang, J. S., & Wang, L. (2019). Metal binding characterization of heterologously expressed metallothionein of the freshwater crab Sinopotamon henanense. *Chemosphere*, *235*, 926–934.

Zhao, C. M., & Wang, W. X. (2012). Importance of surface coatings and soluble silver in silver nanoparticles toxicity to Daphnia magna. *Nanotoxicology*, *6*(4), 361–370.

Zhao, J., Cao, X., Wang, Z., Dai, Y., & Xing, B. (2017). Mechanistic understanding toward the toxicity of graphene-family materials to freshwater algae. *Water Research*, *111*, 18–27.

Zhao, J., Dai, Y., Wang, Z., Ren, W., Wei, Y., Cao, X., & Xing, B. (2018). Toxicity of GO to freshwater algae in the presence of Al2O3 particles with different morphologies: Importance of heteroaggregation. *Environmental Science & Technology*, *52*(22), 13448–13456.

Zheng, Y., & Nowack, B. (2022). Meta-analysis of Bioaccumulation Data for Non-dissolvable Engineered Nanomaterials in Freshwater Aquatic Organisms. *Environmental Toxicology and Chemistry*.

Table of Figures

Figure 1: Illustration of the photocatalytic mechanisms TiO_2-NP may undergo when subjected to UV irradiation, where the radiation energy (hv) is greater than the band gap energy. Reactive Oxygen Species (ROS) produced include the hydroxyl radical ($OH^{\cdot}$), superoxide radical ($O_2^{\cdot -}$) and the non-radical reactive hydrogen peroxide (H_2O_2) molecule.....14

Figure 2: Illustration of electrochemical mechanisms near the charged surface of a cell membrane. The Zeta Potential is defined as the Electric Potential at the interface between the Stern Layer, containing charges strongly bound to the surface, and the Diffuse Layer, containing charges loosely attracted to the surface. 19

Figure 3: Illustration of common uptake (ingestion and adsorption), depuration (excretion) and bioaccumulation pathways of metal contaminants in the freshwater isopod, Asellus aquaticus. Uptake and depuration pathways occur at the organism-environment interface, while bioaccumulation occurs within the cell through the binding of contaminants with receptor molecules. Additional pathways of uptake and depuration include respiratory intake of suspended contaminants from the water phase and desorption of surface-bound contaminants, respectively. 23

Figure 4: Comparison of existing techniques for the quantification of environmental contaminants. Direct measurement can be costly for some analysis types, and relies on post-hoc estimation of ecological impact from environmental concentrations. Traditional biomonitoring assumes that a biological response acts as an effective proxy for environmental presence and/or impact of a contaminant. Passive sampling improves upon direct measurement by selectively amplifying target analytes, but suffers from the additional drawbacks of fouling and selectivity. This thesis proposes that bioaccumulative amplification offers many advantages over these established methods.....30

Figure 5: The freshwater isopod, Asellus aquaticus, has been proposed as a suitable candidate species for use in biomonitoring programmes due to its abundance, range, position at the base of the aquatic food web and tolerance to various contaminants. Image source: "Asellus aquaticus" by Stephen J. McWilliam, iNaturalist (CC0 1.0 Universal). 40

Figure 6: The Periodic Table of Thiophilicity, according to Kepp, 2016. Each element is assigned a value according to their relative affinities to S and O, with higher values denoting a higher affinity to S relative to O. Elements have been colour-coded accordingly. 76

Figure 7: Map of sampling sites (yellow points) for thiophilicity study, located at 51°52'29.5"N, 8°29'00.8"W (T1) and 51°52'30.0"N, 8°29'02.6"W (T2) on the Tramore River (blue line), Cork City, Ireland. 80

Figure 8: Correlation between position on the TS (S) and sediment-associated bioaccumulation factor (BAF_S). Different values of elemental thiophilicity are represented by horizontal position and colour. With the exception of the elements with S=0.9, S values have been rounded down to the nearest multiple of 0.2 for illustrative clarity, and elements with the same thiophilicity have been amalgamated. Pb has been excluded from the calculation of the trend line (shaded area showing 95% confidence interval; $p = .004$, $R^2 = 0.276$).....89

Figure 9: Correlation between position on the TS (S) and sediment-associated bioaccumulation factor (BAF_S), after stratification by species. Different values of elemental thiophilicity are represented by horizontal position and colour. Pb has been excluded from the calculation of the trend line (shaded area showing 95% confidence interval; Asellus aquaticus: $p = .020$, $R^2 = 0.332$; Gammarus sp.: $p = .094$, $R^2 = 0.255$).....90

Figure 10: Correlation between position on the TS (S) and sediment-associated bioaccumulation factor (BAF_S), for a range of previously-published studies. Different values of elemental thiophilicity are represented by horizontal position and colour. Each dot represents a single data point, and the outline represents the normalised distribution of BAF_S values. Pb was omitted from the analysis and determination of the trend line (shaded area showing 95% confidence interval; $p < .001$, $R^2 = 0.409$), but is shown here for illustration.....92

Figure 11: Correlation between position on the TS (S) and sediment-associated bioaccumulation factor (BAF_S) for a range of previously-published studies, after stratification by study. Different values of elemental thiophilicity are represented by horizontal position and colour. Pb was omitted from the analysis and determination of the trend line (shaded area showing 95% confidence interval), but is shown here for illustration. The elements included in each study are listed in Table 2.....93

Figure 12: Map of sampling sites, shown as pink points, for field validation study. A range of freshwater sites with differing characteristics were chosen on the Garryduff (S1: 51°52'36.4"N, 8°23'27.9"W), Tramore (S2: 51°52'22.2"N, 8°27'19.8"W), Owenabue (S3: 51°49'19.1"N, 8°25'18.2"W), Stick (S4: 51°44'25.8"N, 8°29'16.5"W) and Ballybrack (S5: 51°52'10.6"N, 8°26'14.3"W) Rivers..... 101

Figure 13: Histogram of BAFW or accumulation factor from water to benthic macroinvertebrate samples. Most samples exhibted macroinvertebrate matrix concentrations exceeding water matrix concentrations by factors

of 10,000-100,000. The observed values approximate a Gaussian distribution. 104

Figure 14: Correlation between position on the thiophilic scale and BAFS from analysis of field samples (shaded area showing 95% confidence interval; $p < .001$). Different values of elemental thiophilicity are represented by horizontal position and colour. 105

Figure 15: Increased sediment concentrations of Sn, Pd, Ag & Pt were observed at Site 5, compared to other sites. It was noted that Site 5 was located downstream of a garage and active construction site, which may have contributed to heightened concentrations of metals at this site. 107

Figure 16: Increased concentrations of Cr, Fe & Ti were observed in both macroinvertebrate and sediment samples from sites 1 & 2. Cr concentrations can be read from the top axis, while Fe and Ti concentrations can be read from the bottom axis. Site 1 was located adjacent to historical mill and railway station sides, while site 2 was located adjacent to a motocross racing circuit. 108

Figure 17: SEM images showing size and morphology of (a) $bTiO_2$, (b) $nTiO_2$, and (c) $nBaTiO_3$ exposure analytes. These images confirm nanoscale sizing of $nTiO_2$ and $nBaTiO_3$, and macroscale sizing of $bTiO_2$, as well as overall spherical geometry. 118

Figure 18: Comparison of bioaccumulated Ti from exposure of Asellus aquaticus to TiO_2 in nanopowder ($nTiO_2$, blue) and bulk powder ($bTiO_2$, green) forms. It was observed that the nanoscale form was more readily bioaccumulated than the bulk form. 121

Figure 19: Comparison of bioaccumulated Ti from nanopowder TiO_2 ($nTiO_2$, blue) and combined Ba and Ti from nanopowder $BaTiO_3$ ($nBaTiO_3$, red). It was observed that overall ion bioaccumulation from both nanoscale analytes was comparable. 122

Figure 20: Comparison of bioaccumulated Ti from nanopowder TiO_2 ($nTiO_2$, blue), and Ba (red) & Ti (orange), respectively, from nanopowder $BaTiO_3$ ($nBaTiO_3$). The Ba ionic component was more readily bioaccumulated than the Ti ionic component from $nBaTiO_3$, which was less readily accumulated than that of the $nTiO_2$, despite occurring in identical concentrations. 124

Figure 21: Comparison of bioaccumulated Ti from nanopowder TiO_2 ($nTiO_2$, blue), and W from nanopowder WC (nWC, purple). It was found that the nWC was more readily bioaccumulated than $nTiO_2$. 125

Figure 22: Schematic representation of a general overview of the major pathways of metal pollutant uptake (via ingestion, respiration and adsorption), translocation, and loss (via moulting) in a moulting aquatic organism, named Archie Asellus. The dashed arrow represents the elimination of

accumulated pollutants at the time of moulting, which is modelled as a repeating instantaneous event, while the solid arrows represent the continuous pollutant flux. 138

Figure 23: Rate diagram of pollutant flux into and out of the body (B) and moulting exoskeleton (E) compartments. Processes illustrated are respiration (r), ingestion (i), adsorption (a), and internal translocation (t); [r], [i], and [a] represent the concentrations from which respiration, ingestion and adsorption, respectively, occur, B the body compartment concentration. The k_x parameters represent the respective rate constants. 139

Figure 24: Causal diagram showing the connection between bioavailable environmental metal concentrations and measured whole-body metal concentrations, showing the influence of moult stage on the exoskeleton concentration mediator. In this diagram, moult stage and measurement error are two potential causes of in the typical bioaccumulation study. 142

Figure 25: Simulation of theoretical concentration of a metal pollutant in Compartment B (the body of the organism, excluding the moulting exoskeleton) versus time, from application of the described parameters. The dashed black line represents the equilibrium value given by Equation 19 (see text). The lighter lines represent the effects of different values of k_t for the same equilibrium value. 148

Figure 26: Simulation of concentration of a metal pollutant in Compartment E (the moulting exoskeleton of the organism) versus time, from application of the described parameters. Unlike with the concentration in the body compartment, B (see Figure 21), the concentration does not reach an equilibrium state, but oscillates between 0 (complete absence, due to moulting) and a maximum value. The equilibrium maximum value is given by Equation 20 (see text), and is denoted here by the dashed black line. 150

Figure 27: Simulation of overall concentration of a metal pollutant in the organism versus time. The overall concentration is a mass-weighted combination of the concentrations in the body and moulting exoskeleton compartments, B and E. This simulation represents the evolution of the actual measured whole-body concentration over time, where the variation in the concentration beyond day 200 is entirely due to contaminant loss through moulting. The equilibrium minimum and maximum are given by the dashed black lines, and are derived from Equations 19 and 20 (see text) after accounting for body mass. 151

Figure 28: Accumulated concentrations of nickel in the soft-tissue (B) and exoskeleton (E) of multiple Daphnia magna individuals (from Hall,

1982). The corresponding fit of the model qualitatively matches the behaviour seen, where B saturates, but E continues to accumulate indefinitely in the absence of moulting. Hall (1982) also observed indefinite accumulation in the filtering appendages, which contain parts of exoskeleton and soft tissue, so have not been included in this figure. 156

Figure 29: Accumulated concentrations, across time, of nickel in an individual specimen of Daphnia magna (from Hall, 1982). A moulting event occurred between t = 20 h and t = 49 h. A fit of the model, accounting for a moulting event just before t = 49 h, accurately describes the observed behaviour, despite the relative simplicity of the model..... 157

Figure 30: Proportional decrease in moult-induced measurement error with increasing accuracy of moult-synchronous sampling, where a "100%" sampling window is equivalent to ignoring moult stage when sampling. Using a sampling window of 10% of the moult period, for example, would reduce the variance by a factor of 100, for the same sample size. 160

Table of Tables

Table 1: A selection of studies investigating the interaction between various metal species and Asellus aquaticus. 42

Table 2: Studies considered as part of the meta-analysis. 85

Table 3: Determination of bioaccumulation factors from analyzed samples....87

Table 4: Percentage of field analyses showing amplification of macroinvertebrate concentrations over sediment concentrations, stratified by position on the thiophilic scale (around S=0.6)..... 111

Table 5: Multivariate logarithmic regression of key relationships in laboratory data. In each example, the accumulated concentration is regressed on two variables, denoted a and b in the table. 119

Table 6: Model settings producing simulated results presented in the following figures. Full derivation of these figures is supplied in Appendix F5.. 147

Table 7: Studies investigating the contribution of the exoskeleton compartment of organisms to overall measured whole-body accumulated concentrations..... 154

Appendix A

Thiophilicity Study: Field Data

Analyte	Sample	Site	Conc. [ppm]
Al	Freshwater Sediment	1	32452.2457
Ti	Freshwater Sediment	1	2388.1930
V	Freshwater Sediment	1	43.8762
Cr	Freshwater Sediment	1	38.3385
Mn	Freshwater Sediment	1	1458.8086
Fe	Freshwater Sediment	1	22095.4769
Co	Freshwater Sediment	1	8.6617
Ni	Freshwater Sediment	1	22.4913
Cu	Freshwater Sediment	1	15.5446
Zn	Freshwater Sediment	1	386.5625
As	Freshwater Sediment	1	8.1058
Pd	Freshwater Sediment	1	0.6677
Ag	Freshwater Sediment	1	0.8481
Cd	Freshwater Sediment	1	0.8699
Sb	Freshwater Sediment	1	4.4794
W	Freshwater Sediment	1	3.5607
Pt	Freshwater Sediment	1	3.3576
Pb	Freshwater Sediment	1	15.8225
Al	Freshwater Sediment	2	28540.0445
Ti	Freshwater Sediment	2	2710.3628
V	Freshwater Sediment	2	41.2036
Cr	Freshwater Sediment	2	37.9085
Mn	Freshwater Sediment	2	595.0238
Fe	Freshwater Sediment	2	25294.3211
Co	Freshwater Sediment	2	9.5306
Ni	Freshwater Sediment	2	25.0482

Cu	Freshwater Sediment	2	15.3407
Zn	Freshwater Sediment	2	239.4555
As	Freshwater Sediment	2	13.2008
Pd	Freshwater Sediment	2	0.5016
Ag	Freshwater Sediment	2	1.1338
Cd	Freshwater Sediment	2	1.2139
Sb	Freshwater Sediment	2	5.0073
W	Freshwater Sediment	2	6.2956
Pt	Freshwater Sediment	2	4.5302
Pb	Freshwater Sediment	2	36.9230
Al	*Asellus aquaticus*	1	2371.3316
Ti	*Asellus aquaticus*	1	302.3787
V	*Asellus aquaticus*	1	5.9729
Cr	*Asellus aquaticus*	1	8.0531
Mn	*Asellus aquaticus*	1	1024.4884
Fe	*Asellus aquaticus*	1	4150.8580
Co	*Asellus aquaticus*	1	3.2721
Ni	*Asellus aquaticus*	1	9.9191
Cu	*Asellus aquaticus*	1	118.5816
Zn	*Asellus aquaticus*	1	746.7529
As	*Asellus aquaticus*	1	3.7621
Ag	*Asellus aquaticus*	1	0.8937
Cd	*Asellus aquaticus*	1	1.2783
Sb	*Asellus aquaticus*	1	20.9301
W	*Asellus aquaticus*	1	13.7881
Pt	*Asellus aquaticus*	1	4.3348
Pb	*Asellus aquaticus*	1	15.4873
Al	*Gammarus sp.*	2	2136.3068
Ti	*Gammarus sp.*	2	508.4164
Cr	*Gammarus sp.*	2	18.1554
Mn	*Gammarus sp.*	2	845.2614
Fe	*Gammarus sp.*	2	1858.4088
Ni	*Gammarus sp.*	2	19.1141
Cu	*Gammarus sp.*	2	172.6403
Zn	*Gammarus sp.*	2	510.7013
Ag	*Gammarus sp.*	2	6.3488

Cd	*Gammarus sp.*	2	8.2125
Sb	*Gammarus sp.*	2	24.8462
W	*Gammarus sp.*	2	55.6070
Pb	*Gammarus sp.*	2	6.1415

Appendix B

Thiophilicity Study: Meta-Analysis

Study	Site	Analyte	Sample	Taxonomy	Conc. [ppm]
Boubonari et al., 2009		Fe	Sediment		25625.000
Boubonari et al., 2009		Fe	Macrophyte	*Ruppia maritima*	3021.000
Boubonari et al., 2009		Fe	Macrophyte	*Ulva rigida*	8021.000
Boubonari et al., 2009		Fe	Macroinv.	*Abra segmentos*	14271.000
Boubonari et al., 2009		Fe	Macroinv.	*Hediste diversicolor*	6875.000
Boubonari et al., 2009		Fe	Macroinv.	*Corophium orientale*	3854.000
Boubonari et al., 2009		Fe	Macroinv.	*Ventrosia maritima*	1250.000
Boubonari et al., 2009		Fe	Macroinv.	*Gammarus aequicauda*	1250.000
Boubonari et al., 2009		Fe	Macroinv.	*Crangon crangon*	208.000
Boubonari et al., 2009		Pb	Sediment		98.700
Boubonari et al., 2009		Pb	Macrophyte	*Ruppia maritima*	11.000
Boubonari et al., 2009		Pb	Macrophyte	*Ulva rigida*	6.400
Boubonari et al., 2009		Pb	Macroinv.	*Abra segmentos*	52.500

Boubonari et al., 2009	Pb	Macroinv.	*Hediste diversicolor*	15.600
Boubonari et al., 2009	Pb	Macroinv.	*Corophium orientale*	10.300
Boubonari et al., 2009	Pb	Macroinv.	*Ventrosia maritima*	2.800
Boubonari et al., 2009	Pb	Macroinv.	*Gammarus aequicauda*	5.300
Boubonari et al., 2009	Cd	Sediment		0.220
Boubonari et al., 2009	Cd	Macrophyte	*Ruppia maritima*	1.010
Boubonari et al., 2009	Cd	Macrophyte	*Ulva rigida*	1.810
Boubonari et al., 2009	Cd	Macroinv.	*Abra segmentos*	7.430
Boubonari et al., 2009	Cd	Macroinv.	*Hediste diversicolor*	0.960
Boubonari et al., 2009	Cd	Macroinv.	*Corophium orientale*	2.430
Boubonari et al., 2009	Cd	Macroinv.	*Ventrosia maritima*	1.490
Boubonari et al., 2009	Cd	Macroinv.	*Gammarus aequicauda*	1.450
Boubonari et al., 2009	Cd	Macroinv.	*Crangon crangon*	2.380
Boubonari et al., 2009	Zn	Sediment		74.000
Boubonari et al., 2009	Zn	Macrophyte	*Ruppia maritima*	106.000
Boubonari et al., 2009	Zn	Macrophyte	*Ulva rigida*	54.000
Boubonari et al., 2009	Zn	Macroinv.	*Abra segmentos*	146.000
Boubonari et al., 2009	Zn	Macroinv.	*Hediste diversicolor*	241.000
Boubonari et al., 2009	Zn	Macroinv.	*Corophium orientale*	181.000
Boubonari et al., 2009	Zn	Macroinv.	*Ventrosia maritima*	55.000
Boubonari et al., 2009	Zn	Macroinv.	*Gammarus aequicauda*	90.000

Boubonari et al., 2009		Zn	Macroinv.	*Crangon crangon*	93.000
Boubonari et al., 2009		Cu	Sediment		69.280
Boubonari et al., 2009		Cu	Macrophyte	*Ruppia maritima*	39.190
Boubonari et al., 2009		Cu	Macrophyte	*Ulva rigida*	20.060
Boubonari et al., 2009		Cu	Macroinv.	*Abra segmentos*	90.750
Boubonari et al., 2009		Cu	Macroinv.	*Hediste diversicolor*	61.120
Boubonari et al., 2009		Cu	Macroinv.	*Corophium orientale*	107.780
Boubonari et al., 2009		Cu	Macroinv.	*Ventrosia maritima*	68.820
Boubonari et al., 2009		Cu	Macroinv.	*Gammarus aequicauda*	87.950
Boubonari et al., 2009		Cu	Macroinv.	*Crangon crangon*	112.210
Culioli et al., 2009	P2	As	Sediment		9.135
Culioli et al., 2009	P2	Sb	Sediment		1.057
Culioli et al., 2009	P2	As	Macroinv.	*Leuctra budtzi*	1928.000
Culioli et al., 2009	P2	As	Macroinv.	*Leuctra geniculata*	1396.120
Culioli et al., 2009	P2	As	Macroinv.	*Silonella aurata*	574.000
Culioli et al., 2009	P2	As	Macroinv.	*Baetis cyrneus*	432.470
Culioli et al., 2009	P2	As	Macroinv.	*Helichus substriatus*	325.500
Culioli et al., 2009	P2	As	Macroinv.	*Electrogena fallax*	301.000
Culioli et al., 2009	P2	As	Macroinv.	*Ancylus fluviatilis*	271.800
Culioli et al., 2009	P2	As	Macroinv.	*Baetis ingridae*	266.160
Culioli et al., 2009	P2	As	Macroinv.	*Silo rufesens*	149.000

Culioli et al., 2009	P2	As	Macroinv.	*Limnius intermedius*	6.300
Culioli et al., 2009	P2	As	Macroinv.	*Caenis martae*	393.200
Culioli et al., 2009	P2	As	Macroinv.	*Psychomyia pusilla*	27.160
Culioli et al., 2009	P2	As	Macroinv.	*Hydropsyche cyrnotica*	168.200
Culioli et al., 2009	P2	As	Macroinv.	*Hydropsyche fumata*	156.500
Culioli et al., 2009	P2	As	Macroinv.	*Dugesia benazzii*	130.400
Culioli et al., 2009	P2	As	Macroinv.	*Rhyacophila pubescens*	41.900
Culioli et al., 2009	P2	As	Macroinv.	*Isoperla insularis*	23.720
Culioli et al., 2009	P2	As	Macroinv.	*Rhyacophila tarda*	23.500
Culioli et al., 2009	P2	Sb	Macroinv.	*Leuctra budtzi*	197.600
Culioli et al., 2009	P2	Sb	Macroinv.	*Leuctra geniculata*	115.440
Culioli et al., 2009	P2	Sb	Macroinv.	*Silonella aurata*	172.600
Culioli et al., 2009	P2	Sb	Macroinv.	*Baetis cyrneus*	56.700
Culioli et al., 2009	P2	Sb	Macroinv.	*Helichus substriatus*	47.500
Culioli et al., 2009	P2	Sb	Macroinv.	*Electrogena fallax*	75.960
Culioli et al., 2009	P2	Sb	Macroinv.	*Ancylus fluviatilis*	40.880
Culioli et al., 2009	P2	Sb	Macroinv.	*Baetis ingridae*	42.240
Culioli et al., 2009	P2	Sb	Macroinv.	*Silo rufesens*	65.000
Culioli et al., 2009	P2	Sb	Macroinv.	*Limnius intermedius*	63.300
Culioli et al., 2009	P2	Sb	Macroinv.	*Caenis martae*	59.950
Culioli et al., 2009	P2	Sb	Macroinv.	*Psychomyia pusilla*	8.700

Culioli et al., 2009	P2	Sb	Macroinv.	*Hydropsyche cyrnotica*	47.870
Culioli et al., 2009	P2	Sb	Macroinv.	*Hydropsyche fumata*	51.120
Culioli et al., 2009	P2	Sb	Macroinv.	*Dugesia benazzii*	26.400
Culioli et al., 2009	P2	Sb	Macroinv.	*Rhyacophila pubescens*	35.200
Culioli et al., 2009	P2	Sb	Macroinv.	*Isoperla insularis*	21.640
Culioli et al., 2009	P2	Sb	Macroinv.	*Rhyacophila tarda*	16.950
Erasmus et al., 2020	S1	Cr	Sediment		417.600
Erasmus et al., 2020	S1	Ni	Sediment		108.700
Erasmus et al., 2020	S1	Cu	Sediment		64.300
Erasmus et al., 2020	S1	Zn	Sediment		38.000
Erasmus et al., 2020	S1	Cd	Sediment		0.095
Erasmus et al., 2020	S1	Pt	Sediment		0.015
Erasmus et al., 2020	S1	Pb	Sediment		13.000
Erasmus et al., 2020	S2	Cr	Sediment		1258.700
Erasmus et al., 2020	S2	Ni	Sediment		256.000
Erasmus et al., 2020	S2	Cu	Sediment		118.700
Erasmus et al., 2020	S2	Zn	Sediment		82.900
Erasmus et al., 2020	S2	Cd	Sediment		0.391
Erasmus et al., 2020	S2	Pt	Sediment		0.175
Erasmus et al., 2020	S2	Pb	Sediment		40.800
Erasmus et al., 2020	S3	Cr	Sediment		775.800

Erasmus et al., 2020	S3	Ni	Sediment		165.100
Erasmus et al., 2020	S3	Cu	Sediment		59.600
Erasmus et al., 2020	S3	Zn	Sediment		83.200
Erasmus et al., 2020	S3	Cd	Sediment		0.236
Erasmus et al., 2020	S3	Pt	Sediment		0.041
Erasmus et al., 2020	S3	Pb	Sediment		13.900
Erasmus et al., 2020	Mine	Cr	Sediment		1608.700
Erasmus et al., 2020	Mine	Ni	Sediment		198.700
Erasmus et al., 2020	Mine	Cu	Sediment		79.100
Erasmus et al., 2020	Mine	Zn	Sediment		391.100
Erasmus et al., 2020	Mine	Cd	Sediment		0.199
Erasmus et al., 2020	Mine	Pt	Sediment		0.608
Erasmus et al., 2020	Mine	Pb	Sediment		10.900
Erasmus et al., 2020	S1	Cr	Macroinv.	*Lymnaeidae*	0.050
Erasmus et al., 2020	S2	Cr	Macroinv.	*Lymnaeidae*	0.030
Erasmus et al., 2020	S3	Cr	Macroinv.	*Lymnaeidae*	0.020
Erasmus et al., 2020	S1	Ni	Macroinv.	*Lymnaeidae*	0.880
Erasmus et al., 2020	S2	Ni	Macroinv.	*Lymnaeidae*	0.970
Erasmus et al., 2020	S3	Ni	Macroinv.	*Lymnaeidae*	2.270
Erasmus et al., 2020	S1	Cu	Macroinv.	*Lymnaeidae*	4.340
Erasmus et al., 2020	S2	Cu	Macroinv.	*Lymnaeidae*	3.820

Erasmus et al., 2020	S3	Cu	Macroinv.	*Lymnaeidae*	8.810
Erasmus et al., 2020	S1	Zn	Macroinv.	*Lymnaeidae*	3.380
Erasmus et al., 2020	S2	Zn	Macroinv.	*Lymnaeidae*	1.480
Erasmus et al., 2020	S3	Zn	Macroinv.	*Lymnaeidae*	2.540
Erasmus et al., 2020	S1	Cd	Macroinv.	*Lymnaeidae*	1.730
Erasmus et al., 2020	S2	Cd	Macroinv.	*Lymnaeidae*	0.620
Erasmus et al., 2020	S3	Cd	Macroinv.	*Lymnaeidae*	0.230
Erasmus et al., 2020	S1	Pt	Macroinv.	*Lymnaeidae*	0.180
Erasmus et al., 2020	S2	Pt	Macroinv.	*Lymnaeidae*	0.140
Erasmus et al., 2020	S3	Pt	Macroinv.	*Lymnaeidae*	0.170
Erasmus et al., 2020	S1	Pb	Macroinv.	*Lymnaeidae*	0.120
Erasmus et al., 2020	S2	Pb	Macroinv.	*Lymnaeidae*	0.050
Erasmus et al., 2020	S3	Pb	Macroinv.	*Lymnaeidae*	0.090
Erasmus et al., 2020	S1	Cr	Macroinv.	*Baetidae*	0.070
Erasmus et al., 2020	S2	Cr	Macroinv.	*Baetidae*	0.050
Erasmus et al., 2020	S3	Cr	Macroinv.	*Baetidae*	0.020
Erasmus et al., 2020	S1	Ni	Macroinv.	*Baetidae*	0.810
Erasmus et al., 2020	S2	Ni	Macroinv.	*Baetidae*	0.460
Erasmus et al., 2020	S3	Ni	Macroinv.	*Baetidae*	0.430
Erasmus et al., 2020	S1	Cu	Macroinv.	*Baetidae*	2.910
Erasmus et al., 2020	S2	Cu	Macroinv.	*Baetidae*	1.850

Erasmus et al., 2020	S3	Cu	Macroinv.	*Baetidae*	1.730
Erasmus et al., 2020	S1	Zn	Macroinv.	*Baetidae*	10.420
Erasmus et al., 2020	S2	Zn	Macroinv.	*Baetidae*	8.710
Erasmus et al., 2020	S3	Zn	Macroinv.	*Baetidae*	11.170
Erasmus et al., 2020	S1	Cd	Macroinv.	*Baetidae*	6.990
Erasmus et al., 2020	S2	Cd	Macroinv.	*Baetidae*	4.320
Erasmus et al., 2020	S3	Cd	Macroinv.	*Baetidae*	0.230
Erasmus et al., 2020	S1	Pt	Macroinv.	*Baetidae*	0.300
Erasmus et al., 2020	S2	Pt	Macroinv.	*Baetidae*	0.090
Erasmus et al., 2020	S3	Pt	Macroinv.	*Baetidae*	0.080
Erasmus et al., 2020	S1	Pb	Macroinv.	*Baetidae*	0.170
Erasmus et al., 2020	S2	Pb	Macroinv.	*Baetidae*	0.080
Erasmus et al., 2020	S3	Pb	Macroinv.	*Baetidae*	0.060
Erasmus et al., 2020	S2	Cr	Macroinv.	*Hydropsychidae*	0.030
Erasmus et al., 2020	S2	Ni	Macroinv.	*Hydropsychidae*	0.310
Erasmus et al., 2020	S2	Cu	Macroinv.	*Hydropsychidae*	1.380
Erasmus et al., 2020	S2	Zn	Macroinv.	*Hydropsychidae*	4.160
Erasmus et al., 2020	S2	Cd	Macroinv.	*Hydropsychidae*	1.000
Erasmus et al., 2020	S2	Pt	Macroinv.	*Hydropsychidae*	0.020
Erasmus et al., 2020	S2	Pb	Macroinv.	*Hydropsychidae*	0.080
Erasmus et al., 2020	S3	Cr	Macroinv.	*Chironomidae*	0.060

Erasmus et al., 2020	S3	Ni	Macroinv.	*Chironomidae*	0.880
Erasmus et al., 2020	S3	Cu	Macroinv.	*Chironomidae*	2.830
Erasmus et al., 2020	S3	Zn	Macroinv.	*Chironomidae*	4.330
Erasmus et al., 2020	S3	Cd	Macroinv.	*Chironomidae*	0.190
Erasmus et al., 2020	S3	Pt	Macroinv.	*Chironomidae*	0.140
Erasmus et al., 2020	S3	Pb	Macroinv.	*Chironomidae*	0.160
Erasmus et al., 2020	S2	Cr	Macroinv.	*Tubificidae*	0.070
Erasmus et al., 2020	S2	Ni	Macroinv.	*Tubificidae*	0.780
Erasmus et al., 2020	S2	Cu	Macroinv.	*Tubificidae*	1.420
Erasmus et al., 2020	S2	Zn	Macroinv.	*Tubificidae*	7.750
Erasmus et al., 2020	S2	Cd	Macroinv.	*Tubificidae*	1.640
Erasmus et al., 2020	S2	Pt	Macroinv.	*Tubificidae*	0.500
Erasmus et al., 2020	S2	Pb	Macroinv.	*Tubificidae*	0.150
Erasmus et al., 2020	S1	Cr	Macroinv.	*Potamonautidae*	0.020
Erasmus et al., 2020	S2	Cr	Macroinv.	*Potamonautidae*	0.010
Erasmus et al., 2020	S3	Cr	Macroinv.	*Potamonautidae*	0.010
Erasmus et al., 2020	S1	Ni	Macroinv.	*Potamonautidae*	0.470
Erasmus et al., 2020	S2	Ni	Macroinv.	*Potamonautidae*	0.410
Erasmus et al., 2020	S3	Ni	Macroinv.	*Potamonautidae*	0.950
Erasmus et al., 2020	S1	Cu	Macroinv.	*Potamonautidae*	3.870
Erasmus et al., 2020	S2	Cu	Macroinv.	*Potamonautidae*	4.210

Erasmus et al., 2020	S3	Cu	Macroinv.	*Potamonautidae*	7.960
Erasmus et al., 2020	S1	Zn	Macroinv.	*Potamonautidae*	6.370
Erasmus et al., 2020	S2	Zn	Macroinv.	*Potamonautidae*	2.680
Erasmus et al., 2020	S3	Zn	Macroinv.	*Potamonautidae*	3.630
Erasmus et al., 2020	S1	Cd	Macroinv.	*Potamonautidae*	0.660
Erasmus et al., 2020	S2	Cd	Macroinv.	*Potamonautidae*	0.520
Erasmus et al., 2020	S3	Cd	Macroinv.	*Potamonautidae*	0.170
Erasmus et al., 2020	S1	Pt	Macroinv.	*Potamonautidae*	0.050
Erasmus et al., 2020	S2	Pt	Macroinv.	*Potamonautidae*	0.030
Erasmus et al., 2020	S3	Pt	Macroinv.	*Potamonautidae*	0.060
Erasmus et al., 2020	S1	Pb	Macroinv.	*Potamonautidae*	0.050
Erasmus et al., 2020	S2	Pb	Macroinv.	*Potamonautidae*	0.020
Erasmus et al., 2020	S3	Pb	Macroinv.	*Potamonautidae*	0.040
Erasmus et al., 2020	S1	Cr	Macroinv.	*Coenagrionidae*	0.070
Erasmus et al., 2020	S2	Cr	Macroinv.	*Coenagrionidae*	0.020
Erasmus et al., 2020	S3	Cr	Macroinv.	*Coenagrionidae*	0.020
Erasmus et al., 2020	S1	Ni	Macroinv.	*Coenagrionidae*	0.830
Erasmus et al., 2020	S2	Ni	Macroinv.	*Coenagrionidae*	0.180
Erasmus et al., 2020	S3	Ni	Macroinv.	*Coenagrionidae*	0.550
Erasmus et al., 2020	S1	Cu	Macroinv.	*Coenagrionidae*	2.020
Erasmus et al., 2020	S2	Cu	Macroinv.	*Coenagrionidae*	1.160

Erasmus et al., 2020	S3	Cu	Macroinv.	*Coenagrionidae*	1.760
Erasmus et al., 2020	S1	Zn	Macroinv.	*Coenagrionidae*	11.040
Erasmus et al., 2020	S2	Zn	Macroinv.	*Coenagrionidae*	4.970
Erasmus et al., 2020	S3	Zn	Macroinv.	*Coenagrionidae*	4.680
Erasmus et al., 2020	S1	Cd	Macroinv.	*Coenagrionidae*	1.630
Erasmus et al., 2020	S2	Cd	Macroinv.	*Coenagrionidae*	1.480
Erasmus et al., 2020	S3	Cd	Macroinv.	*Coenagrionidae*	0.090
Erasmus et al., 2020	S1	Pt	Macroinv.	*Coenagrionidae*	0.210
Erasmus et al., 2020	S2	Pt	Macroinv.	*Coenagrionidae*	0.020
Erasmus et al., 2020	S3	Pt	Macroinv.	*Coenagrionidae*	0.080
Erasmus et al., 2020	S1	Pb	Macroinv.	*Coenagrionidae*	0.130
Erasmus et al., 2020	S2	Pb	Macroinv.	*Coenagrionidae*	0.030
Erasmus et al., 2020	S3	Pb	Macroinv.	*Coenagrionidae*	0.060
Erasmus et al., 2020	S1	Cr	Macroinv.	*Libellulidae*	0.060
Erasmus et al., 2020	S2	Cr	Macroinv.	*Libellulidae*	0.030
Erasmus et al., 2020	S3	Cr	Macroinv.	*Libellulidae*	0.030
Erasmus et al., 2020	Mine	Cr	Macroinv.	*Libellulidae*	0.040
Erasmus et al., 2020	S1	Ni	Macroinv.	*Libellulidae*	0.520
Erasmus et al., 2020	S2	Ni	Macroinv.	*Libellulidae*	0.300
Erasmus et al., 2020	S3	Ni	Macroinv.	*Libellulidae*	0.800
Erasmus et al., 2020	Mine	Ni	Macroinv.	*Libellulidae*	0.820

Erasmus et al., 2020	S1	Cu	Macroinv.	*Libellulidae*	1.420
Erasmus et al., 2020	S2	Cu	Macroinv.	*Libellulidae*	1.650
Erasmus et al., 2020	S3	Cu	Macroinv.	*Libellulidae*	2.250
Erasmus et al., 2020	Mine	Cu	Macroinv.	*Libellulidae*	1.500
Erasmus et al., 2020	S1	Zn	Macroinv.	*Libellulidae*	8.440
Erasmus et al., 2020	S2	Zn	Macroinv.	*Libellulidae*	4.150
Erasmus et al., 2020	S3	Zn	Macroinv.	*Libellulidae*	4.070
Erasmus et al., 2020	Mine	Zn	Macroinv.	*Libellulidae*	1.250
Erasmus et al., 2020	S1	Cd	Macroinv.	*Libellulidae*	0.580
Erasmus et al., 2020	S2	Cd	Macroinv.	*Libellulidae*	0.520
Erasmus et al., 2020	S3	Cd	Macroinv.	*Libellulidae*	0.100
Erasmus et al., 2020	Mine	Cd	Macroinv.	*Libellulidae*	0.150
Erasmus et al., 2020	S1	Pt	Macroinv.	*Libellulidae*	0.230
Erasmus et al., 2020	S2	Pt	Macroinv.	*Libellulidae*	0.030
Erasmus et al., 2020	S3	Pt	Macroinv.	*Libellulidae*	0.060
Erasmus et al., 2020	Mine	Pt	Macroinv.	*Libellulidae*	0.100
Erasmus et al., 2020	S1	Pb	Macroinv.	*Libellulidae*	0.140
Erasmus et al., 2020	S2	Pb	Macroinv.	*Libellulidae*	0.040
Erasmus et al., 2020	S3	Pb	Macroinv.	*Libellulidae*	0.090
Erasmus et al., 2020	Mine	Pb	Macroinv.	*Libellulidae*	0.170
Farag et al., 2007	LBR	As	Sediment		20.000

Farag et al., 2007	UBR	As	Sediment	13.000
Farag et al., 2007	REF 1	As	Sediment	17.000
Farag et al., 2007	LHO	As	Sediment	740.000
Farag et al., 2007	LCC	As	Sediment	580.000
Farag et al., 2007	MCC	As	Sediment	250.000
Farag et al., 2007	UCC	As	Sediment	96.000
Farag et al., 2007	LBC	As	Sediment	140.000
Farag et al., 2007	JC	As	Sediment	330.000
Farag et al., 2007	BRRCREF 2	As	Sediment	8.300
Farag et al., 2007	BRBC	As	Sediment	20.000
Farag et al., 2007	BRCC	As	Sediment	55.000
Farag et al., 2007	BRGG	As	Sediment	99.000
Farag et al., 2007	LHO	Cd	Sediment	14.000
Farag et al., 2007	LCC	Cd	Sediment	11.000
Farag et al., 2007	MCC	Cd	Sediment	9.300
Farag et al., 2007	UCC	Cd	Sediment	3.000
Farag et al., 2007	LBC	Cd	Sediment	3.900
Farag et al., 2007	JC	Cd	Sediment	4.200
Farag et al., 2007	BRCC	Cd	Sediment	3.200
Farag et al., 2007	BRGG	Cd	Sediment	2.800
Farag et al., 2007	LBR	Cu	Sediment	13.000

Farag et al., 2007	UBR	Cu	Sediment	7.800
Farag et al., 2007	REF 1	Cu	Sediment	10.000
Farag et al., 2007	LHO	Cu	Sediment	140.000
Farag et al., 2007	LCC	Cu	Sediment	440.000
Farag et al., 2007	MCC	Cu	Sediment	450.000
Farag et al., 2007	UCC	Cu	Sediment	110.000
Farag et al., 2007	LBC	Cu	Sediment	98.000
Farag et al., 2007	JC	Cu	Sediment	180.000
Farag et al., 2007	BRRCREF 2	Cu	Sediment	16.000
Farag et al., 2007	BRBC	Cu	Sediment	38.000
Farag et al., 2007	BRCC	Cu	Sediment	110.000
Farag et al., 2007	BRGG	Cu	Sediment	84.000
Farag et al., 2007	LBR	Pb	Sediment	26.000
Farag et al., 2007	UBR	Pb	Sediment	10.000
Farag et al., 2007	REF 1	Pb	Sediment	18.000
Farag et al., 2007	LHO	Pb	Sediment	1100.000
Farag et al., 2007	LCC	Pb	Sediment	390.000
Farag et al., 2007	MCC	Pb	Sediment	280.000
Farag et al., 2007	UCC	Pb	Sediment	220.000
Farag et al., 2007	LBC	Pb	Sediment	150.000
Farag et al., 2007	JC	Pb	Sediment	190.000

Farag et al., 2007	BRRCREF 2	Pb	Sediment	13.000
Farag et al., 2007	BRBC	Pb	Sediment	27.000
Farag et al., 2007	BRCC	Pb	Sediment	80.000
Farag et al., 2007	BRGG	Pb	Sediment	99.000
Farag et al., 2007	LBR	Zn	Sediment	100.000
Farag et al., 2007	UBR	Zn	Sediment	40.000
Farag et al., 2007	REF 1	Zn	Sediment	70.000
Farag et al., 2007	LHO	Zn	Sediment	3400.000
Farag et al., 2007	LCC	Zn	Sediment	1300.000
Farag et al., 2007	MCC	Zn	Sediment	930.000
Farag et al., 2007	UCC	Zn	Sediment	440.000
Farag et al., 2007	LBC	Zn	Sediment	640.000
Farag et al., 2007	JC	Zn	Sediment	490.000
Farag et al., 2007	BRRCREF 2	Zn	Sediment	74.000
Farag et al., 2007	BRBC	Zn	Sediment	180.000
Farag et al., 2007	BRCC	Zn	Sediment	430.000
Farag et al., 2007	BRGG	Zn	Sediment	490.000
Farag et al., 2007	LBR	As	Macroinv.	2.300
Farag et al., 2007	UBR	As	Macroinv.	3.700
Farag et al., 2007	REF 1	As	Macroinv.	3.000
Farag et al., 2007	LHO	As	Macroinv.	60.000

Farag et al., 2007	LCC	As	Macroinv.	63.000
Farag et al., 2007	MCC	As	Macroinv.	80.100
Farag et al., 2007	UCC	As	Macroinv.	7.500
Farag et al., 2007	LBC	As	Macroinv.	21.500
Farag et al., 2007	JC	As	Macroinv.	77.000
Farag et al., 2007	BRRCREF 2	As	Macroinv.	4.600
Farag et al., 2007	BRBC	As	Macroinv.	5.300
Farag et al., 2007	BRCC	As	Macroinv.	13.100
Farag et al., 2007	BRGG	As	Macroinv.	26.700
Farag et al., 2007	LBR	Cd	Macroinv.	3.700
Farag et al., 2007	UBR	Cd	Macroinv.	0.900
Farag et al., 2007	REF 1	Cd	Macroinv.	2.300
Farag et al., 2007	LHO	Cd	Macroinv.	16.700
Farag et al., 2007	LCC	Cd	Macroinv.	59.300
Farag et al., 2007	MCC	Cd	Macroinv.	35.000
Farag et al., 2007	UCC	Cd	Macroinv.	15.900
Farag et al., 2007	LBC	Cd	Macroinv.	18.100
Farag et al., 2007	JC	Cd	Macroinv.	10.000
Farag et al., 2007	BRRCREF 2	Cd	Macroinv.	1.100
Farag et al., 2007	BRBC	Cd	Macroinv.	10.600
Farag et al., 2007	BRCC	Cd	Macroinv.	16.200

Farag et al., 2007	BRGG	Cd	Macroinv.	11.700
Farag et al., 2007	LBR	Cu	Macroinv.	38.000
Farag et al., 2007	UBR	Cu	Macroinv.	30.000
Farag et al., 2007	REF 1	Cu	Macroinv.	34.000
Farag et al., 2007	LHO	Cu	Macroinv.	74.000
Farag et al., 2007	LCC	Cu	Macroinv.	340.000
Farag et al., 2007	MCC	Cu	Macroinv.	268.000
Farag et al., 2007	UCC	Cu	Macroinv.	77.000
Farag et al., 2007	LBC	Cu	Macroinv.	92.000
Farag et al., 2007	JC	Cu	Macroinv.	319.000
Farag et al., 2007	BRRCREF 2	Cu	Macroinv.	29.000
Farag et al., 2007	BRBC	Cu	Macroinv.	85.000
Farag et al., 2007	BRCC	Cu	Macroinv.	111.000
Farag et al., 2007	BRGG	Cu	Macroinv.	98.000
Farag et al., 2007	LBR	Pb	Macroinv.	1.200
Farag et al., 2007	UBR	Pb	Macroinv.	1.000
Farag et al., 2007	REF 1	Pb	Macroinv.	1.200
Farag et al., 2007	LHO	Pb	Macroinv.	36.000
Farag et al., 2007	LCC	Pb	Macroinv.	34.000
Farag et al., 2007	MCC	Pb	Macroinv.	24.100
Farag et al., 2007	UCC	Pb	Macroinv.	11.200

Farag et al., 2007	LBC	Pb	Macroinv.		12.400
Farag et al., 2007	JC	Pb	Macroinv.		12.600
Farag et al., 2007	BRRCREF 2	Pb	Macroinv.		1.600
Farag et al., 2007	BRBC	Pb	Macroinv.		3.300
Farag et al., 2007	BRCC	Pb	Macroinv.		8.500
Farag et al., 2007	BRGG	Pb	Macroinv.		38.000
Farag et al., 2007	LBR	Zn	Macroinv.		340.000
Farag et al., 2007	UBR	Zn	Macroinv.		235.000
Farag et al., 2007	REF 1	Zn	Macroinv.		288.000
Farag et al., 2007	LHO	Zn	Macroinv.		3090.000
Farag et al., 2007	LCC	Zn	Macroinv.		2410.000
Farag et al., 2007	MCC	Zn	Macroinv.		2070.000
Farag et al., 2007	UCC	Zn	Macroinv.		1050.000
Farag et al., 2007	LBC	Zn	Macroinv.		929.000
Farag et al., 2007	JC	Zn	Macroinv.		580.000
Farag et al., 2007	BRRCREF 2	Zn	Macroinv.		237.000
Farag et al., 2007	BRBC	Zn	Macroinv.		584.000
Farag et al., 2007	BRCC	Zn	Macroinv.		977.000
Farag et al., 2007	BRGG	Zn	Macroinv.		669.000
Levit et al., 2020	S1	Zn	Macroinv.	*Amphipoda*	63.100
Levit et al., 2020	S2	Zn	Macroinv.	*Amphipoda*	59.500

Levit et al., 2020	S3	Zn	Macroinv.	*Amphipoda*	61.300
Levit et al., 2020	S4	Zn	Macroinv.	*Amphipoda*	72.600
Levit et al., 2020	S5	Zn	Macroinv.	*Amphipoda*	57.200
Levit et al., 2020	S6	Zn	Macroinv.	*Amphipoda*	58.100
Levit et al., 2020	S1	Zn	Macroinv.	*Bivalvia*	21.800
Levit et al., 2020	S4	Zn	Macroinv.	*Bivalvia*	24.800
Levit et al., 2020	S1	Zn	Macroinv.	*Gastropoda*	27.700
Levit et al., 2020	S4	Zn	Macroinv.	*Gastropoda*	44.600
Levit et al., 2020	S1	Zn	Macroinv.	*Hirudinea*	110.000
Levit et al., 2020	S4	Zn	Macroinv.	*Hirudinea*	381.000
Levit et al., 2020	S4	Zn	Macroinv.	*Oligochaeta*	145.000
Levit et al., 2020	S6	Zn	Macroinv.	*Oligochaeta*	71.500
Levit et al., 2020	S1	Cd	Macroinv.	*Amphipoda*	0.410
Levit et al., 2020	S2	Cd	Macroinv.	*Amphipoda*	0.200
Levit et al., 2020	S3	Cd	Macroinv.	*Amphipoda*	0.330
Levit et al., 2020	S4	Cd	Macroinv.	*Amphipoda*	0.170
Levit et al., 2020	S5	Cd	Macroinv.	*Amphipoda*	0.180
Levit et al., 2020	S6	Cd	Macroinv.	*Amphipoda*	0.130
Levit et al., 2020	S1	Cd	Macroinv.	*Bivalvia*	0.180
Levit et al., 2020	S4	Cd	Macroinv.	*Bivalvia*	0.140
Levit et al., 2020	S1	Cd	Macroinv.	*Gastropoda*	0.330

Levit et al., 2020	S4	Cd	Macroinv.	*Gastropoda*	0.110
Levit et al., 2020	S1	Cd	Macroinv.	*Hirudinea*	0.800
Levit et al., 2020	S4	Cd	Macroinv.	*Hirudinea*	0.170
Levit et al., 2020	S4	Cd	Macroinv.	*Oligochaeta*	0.370
Levit et al., 2020	S6	Cd	Macroinv.	*Oligochaeta*	0.320
Levit et al., 2020	S1	Pb	Macroinv.	*Amphipoda*	1.890
Levit et al., 2020	S2	Pb	Macroinv.	*Amphipoda*	1.180
Levit et al., 2020	S3	Pb	Macroinv.	*Amphipoda*	2.940
Levit et al., 2020	S4	Pb	Macroinv.	*Amphipoda*	2.830
Levit et al., 2020	S5	Pb	Macroinv.	*Amphipoda*	1.440
Levit et al., 2020	S6	Pb	Macroinv.	*Amphipoda*	1.500
Levit et al., 2020	S1	Pb	Macroinv.	*Bivalvia*	1.670
Levit et al., 2020	S4	Pb	Macroinv.	*Bivalvia*	1.520
Levit et al., 2020	S1	Pb	Macroinv.	*Gastropoda*	1.810
Levit et al., 2020	S4	Pb	Macroinv.	*Gastropoda*	1.430
Levit et al., 2020	S1	Pb	Macroinv.	*Hirudinea*	10.100
Levit et al., 2020	S4	Pb	Macroinv.	*Hirudinea*	10.500
Levit et al., 2020	S4	Pb	Macroinv.	*Oligochaeta*	21.300
Levit et al., 2020	S6	Pb	Macroinv.	*Oligochaeta*	3.220
Levit et al., 2020	S1	Cu	Macroinv.	*Amphipoda*	49.800
Levit et al., 2020	S2	Cu	Macroinv.	*Amphipoda*	22.100

Levit et al., 2020	S3	Cu	Macroinv.	*Amphipoda*	22.100
Levit et al., 2020	S4	Cu	Macroinv.	*Amphipoda*	55.500
Levit et al., 2020	S5	Cu	Macroinv.	*Amphipoda*	49.100
Levit et al., 2020	S6	Cu	Macroinv.	*Amphipoda*	39.900
Levit et al., 2020	S1	Cu	Macroinv.	*Bivalvia*	3.400
Levit et al., 2020	S4	Cu	Macroinv.	*Bivalvia*	8.100
Levit et al., 2020	S1	Cu	Macroinv.	*Gastropoda*	26.200
Levit et al., 2020	S4	Cu	Macroinv.	*Gastropoda*	20.100
Levit et al., 2020	S1	Cu	Macroinv.	*Hirudinea*	30.600
Levit et al., 2020	S4	Cu	Macroinv.	*Hirudinea*	18.200
Levit et al., 2020	S4	Cu	Macroinv.	*Oligochaeta*	14.500
Levit et al., 2020	S6	Cu	Macroinv.	*Oligochaeta*	8.900
Levit et al., 2020	S1	Mn	Macroinv.	*Amphipoda*	185.000
Levit et al., 2020	S2	Mn	Macroinv.	*Amphipoda*	158.000
Levit et al., 2020	S3	Mn	Macroinv.	*Amphipoda*	152.000
Levit et al., 2020	S4	Mn	Macroinv.	*Amphipoda*	101.000
Levit et al., 2020	S5	Mn	Macroinv.	*Amphipoda*	104.000
Levit et al., 2020	S6	Mn	Macroinv.	*Amphipoda*	173.000
Levit et al., 2020	S1	Mn	Macroinv.	*Bivalvia*	147.000
Levit et al., 2020	S4	Mn	Macroinv.	*Bivalvia*	200.000
Levit et al., 2020	S1	Mn	Macroinv.	*Gastropoda*	155.000

Levit et al., 2020	S4	Mn	Macroinv.	*Gastropoda*	83.000
Levit et al., 2020	S1	Mn	Macroinv.	*Hirudinea*	204.000
Levit et al., 2020	S4	Mn	Macroinv.	*Hirudinea*	119.000
Levit et al., 2020	S4	Mn	Macroinv.	*Oligochaeta*	200.000
Levit et al., 2020	S6	Mn	Macroinv.	*Oligochaeta*	523.000
Levit et al., 2020	S1	Fe	Macroinv.	*Amphipoda*	1370.000
Levit et al., 2020	S2	Fe	Macroinv.	*Amphipoda*	541.000
Levit et al., 2020	S3	Fe	Macroinv.	*Amphipoda*	1430.000
Levit et al., 2020	S4	Fe	Macroinv.	*Amphipoda*	550.000
Levit et al., 2020	S5	Fe	Macroinv.	*Amphipoda*	574.000
Levit et al., 2020	S6	Fe	Macroinv.	*Amphipoda*	1105.000
Levit et al., 2020	S1	Fe	Macroinv.	*Bivalvia*	479.000
Levit et al., 2020	S4	Fe	Macroinv.	*Bivalvia*	541.000
Levit et al., 2020	S1	Fe	Macroinv.	*Gastropoda*	731.000
Levit et al., 2020	S4	Fe	Macroinv.	*Gastropoda*	622.000
Levit et al., 2020	S1	Fe	Macroinv.	*Hirudinea*	2580.000
Levit et al., 2020	S4	Fe	Macroinv.	*Hirudinea*	2590.000
Levit et al., 2020	S4	Fe	Macroinv.	*Oligochaeta*	5020.000
Levit et al., 2020	S6	Fe	Macroinv.	*Oligochaeta*	3830.000
Levit et al., 2020	S1	Zn	Sediment		27.800
Levit et al., 2020	S2	Zn	Sediment		20.900

Levit et al., 2020	S3	Zn	Sediment	19.900
Levit et al., 2020	S4	Zn	Sediment	59.000
Levit et al., 2020	S5	Zn	Sediment	9.700
Levit et al., 2020	S6	Zn	Sediment	11.700
Levit et al., 2020	S1	Cd	Sediment	0.180
Levit et al., 2020	S2	Cd	Sediment	0.100
Levit et al., 2020	S3	Cd	Sediment	0.080
Levit et al., 2020	S4	Cd	Sediment	0.290
Levit et al., 2020	S5	Cd	Sediment	0.030
Levit et al., 2020	S6	Cd	Sediment	0.050
Levit et al., 2020	S1	Pb	Sediment	25.700
Levit et al., 2020	S2	Pb	Sediment	20.900
Levit et al., 2020	S3	Pb	Sediment	36.700
Levit et al., 2020	S4	Pb	Sediment	24.200
Levit et al., 2020	S5	Pb	Sediment	14.000
Levit et al., 2020	S6	Pb	Sediment	13.200
Levit et al., 2020	S1	Cu	Sediment	13.400
Levit et al., 2020	S2	Cu	Sediment	1.320
Levit et al., 2020	S3	Cu	Sediment	2.980
Levit et al., 2020	S4	Cu	Sediment	5.910
Levit et al., 2020	S5	Cu	Sediment	1.010

Levit et al., 2020	S6	Cu	Sediment		1.250
Levit et al., 2020	S1	Mn	Sediment		204.000
Levit et al., 2020	S2	Mn	Sediment		189.000
Levit et al., 2020	S3	Mn	Sediment		291.000
Levit et al., 2020	S4	Mn	Sediment		295.000
Levit et al., 2020	S5	Mn	Sediment		64.000
Levit et al., 2020	S6	Mn	Sediment		291.000
Levit et al., 2020	S1	Fe	Sediment		8040.000
Levit et al., 2020	S2	Fe	Sediment		4520.000
Levit et al., 2020	S3	Fe	Sediment		7850.000
Levit et al., 2020	S4	Fe	Sediment		8060.000
Levit et al., 2020	S5	Fe	Sediment		9820.000
Levit et al., 2020	S6	Fe	Sediment		8900.000
Pourang, 1996		Pb	Sediment		24.200
Pourang, 1996		Pb	Macroinv.	*Chironomidae*	13.900
Pourang, 1996		Pb	Macroinv.	*Tubifex tubifex*	19.200
Pourang, 1996		Pb	Macroinv.	*Mytilaster lineatus*	24.300
Pourang, 1996		Pb	Macroinv.	*Corbicula fluminalis*	5.800
Pourang, 1996		Cu	Sediment		38.300
Pourang, 1996		Cu	Macroinv.	*Chironomidae*	49.900
Pourang, 1996		Cu	Macroinv.	*Tubifex tubifex*	77.400

Pourang, 1996	Cu	Macroinv.	*Mytilaster lineatus*	35.600
Pourang, 1996	Cu	Macroinv.	*Corbicula fluminalis*	24.800
Pourang, 1996	Zn	Sediment		87.500
Pourang, 1996	Zn	Macroinv.	*Chironomidae*	79.500
Pourang, 1996	Zn	Macroinv.	*Tubifex tubifex*	154.300
Pourang, 1996	Zn	Macroinv.	*Mytilaster lineatus*	262.900
Pourang, 1996	Zn	Macroinv.	*Corbicula fluminalis*	53.100
Pourang, 1996	Mn	Sediment		840.200
Pourang, 1996	Mn	Macroinv.	*Chironomidae*	3.300
Pourang, 1996	Mn	Macroinv.	*Tubifex tubifex*	8.400
Pourang, 1996	Mn	Macroinv.	*Mytilaster lineatus*	6.200
Pourang, 1996	Mn	Macroinv.	*Corbicula fluminalis*	4.300

Appendix C

Field Data

C1. Measured water concentrations

Analyte	Site 1 [ppb]	Site 2 [ppb]	Site 3 [ppb]	Site 4 [ppb]	Site 5 [ppb]
Mg	6520.31	7374.19	5730.00	5666.83	7273.32
Ti	0.60	0.26	1.15	1.55	0.52
Cr	0.31	0.34	0.42	0.36	0.32
Mn	36.69	7.43	200.71	141.16	45.36
Co	0.21	0.15	1.79	1.42	0.25
Ni	0.46	0.39	8.46	4.40	0.51
Cu	1.23	0.63	4.90	3.90	1.73
Zn	3.70	2.13	45.69	19.79	5.76
As	0.39	0.25	1.04	0.82	0.42
Ba	7.97	12.27	10.74	7.97	14.29
Fe	91.81	19.22	1015.68	790.56	111.27
Li	0.56	0.76	1.59	2.23	0.58
Se	0.85	1.31	0.86	1.10	0.72
Pd	*n.d.*	*n.d.*	*n.d.*	*n.d.*	*n.d.*
Ag	*n.d.*	*n.d.*	*n.d.*	*n.d.*	*n.d.*
Cd	*n.d.*	*n.d.*	0.46	0.10	*n.d.*
Sn	*n.d.*	*n.d.*	*n.d.*	*n.d.*	*n.d.*
Sb	0.06	0.03	0.08	0.06	0.08
W	*n.d.*	*n.d.*	0.61	*n.d.*	2.69
Pt	*n.d.*	*n.d.*	*n.d.*	*n.d.*	*n.d.*
Au	0.03	0.02	0.03	0.04	0.02

Hg	0.12	0.10	0.15	0.12	0.30
Pb	0.53	0.19	2.83	1.22	0.56
Bi	0.01	0.01	0.01	0.01	0.00

C2. Measured sediment concentrations

Analyte	Site 1 [ppm]	Site 2 [ppm]	Site 3 [ppm]	Site 4 [ppm]	Site 5 [ppm]
Mg	3118.79	2501.81	4373.97	8059.23	3710.02
Ti	4335.17	4837.12	3771.83	2631.23	3311.89
Cr	94.91	84.42	59.79	50.71	59.92
Mn	1525.85	431.89	489.14	484.46	547.18
Co	15.82	12.05	17.05	9.80	10.76
Ni	39.51	37.11	37.44	28.87	31.94
Cu	13.60	17.25	17.65	21.60	15.08
Zn	195.90	228.92	295.07	408.56	248.25
As	14.68	18.20	18.46	14.47	9.43
Ba	310.68	410.33	350.21	249.52	298.16
Fe	38361.72	33264.87	24834.24	27128.02	23772.28
Li	37.56	51.98	41.61	30.37	33.88
Se	0.69	0.51	1.29	0.64	0.57
Pd	5.09	4.00	3.04	2.56	10.94
Ag	0.71	0.56	0.41	0.29	1.48
Cd	0.17	0.13	0.56	0.12	0.23
Sn	12.83	6.87	8.68	6.37	68.36
Sb	2.91	4.05	3.15	3.15	3.25
W	15.70	23.62	34.05	59.59	9.63
Pt	0.06	*n.d.*	*n.d.*	*n.d.*	2.54
Au	*n.d.*	*n.d.*	*n.d.*	*n.d.*	*n.d.*
Hg	1.01	1.23	1.78	3.56	3.97
Pb	36.56	12.03	24.86	11.74	21.83
Bi	0.70	0.26	0.28	0.29	0.36

C3. Measured macroinvertebrate concentrations

Analyte	Site 1 [ppm]	Site 2 [ppm]	Site 3 [ppm]	Site 4 [ppm]	Site 5 [ppm]
Mg	4107.91	1620.84	2542.19	1950.00	1250.31
Ti	2536.58	3234.65	1196.71	845.60	666.41
Cr	56.16	56.96	24.33	18.32	18.50
Mn	425.10	376.54	1477.77	1265.71	918.99
Co	12.15	8.09	63.05	13.84	7.56
Ni	37.12	25.02	42.11	21.24	14.62
Cu	27.99	29.92	86.94	240.27	134.24
Zn	186.61	314.40	1363.68	649.45	660.07
As	9.62	15.83	27.47	18.26	14.16
Ba	314.60	353.10	247.57	128.19	174.07
Fe	28587.26	26486.97	11507.83	10237.54	13564.48
Li	37.90	22.80	11.61	6.90	5.40
Se	1.39	1.28	4.49	12.19	9.90
Pd	1.96	3.04	0.79	0.07	0.57
Ag	0.32	0.47	*n.d.*	0.57	0.22
Cd	0.21	0.36	5.80	2.04	0.12
Sn	1.93	3.76	17.10	10.68	15.36
Sb	1.35	2.65	10.03	5.19	6.49
W	21.04	59.30	90.34	47.54	37.94
Pt	0.07	*n.d.*	*n.d.*	*n.d.*	*n.d.*
Au	*n.d.*	*n.d.*	*n.d.*	*n.d.*	*n.d.*
Hg	1.32	3.91	7.31	4.16	4.53
Pb	19.88	25.03	19.38	9.40	17.58
Bi	0.17	0.30	1.22	2.90	0.54

Appendix D

Lab Data

D1. TiO2 exposure assays

Concentration [ppm]	Ti in bTiO2 [ppm]	Ti in nTiO2 [ppm]
0.00	8.45	49.84
0.01	39.00	341.64
0.05	117.39	1150.99
0.10	125.62	2179.32
0.50	324.23	3486.00

D2. BaTiO3 exposure assays

Concentration [ppm]	Ba in nBaTiO3 [ppm]	Ti in nBaTiO3 [ppm]
0.00	13.85	2.25
0.01	400.00	288.36
0.05	707.88	224.41
0.10	1675.43	356.70
0.50	1726.32	460.85

D3. WC exposure assays

Concentration [ppm]	W in nWC [ppm]
0.00	27.59
0.01	1469.70
0.05	12426.28
0.10	8010.36
0.50	36338.55

Appendix E

Moulting Model: Data

E1. V Concentration Factors, from (Miramand et al., 1981)

Days	CF
1	3.154
2	4.379
4	5.187
5	5.527
7	6.145
8	6.548
11	7.594
12	7.675
16	10.214
18	10.106
21	10.327

E2. Ni Concentrations, from Figure 4 of (Hall, 1982)

Hours	*B*	*E*
0.7	0.47	0.20
2.2	1.41	0.61
3.1	1.79	1.02
5.1	2.52	1.96
10.2	3.98	2.43
15.1	3.96	3.30
20.0	4.52	4.00
32.9	3.34	4.86
39.9	3.72	6.00
48.9	5.03	5.52
59.0	5.66	7.80
64.5	4.19	8.11
70.8	5.44	7.31
79.2	5.03	7.94

E3. Ni Concentrations, from Figure 2(a) of (Hall, 1982)

Hours	*B* + *E*	Std. Err. (low)	Std. Err. (high)
1	0.88	0.82	1.01
5	3.52	3.24	3.77
9	4.79	4.36	5.14
20	7.90	7.28	8.52
49	5.41	4.85	6.03
72	6.33	5.72	6.95
91	8.47	7.66	9.33

E4. Extracted Data, from (Bergey and Weis, 2007)

	ST	CP	ST	CP	All ST	All CP	% CP
Cu	639.69	152.71	518.89	136.66	1158.58	289.37	20.0
Pb	41.37	41.28	0.36	27.03	41.73	68.31	62.1
Zn	135.78	46.58	149.85	46.64	285.63	93.22	24.6

E5. Extracted Data, from (Hennig, 1984)

	Zn	Sr	Cu	Fe
	9.40	90.49	8.59	62.43
	14.39	97.49	10.19	84.59
	24.14	92.00	14.93	81.97
	29.21	103.37	16.27	94.27
	35.83	100.99	17.86	118.70
	46.96	94.35	19.83	148.41
	56.12	119.98	20.65	162.56
	57.92	125.30	24.74	179.74
	73.32	133.11	38.13	268.84
Mean	38.59	106.34	19.02	133.50
Exuviae	129	858	105	498
% Exuviae	77.0	89.0	84.7	78.9

E6. Extracted Data, from (Keteles and Fleeger, 2001)

	Cu	Zn	Cd
Intermolt	94.22	156.88	2.92
Post-ecdysis	81.16	43.13	1.72
E	13.06	113.75	1.20
% E	13.86	72.51	41.13

E7. Extracted Data, from (Reinecke *et al.,* 2003)

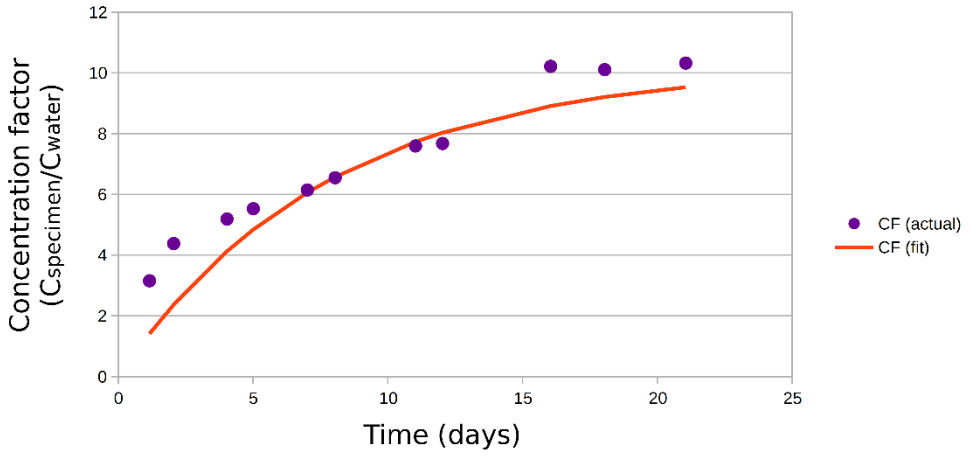
	Carapace	Muscle	D. Gland	Gills	Gonads	B	% E
Pb	23.53	17.94	7.49	14.18	23.50	63.11	27.2
Cd	3.96	2.71	2.14	3.29	5.26	13.40	22.8

Appendix F

Moulting Model: Details

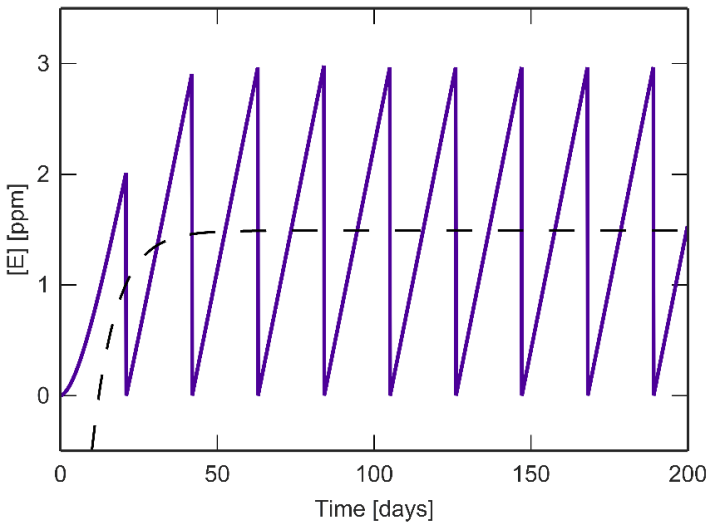
F1. Accumulation Data from (Miramand *et al.,* 1981)

Red line shows fit to Equation 3, with $T_M = 21$ days and $G = 1$.

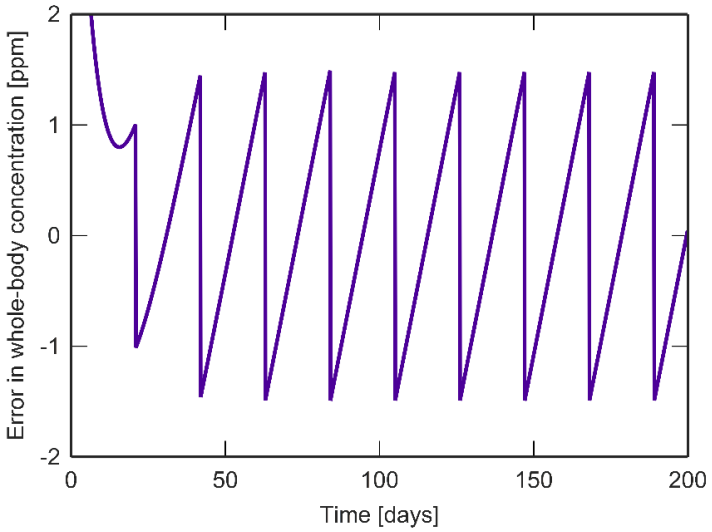


F2. Simulated Exoskeleton Pollutant Concentration

Continuous moulting approximation (given by Equation S14) is overlaid in dashed black.



F3. Error when Modelling Moulting as a Continuous Process



F4. Expanding the Model Derivation

This section will provide a more explicit derivation of the equations treated in the chapter.

Eq. 15 is a direct statement of the model presented in Figure 23:

$$\frac{\mathrm{d}B}{\mathrm{d}t} = k_i[i] + k_r[r] - k_t[B] \qquad (15 \textit{ supra})$$

The uptake rates can be grouped together, and will be denoted U, where $U = k_i\,[i] + k_r\,[r]$:

$$\frac{\mathrm{d}B}{\mathrm{d}t} = U - k_t[B] \qquad (S1)$$

Dividing the rate constants by the growth factor, G, allows us to account for the multidimensional growth of the isopod:

$$\frac{\mathrm{d}B}{\mathrm{d}t} = \frac{U}{G} - \frac{k_t[B]}{G} \qquad (S2)$$

This can be reformulated as a first-order linear equation in terms of the body compartment concentration, $[B]$:

$$\frac{\mathrm{d}B}{\mathrm{d}t} + \left(\frac{k_t}{G}\right)[B] = \frac{U}{G} \qquad (S3)$$

The solution to this equation for $[B] = 0$ at $t = 0$ is given by:

$$[B] = A\left(1 - e^{-t/\tau}\right) \qquad (S4)$$

where $A = U/k_t$, and $\tau = G/k_t$. This agrees with Eq. 17.

Eq. 16 can then be expanded by substituting Eq. S4 for $[B]$:

$$\frac{\mathrm{d}[E]}{\mathrm{d}t} = k_t A \left(1 - e^{-t/\tau}\right) + k_a[a] \tag{S5}$$

$$\frac{\mathrm{d}[E]}{\mathrm{d}t} = U \left(1 - e^{-t/\tau}\right) + k_a[a] \tag{S6}$$

This can be reformulated in terms of constants and functions of time:

$$\frac{\mathrm{d}[E]}{\mathrm{d}t} = (U + k_a[a]) - U \left(1 - e^{-t/\tau}\right) \tag{S7}$$

An expression for the exoskeleton body concentration can then be determined through direct integration, applying $[E] = 0$ at $t = 0$:

$$\int_0^{[E]} \mathrm{d}[E] = \int_0^t (U + k_a[a])\,\mathrm{d}t - \int_0^t U \left(1 - e^{-t/\tau}\right) \mathrm{d}t \tag{S8}$$

$$[E] = (U + k_a[a])\, t - U\tau \left(1 - e^{-t/\tau}\right) \tag{18 \textit{supra}}$$

The steady-state limit for $[B]$ can be determined by observing its behaviour as *t* increases. The $e^{-t/\tau}$ term approaches zero, leaving behind the A term, which produces Eq. 19.

When $[B]$ has reached steady-state, Eq. 16 can be simplified using Eq. 19 to obtain:

$$\frac{\mathrm{d}[E]}{\mathrm{d}t} = U + k_a[a] \tag{S9}$$

$$[E] = (U + k_a[a])\, t \tag{S10}$$

Pollutant flow is assumed to be uni-directional into the exoskeleton, therefore, the exoskeleton compartment concentration, $[E]$, reaches a maximum just before moulting occurs, ie. after a time period of T_M:

$$[E]_{\mathrm{MAX}} = (U + k_a[a])\, T_M \qquad (20\ \textit{supra})$$

F5. Derivation of Parameters from (Miramand *et al.*, 1981)

Miramand *et al.* (1981), reports accumulated concentrations in the shrimp *Lysmata seticaudata*, via a Vanadium uptake study using radioisotope tracing to determine internal concentrations. These results were used to derive approximately realistic values for the model.

Accumulations of Vanadium are presented in the former, referenced to the aquatic concentrations, for a number of non-moulting organisms in that publication's Figure 1b (filled circles). The values are presented in Table E1. It is assumed that these correspond to $[B]$ in the model (ie. that the contributions of $[E]$ average out); therefore, the data was fit to Eq. 17, taking an average of the final 3 values to estimate the steady-state body concentration $[B]_{\mathrm{MAX}}$. The original data and fit are shown in Figure F1.

This produced the coefficients $(1/\tau) = 0.12823\ \mathrm{day}^{-1}$ and $(U/k_t) = 10.21437\ (\mathrm{cpm\ organism})/(\mathrm{cpm\ water})$. Water concentrations of 25,

50 and 100 ppb were studied; the larger of these values was chosen, 0.1 ppm, resulting in a body concentration-referred value of $(U/k_t) = 1.021$ ppm.

From the derived value of $(1/\tau)$ and the chosen value for G, since $(1/\tau) = k_t/G$, this reduced to $k_t = 0.128\ \text{day}^{-1}$, which was rounded to $k_t = 0.13\ \text{day}^{-1}$. From $(U/k_t) = 1.021$ ppm, it follows that $U = k_i[i] + k_r[r] = 0.133$. $[r]$ corresponds to the water concentration, 0.1 ppm, while $[i]$ was estimated to be less than this, 0.07 ppm, with the rate constants chosen to satisfy the above value of U.

Miramand *et al.* (1981) estimate that moulting contributed to a loss of 74.4% of the overall accumulated concentration, in other words, $[B]/([B] + [E]_{\text{MAX}}) = 0.744$, from which it can be determined (using Eqs. 5-6) that $k_a[a] = 0.00857$. Since $[a]$ refers to the water concentration, 0.1 ppm, k_a was set to $0.09\ \text{day}^{-1}$ in order to achieve $k_a[a] = 0.009$.

F6. Derivation of Parameters from (Hall, 1982)

(Hall, 1982) presents a study of the uptake of Ni by *Daphnia magna*. Contained within this paper are:

a) measured time-series Ni accumulations in *D. magna* exposed to water containing 50, 250 and $750\ \text{ppb}$ of Ni, respectively (Figures 2 & 3), and

b) measurements of Ni accumulation in different body compartments of *D. magna* exposed to water containing $250\ \text{ppb}$ of Ni (Figure 4).

Data was extracted from Figure 4, and the relevant concentrations for the "body fluids" (B) and "carapace" (E) compartments are presented in Table E2. These measurements indicate that the body concentrations saturate after $20\ \text{h}$, while the carapace concentrations continue to increase indefinitely. This behaviour agrees with our model. Two other compartments, "gut tissues" and "filtering appendages, were not included in our analysis, as gut contents are often excreted directly without uptake occurring, while filtering appendages consist of both exoskeleton and soft tissue components.

The model was fit to the above data as follows. Compartment B saturates after $t = 20\ \text{h}$, so pre-saturation and post-saturation periods are dealt differently. The saturation value was found to equal (U/k_t), so this parameter was set to the mean value of B after $t = 20\ \text{h}$. Measured values

before $t = 20\,\mathrm{h}$ were then fitted to Eq, 17 with this saturation value, using a least squares method. In this manner the values $(U/k_t) = 4.63\,\mathrm{ng}$ and $\tau = 5.90\,\mathrm{h}^{-1}$ are obtained.

For ease of fitting, the steady-state version of Eq. 18 was employed, namely $E(t) = (U + k_a[a])t$. The parameter $(U + k_a[a])$ was determined using a simple linear regression with intercept through the origin, and produced the result $(U + k_a[a]) = 0.12\,\mathrm{ng\,h}^{-1}$. These three parameters completely describe the behaviour shown in Figure 26.

The time-series data is interesting as Figure 2(a) shows time-series measurements of Ni accumulation before and after a moult event (unfortunately, Figure 2(c) ends just after a moult event, while Figures 2(b) and 3 do not span moult events). Data from Figure 2(a) was extracted, and is presented in Table E3.

The moult event happens between $t = 20\,\mathrm{h}$ and $t = 49\,\mathrm{h}$, so a value of $T_M = 48\,\mathrm{h}$ is assumed. It is also assumed that the uptake conditions were relatively similar to those in Figure 4, which leads to the evaluations $(U + k_a[a]) = (k_i[i] + k_r[r] + k_a[a]) = 0.12\,\mathrm{ng\,h}^{-1}$ and $\tau = G/k_t = 5.90\,\mathrm{h}^{-1}$, as before, and the only change was in the translocation kinetics.

A least squares fit was then applied to the sum of Eq. 17 and the steady-state version of Eq. 18 using the above parameters. This obtained a value of $(U/k_t) = 4.51$. These values completely describe the behaviour shown in Figure 27.

F7. Continuous Approximation

A key property of the model is the discontinuous contribution of moulting to the whole-body concentration. An important consequence of this is that the whole-body concentration cannot be modelled by continuous processes. In this section an attempt is made to approximate the contribution of moulting as a continuous process, and illustrate the error introduced by this approach.

We begin by modifying Eq. S8 to consider a time t_2 which occurs after a moult event at time t_1.

$$\int_0^{[E]} \mathrm{d}[E] = \int_{t_1}^{t_2} (U + k_a[a])\,\mathrm{d}t - \int_{t_1}^{t_2} U\left(1 - e^{-t/\tau}\right)\mathrm{d}t \quad \text{(S11)}$$

$$[E] = (U + k_a[a])\,(t_2 - t_1) - U\tau\left(e^{-t_1/\tau} - e^{-t_2/\tau}\right) \quad \text{(S12)}$$

We are initially interested in the maximum value obtained before the next moult, which occurs when the subsequent moult is about to occur, ie. $t_2 = t_1 + T_M$. Eq. S12 then becomes:

$$[E]_{\mathrm{MAX}} = (U + k_a[a])\, T_M - U\tau \left(e^{-(t_2 - T_M)/\tau} - e^{-t_2/\tau}\right) \quad \text{(S13)}$$

The maximum value of $[E]$ obtained is zero, which occurs after each moult. Approximating $[E]$ as a sawtooth pattern, the mean value of $[E]$ is simply given by:

$$[E]_{\mathrm{MEAN}} = \frac{[E]_{\mathrm{MAX}}}{2} \quad \text{(S14)}$$

The resulting approximation for $[E]$, where moulting is modelled as a continuous depuration process, is illustrated in Figure F2. Figure F3 shows the resulting error in the whole-body concentration, which is not a simple periodic sequence.

F8.Sample Implementation

What follows is sample code for modelling the pollutant concentrations accumulated by an aquatic invertebrate. This model accounts for the mechanism of moulting, and is written for Octave, but is also valid MATLAB code. It can be amended with ease to be applicable to a great number of alternative programming packages.

```
%%% PARAMETERS %%%
% Adjust these parameters according to species, pollutant etc.

delt = 0.1 ;% Time step
numpoints = 2000; % Length of simulation
t = 0 * ones(1, numpoints);

% Assume growth factor, G = 1 for simplicity

% Respiration
kr = 0.70; % Rate of respiration
Cr = 0.10 * ones(1, numpoints);% Concentration taken in via
respiration

% Ingestion
ki = 0.90; % Rate of ingestion
Ci = 0.07 * ones(1, numpoints); % Concentration taken in via ingestion

% Body
kt = 0.13; % Rate of translocation from the body to the exoskeleton
Cb = 0 * ones(1, numpoints); % Concentration in the body

% Adsorption
ka = 0.09; % Rate of adsorption
Ca = 0.10 * ones(1, numpoints); % Concentration taken in via
adsorption

% Exoskeleton
Ce = 0 * ones(1, numpoints); % Concentration in the exoskeleton
moultperiod = 21; % How often is the exoskeleton moulted?

%%%%%%%%%%%%%%%%%%%%%%%%%%%%%%%%%%%%%%%%%%%%%%%%%%%%%%%%%%%%%%%%%%%%%%%%%%%%
%%%%%%%%%%

    for n = 2 : numpoints
    |   t(n) = t(n-1) + delt;
    |
    |   delCb = (ki * Ci(n-1) + kr * Cr(n-1) - kt * Cb(n-1)) * delt;
    |   delCe = (ka * Ca(n-1) + kt * Cb(n-1)) * delt;
    |
    |   Cb(n) = Cb(n-1) + delCb;
    |   Ce(n) = Ce(n-1) + delCe;
    |
    |   % Accounting for moulting
    |   if (floor (t(n)/moultperiod) > floor (t(n-1)/moultperiod))
    |   |   Ce(n) = 0;          % Moult has occurred, new exoskeleton!
    |   end
    end

% Making predictions
Abody = (ki * Ci + kr * Cr) / kt;
Amoult = (ki * Ci + kr * Cr + ka * Ca) * moultperiod;

fprintf("Equilibrium body concentration [B](infinity): %0.3f\n",
Abody(1))
fprintf("Peak moult concentration [E]max: %0.3f\n", Amoult(1))
```

```
fprintf("Maximum percentage moult concentration: %0.2f percent\n", 100
* Amoult(1) / (Amoult(1) + Abody(1)))
fprintf("Mean percentage moult concentration: %0.2f percent\n", 50 *
Amoult(1) / (Amoult(1) + Abody(1)))

% Plotting as figures

%% Fig. 1: Body
figure()
plot(t, Cb, 'linewidth', 3, 'Colour', [76, 0, 153]/256)
xlabel('Time (days)')
ylabel('[B] (ppm)')
xlim([0, numpoints*delt])
hold('on')
plot(t, Abody(1) * ones (1, numpoints), '--k', 'linewidth', 2)
hold('off')
set(gca, 'fontsize', 18, 'linewidth', 2)
xlabel('Time [days]', 'fontsize', 18)
ylabel('[B] [ppm]', 'fontsize', 18)

%% Fig. 2: Exoskeleton
figure()
plot(t, Ce, 'linewidth', 3, 'Colour', [76, 0, 153]/256)
xlabel('Time (days)')
ylabel('[E] (ppm)')
xlim([0, numpoints*delt])
ylim([0,3.5])
hold('on')
plot(t, Amoult(1) * ones (1, numpoints), '--k', 'linewidth', 2)
hold('off')
set(gca, 'fontsize', 18, 'linewidth', 2)
xlabel('Time [days]', 'fontsize', 18)
ylabel('[E] [ppm]', 'fontsize', 18)

%% Fig. 3: Overall (whole-body) concentration
figure()
plot(t, Cb + Ce, 'linewidth', 3, 'Colour', [76, 0, 153]/256)
xlabel('Time (days)')
ylabel('Whole body conc. (ppm)')
xlim([0, numpoints*delt])
ylim([0,4.5])
hold('on')
plot(t, Abody(1) * ones (1, numpoints), '--k', 'linewidth', 2)
plot(t, (Abody(1) + Amoult(1)) * ones (1, numpoints), '--k',
'linewidth', 2)
hold('off')
set(gca, 'fontsize', 18, 'linewidth', 2)
xlabel('Time [days]', 'fontsize', 18)
ylabel('Whole body conc. [ppm]', 'fontsize', 18)
```

The simulation code presented above is an Octave/MATLAB-based fixed-timestep implementation of the model. A textual description of the model follows, with reference to the code listing.

Because brackets cannot be used as variable names in Octave/MATLAB, the letter 'C' is used to denote concentrations, ie. `Cb` = $[B]$ and `Ce` = $[E]$.

The simulation is run for a finite number of timesteps (`numpoints`), with each timestep separated by a fixed time period (`delt`).

```
for n = 2 : numpoints
|   t(n) = t(n-1) + delt;
|                                   % simulation code...
end
```

Eq. 15 is a differential equation giving the rate of change of the concentration in the body compartment, $[B]$, versus time:

$$\frac{\mathrm{d}B}{\mathrm{d}t} = k_i[i] + k_r[r] - k_t[B] \qquad \text{(15 supra)}$$

For a sufficiently small timestep, it can be approximated as a difference equation by replacing the derivative on the left-hand side with $\Delta[B]/\Delta t$, producing the following expression for the change in concentration during each timestep:

$$\Delta[B] = (k_i[i] + k_r[r] - k_t[B])\,\Delta t \qquad \text{(S15)}$$

Similarly, Eq. 16 can be transformed into a difference equation and reformulated as follows:

$$\Delta[E] = (k_t[B] + k_a[a])\,\Delta t \qquad \text{(S16)}$$

This can be formulated in code as:

```
delCb = (ki * Ci(n-1) + kr * Cr(n-1) - kt * Cb(n-1)) * delt;
delCe = (ka * Ca(n-1) + kt * Cb(n-1)) * delt;
```

An alternative approach would be to implement Eqs. 17 & 18 instead; either approach will yield similar results.

The change in concentration is simply applied to the concentration of the previous timestep to obtain the concentration of the current timestep.

```
Cb(n) = Cb(n-1) + delCb;
Ce(n) = Ce(n-1) + delCe;
```

Moulting occurs whenever the current time, t, passes a multiple of the moult period, T_M. When this happens, the floor of t/T_M changes.

Moult occurs if:

$$\lfloor t/T_M \rfloor \neq \lfloor (t-1)/T_M \rfloor \qquad (S17)$$

When moulting occurs, the concentration of the exoskeleton, $[E]$, goes to zero. This formulation of the moulting condition can be directly coded as follows:

```
if (floor (t(n)/moultperiod) > floor (t(n-1)/moultperiod))
    Ce(n) = 0;          % Moult has occurred, new exoskeleton!
end
```

The predictions, given by Eqs. 19 & 20, can also be directly coded:

```
Abody = (ki * Ci + kr * Cr) / kt;
Amoult = (ki * Ci + kr * Cr + ka * Ca) * moultperiod;
```